

# BONE PERFUSION ALTERATIONS IN CHRONIC KIDNEY DISEASE

Mohammad W. Aref

Submitted to the faculty of the University Graduate School  
in partial fulfillment of the requirements  
for the degree  
Doctor of Philosophy  
in the Department of Anatomy and Cell Biology,  
Indiana University

May 2019

Accepted by the Graduate Faculty of Indiana University, in partial fulfillment of the requirements for the degree of Doctor of Philosophy.

Doctoral Committee

---

Matthew R. Allen, Ph.D., Chair

---

Jason M. Organ, Ph.D.

February 5, 2019

---

Jonathan D. Tune, Ph.D.

---

Joseph M. Wallace, Ph.D.

---

Sharon M. Moe, M.D.

© 2019

Mohammad W. Aref

Mohammad W. Aref

## BONE PERFUSION ALTERATIONS IN CHRONIC KIDNEY DISEASE

Patients with chronic kidney disease (CKD) are at an alarming risk of fracture and cardiovascular disease-associated mortality. There is a critical need to better understand the underlying mechanism driving altered cardiovascular and skeletal homeostasis, as well as any connection between the two. CKD has been shown to have negative effects on many vascular properties including end-organ perfusion. Surprisingly, exploration of skeletal perfusion and vasculature has not been undertaken in CKD. Alterations in bone perfusion are linked to dysregulation of bone remodeling and mass in multiple conditions. An understanding of the detrimental impact of CKD on bone perfusion is a crucial step in understanding bone disease in these patients. The goal of this series of studies was to test the global hypothesis that skeletal perfusion is altered in CKD and that alterations can be modulated through treatments that affect metabolic dysfunction. These studies utilized a rat model of CKD to conduct metabolic assessments, bone perfusion measurements, bone imaging studies, and isolated vessel reactivity experiments. Our results showed that animals with CKD had higher levels of parathyroid hormone (PTH), leading to substantial bone resorption. Bone perfusion measurements showed CKD-induced elevations in cortical bone perfusion with levels progressing alongside CKD severity. Conversely we show that marrow perfusion was lower in advanced CKD. PTH suppression therapy in animals with CKD resulted in the normalization of cortical bone perfusion and cortical bone mass, but did not normalize marrow bone

perfusion. These results show a clear association between bone deterioration and altered bone perfusion in CKD. While the relationship of altered bone perfusion and bone deterioration in CKD necessitates further work, these results indicate that determining the mechanisms of bone perfusion alterations and whether they are drivers, propagators, or consequences of skeletal deterioration in CKD could help untangle a key player in CKD-induced bone alterations.

Matthew R. Allen, Ph.D., Chair

## TABLE OF CONTENTS

Chapter 1. Introduction .....	1
Chapter 2. Assessment of regional bone tissue perfusion in rats using fluorescent microspheres .....	22
Chapter 3. Skeletal vascular perfusion is altered in chronic kidney disease .....	39
Chapter 4. Suppression of parathyroid hormone normalizes chronic kidney disease-induced elevations in cortical bone vascular perfusion.....	59
Chapter 5. Effects of CKD on Isolated Vessel Properties: Preliminary Investigation .....	79
Chapter 6. Discussion .....	89
References .....	107
Curriculum Vitae	

## LIST OF TABLES

Table 1-1: Summary of bone vascular dysfunction in diseases, conditions and treatments.....	12
Table 2-1: Tissue fluorescence density in the femur and tibia following intra-cardiac injection of microspheres .....	36
Table 2-2: Tibia tissue fluorescence density following cardiac versus tail vein microsphere injection.....	37
Supplemental Table 2-1: Femur and tibia mass data (in grams).....	38
Table 3-1: Serum biochemistries .....	46
Table 3-2: 35 week correlations between PTH and tissue fluorescence density .....	48
Supplemental Table 3-1: Body Masses .....	56
Supplemental Table 3-2: Tissue Masses .....	57
Supplemental Table 3-3: Kidney Perfusion .....	58
Table 4-1: Serum biochemistries at end point (35 weeks) .....	66
Table 4-2: Proximal tibia cortical geometry .....	68
Table 6-1: Bone perfusion, bone formation rate, and bone volume in different conditions .....	94
Table 6-2: Description of future studies .....	103

## LIST OF FIGURES

Figure 1-1: Changes to mineral metabolism in CKD .....	3
Figure 1-2: Cardiac calcification and cortical porosity in the Cy/+ model .....	9
Figure 1-3: Diaphyseal bone perfusion.....	17
Figure 1-4: Bone vascular dysfunction and bone disease .....	21
Figure 2-1: Graphical depiction of microsphere protocol including microsphere injection, tissue processing and fluorescence quantification .....	26
Figure 2-2: Microsphere standard curves displayed as bead quantity and fluorescence .....	30
Figure 2-3: Tissue fluorescent density (TFD) of segmented femur (A,C) and tibia (B,D).....	31
Figure 3-1: 30 week time point bone perfusion data .....	49
Figure 3-2: 35 week time point bone perfusion data .....	50
Figure 4-1: MicroCT of proximal tibia 2.5mm distal to the proximal growth plate .....	69
Figure 4-2: Bone perfusion data .....	71
Figure 4-3: Combined graphs with data from Experiments 1 & 2 .....	74
Figure 4-4: Potential mechanism of elevated PTH effect on cortical perfusion .....	75
Figure 5-1: Aortic and femoral wire myography.....	84
Figure 5-2: Potential causes and consequences of decreased marrow perfusion.....	86



## CHAPTER 1

### INTRODUCTION

Patients with chronic kidney disease are at an alarming risk of cardiovascular disease and fracture-associated mortality. One in ten Americans suffers from chronic kidney disease (CKD) [1]. CKD results in a sequelae of physiological changes, including a triad of abnormal biochemistries, bone remodeling changes and vascular calcification, that culminate in increased morbidity and mortality. In CKD patients, the risk of cardiovascular disease is increased 2-3-fold and the risk of fracture 17-fold compared to the normal population with progressive rise in risk as kidney function deteriorates. More striking, cardiovascular disease accounts for nearly 60% of deaths in those with CKD (compared to 28% in the normal population); similarly over 60% of CKD patients that sustain a hip fracture die within a year (compared to 20% in the normal population) [2]. These striking statistics emphasize the critical need to better understand the underlying mechanism driving altered cardiovascular and skeletal homeostasis, as well as any connection between the two.

The pathogenesis of chronic kidney disease—mineral and bone disorder (CKD-MBD) is driven by complex alterations in mineral metabolism. Disturbances in bone and mineral metabolism are a hallmark of CKD [3], [4]. Along with hyperphosphatemia, secondary hyperparathyroidism, and vascular calcification, patients exhibit alarming increases in the risk of cardiovascular disease and skeletal fractures [2,5-11,14-23]. Given the complexities of normal mineral metabolism, CKD-MBD encapsulates the compensatory mechanisms (and their

failure) that preserve calcium and phosphate homeostasis in the face of declining kidney function [12] (**Figure 1-1**). These physiological and pathological adaptations play a significant role in fracture risk and cardiovascular mortality [13-16].

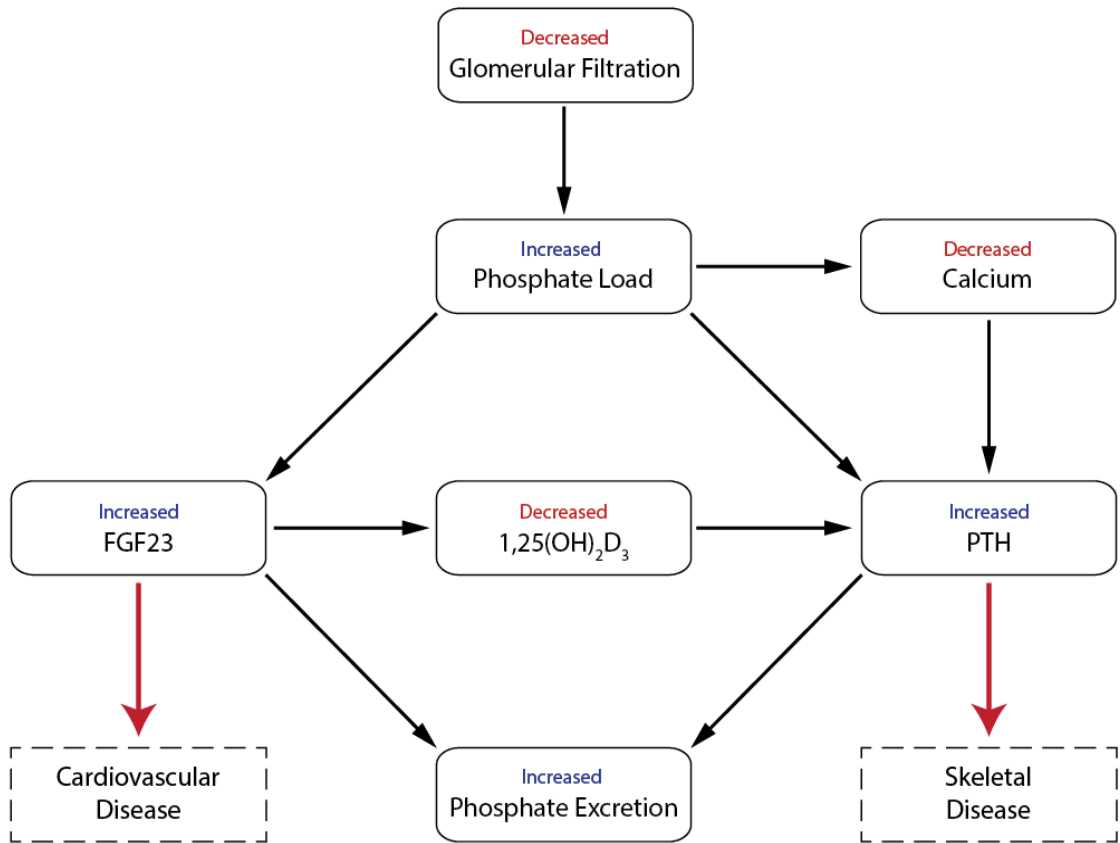


**Figure 1-1.** Changes to mineral metabolism in CKD.

As kidney function begins to decline, there is an increased demand on the remaining nephrons to maintain mineral homeostasis and normal excretory functions[17,18]. Changes in phosphate excretion drive the metabolic derangements that characterize CKD-MBD. In response to increased phosphate load in the circulation, osteocytes increase secretion of FGF23, which acts on tubular epithelial cells in the kidney to decrease phosphate reabsorption. Elevated levels of FGF23 have been linked to ventricular hypertrophy and cardiovascular mortality [19-37]. In concert with elevated FGF23, parathyroid hormone (PTH) levels also increase to compensate for the rises in serum phosphate (though simultaneous declines in vitamin D synthesis occur in an attempt to temper PTH rises). While recent evidence indicates that FGF23 normally suppresses PTH activity [38,39], secondary hyperparathyroidism ensues nonetheless, presumably due to the decreased expression of Klotho resulting in impaired FGF23 function. Initially, these responses effectively maintain normal serum phosphate levels. Eventually though, this process fails, and serum phosphate levels begin to increase despite continued elevations in PTH and FGF23. Rises in PTH levels lead to enormous increases in osteoclast differentiation and activity, which ultimately leads to the bone deterioration often present in CKD-MBD. While these pathways are beginning to be elucidated, the metabolic complexity of CKD has led to great challenges in understanding and treating skeletal and cardiovascular manifestations, resulting in an inability to minimize fracture risk and mortality in this population.

Metabolic changes in CKD lead to significant changes in structure/function of cardiovascular and skeletal tissue. The connection between kidney disease and cardiovascular abnormalities was first made in the 19<sup>th</sup> century [15]. Since then, numerous studies have illustrated the connection between decreased kidney function in CKD [40-46] and disorders of mineral metabolism [61][62-64][65-67] with a wide array of cardiovascular diseases. In a rat model of CKD, chronic elevations of PTH have been implicated in lowering cardiac contractility and adversely affecting energy utilization in myocardial tissue [54], increasing myocardial calcium deposition, hypertrophy and fibrosis and vascular calcification [55,56], increasing mitral annular calcification [57], impairing arterial vasodilation [58], and causing wall-thickening of intramyocardial arterioles independent of blood pressure [59].

Patients with chronic kidney disease have more than double the risk of having a fracture compared to the general population [6,7]. Of even greater concern, mortality rates in CKD patients with hip fractures more than double that of non-CKD patients with hip fractures [8]. The presence of secondary hyperparathyroidism causes changes in bone metabolism that lead to the preferential breakdown of cortical bone. Specifically, chronic elevations in PTH can lead to subperiosteal and intracortical erosion, resulting in drastic increases in cortical porosity [60]. The impact on cancellous bone is more variable. In cases of mild hyperparathyroidism, cancellous bone is usually unchanged or even increased [61]. Other imaging studies indicate that hyperparathyroidism can also detrimentally impact trabecular bone in CKD [62]. Nevertheless, cortical bone is

most prominently impacted, which may explain why BMD estimates in the distal radius and tibia (and not the hip or spine) are the strongest predictors of fracture in these patients. Specifically, CKD patients with a history of fracture have lower volumetric BMD and thinner cortices than those without fractures [60].

Animal models present an opportunity to explore the relationship between cardiovascular alterations and skeletal deterioration in CKD. Because of the widespread impact of CKD on human health, numerous animal models have been developed to address the systemic repercussions of kidney disease. The most common approach is to induce end stage renal disease by surgical subtotal nephrectomy (with numerous variations), electrocautery, or the administration of adenine. These models represent an acute injury that leads to chronic renal failure. Given that the vast majority of patients with CKD have either hypertensive nephropathy or diabetic nephropathy [63], sudden trauma does not accurately represent the progression of disease that occurs in the majority of human CKD cases. While adenine does provide a slower disease progression (three to four weeks), animals exhibit severe weight loss not seen in other models [64]. The consequences of this weight loss on pertinent disease parameters are unclear. Despite the drawbacks of acute onset, these models still have important potential for examining the impact of CKD on mature cardiovascular and skeletal tissue.

The effects of subtotal nephrectomy in rodents on the cardiovascular system resemble those seen in human CKD [65], although severe hypertension is not common in this model. Pathologies documented in the subtotal nephrectomy model include left ventricular hypertrophy [66] along with increases

in myocyte cross-sectional area [67], interstitial fibrosis [67], and increases in capillary density [68]. With regards to skeletal tissue, most of these data derive from experiments in which CKD is induced in skeletally immature animals with actively growing bones [69] [70]. Not only do these animals exhibit rapid bone modeling not present in adult rodents, but there also is no way to distinguish the direct impact of kidney disease on bone from its impact on altered skeletal development.

Alternative models use genetic manipulation to induce kidney failure, primarily in the form of polycystic kidney disease [71]. For example, the *jck* mouse has a primary ciliary defect that leads to cystic kidney disease by four weeks of age. Similarly, *pcy* mice exhibit ciliary disease leading to cysts by three weeks. The greatest challenge with most genetic models is the rapid onset of disease during early growth and development. As above, this makes it exceedingly difficult to determine if skeletal manifestations are a direct result of the disease or rather an indirect byproduct of disturbed skeletal development. While these are important models for pediatric CKD, their application to end stage disease in adults is limited.

The model utilized in the current study (the Cy/+ rat) avoids many of these drawbacks. The Cy/+ rat, developed here at IUSM by the late Dr. Vince Gattone, is characterized by autosomal dominant polycystic kidney disease [72]. Based upon its gradual development of mineral disturbances and similar response to current therapies, our laboratory has demonstrated that it accurately recapitulates several aspects of human CKD [72,73]. Blood urea nitrogen (BUN)

and creatinine are elevated by 20 weeks while progressive hyperphosphatemia, hyperparathyroidism, and skeletal abnormalities, are all present by 30 weeks. By 35 weeks of age there are dramatic manifestations of cardiac and vascular calcification as well as severe cortical porosity and compromised mechanical properties (**Figure 1-2**). The apparent and clinically relevant dysfunction in cortical bone observed in this model provides an opportunity to study the possibility of dysfunctions in skeletal blood flow in CKD. Although both males and females display disease progression, males do so more quickly and thus have been the focus of most previous experiments [73,74]. Because of this preponderance of data, males will be utilized here with the long-term goal of assessing sex-differences.



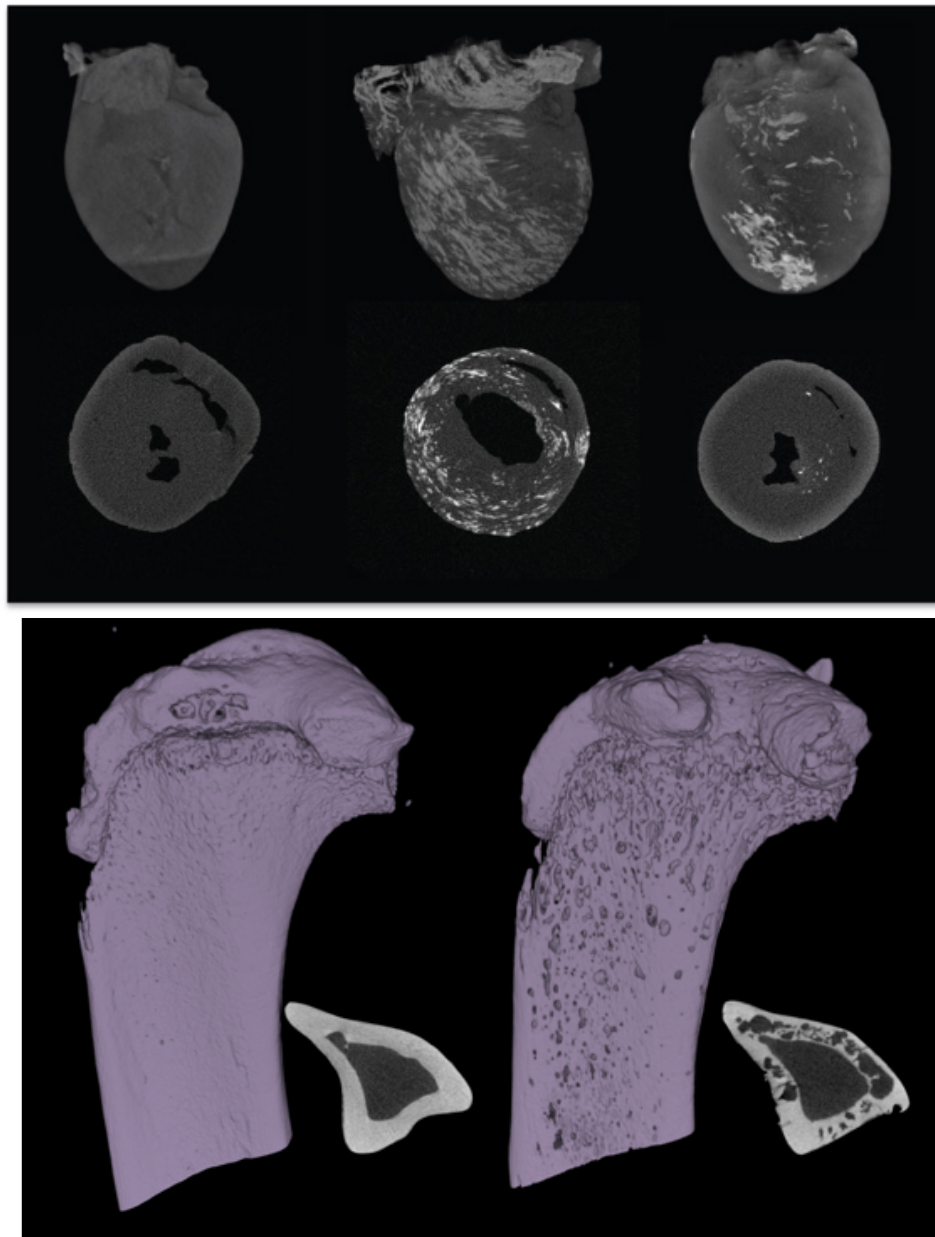


**Figure 1-2.** Cardiac calcification and cortical porosity in the Cy/+ model. The Cy/+ model develops cardiac calcifications (upper panels show normal (on left) and two Cy/+ animals at 35 weeks via CT) and severe skeletal destruction (lower panels (left is normal; right is CT image of a Cy/+ tibia at 35 weeks)).

Overall, the Cy/+ rat provides an advantage as it allows for the analysis of skeletal defects in a model that exhibits progressive development of both CKD mineral metabolism and skeletal abnormalities [64]. Normal bone is allowed to develop prior to the onset of disease, mimicking the gradual development of CKD in human adults.

Skeletal perfusion is essential to bone health. Bone blood flow plays a crucial role in bone growth [75], fracture repair [76-78], and bone homeostasis [79,80]. The vascularity of bone dictates its degree of cellularity, remodeling and repair [81]. Disturbances to bone blood flow have been shown to have deleterious effects on bone health and function [79,82-85]. Conditions that alter bone remodeling (diabetes, disuse, aging, estrogen withdrawal, anabolic drug treatment) have all been associated to changes in bone blood flow and properties of the principal nutrient artery (PNA), the main resistance vessel to each long bone [82,83,86-91]. Moreover, disturbances to bone vasculature, due to any of a number of potential causes, result in alterations in tissue perfusion and local hypoxia [92]. Reduced bone perfusion has been associated with bone loss [93] in a number of conditions, including aging, inflammation, infection, fractures, unloading, tumors, diabetes, smoking, and glucocorticoids (**Table 1-1**). Additionally, impairments to bone blood supply have been shown to reduce growth and repair [94]. The effects of local hypoxia on bone cell function dictate the effects of disturbances to bone vasculature on bone health. Hypoxia has been shown to stimulate bone resorption by accelerating the formation of osteoclasts and ultimately increasing osteoclast number [95]. The formation of

functional osteoclasts occurs through the differentiation of mononuclear precursors following extravasation into oxygen-deficient bone microenvironments [93,96,97]. Hypoxia has also been shown to inhibit osteogenesis due to decreased differentiation of osteoblasts, along with inhibition of cell proliferation, collagen production, and alkaline phosphatase expression [93,98].

**Table 1-1.** Summary of bone vascular dysfunction in diseases, conditions and treatments

<b>Condition</b>	<b>Effect of disease on bone vascular properties</b>
<b><u>Skeletal Disease</u></b>	
<b>Post-menopausal Osteoporosis</b>	<ul style="list-style-type: none"> <li>• Decrease in blood vessel volume - Reduced medullary canal vascularity, including capillary rarefaction and decrease expression of angiogenesis-related HIF-1a, HIF-2a, and VEGF proteins in aging humans and ovariectomized mice [99]</li> </ul>
<b>Osteonecrosis</b>	<ul style="list-style-type: none"> <li>• Reduced bone blood supply that results in increased osteoclast differentiation [100]</li> </ul>
<b>Avascular necrosis of the femoral head</b>	<ul style="list-style-type: none"> <li>• Decreased neovascularization caused by low number of endothelial progenitor cells (EPCs), their diminished capacity to migrate and increased senescence in humans [101]</li> <li>• Blood flow interruption caused by damage of the endothelial cell membrane [101]</li> </ul>
<b>Osteopetrosis</b>	<ul style="list-style-type: none"> <li>• Blood perfusion to the bone affected by the obliteration of medullary spaces combined with granulocytopenia, anemia and ischemia, commonly lead to necrosis and osteomyelitis [102]</li> </ul>
<b><u>Vascular Disease</u></b>	
<b>Atherosclerosis</b>	<ul style="list-style-type: none"> <li>• Oxidized lipids produced during atherosclerotic plaque formation within bone blood vessels negatively affect bone mass by increasing anti-osteoblastic inflammatory cytokines and decreasing pro-osteoblastogenic Wnt ligands in ApoE-knockout, high-fat-diet-fed mice [103]</li> </ul>
<b><u>Systemic Disease</u></b>	
<b>Diabetes Mellitus</b>	<ul style="list-style-type: none"> <li>• Diabetes-induced microangiopathy causes vasoconstriction and impairs blood flow with long bones of rats [84]</li> <li>• Decreased blood vessel supply - decreased marrow vascularity [104]</li> <li>• Advanced glycation end products (AGEs), produced in diabetes may also disrupt bone vasculature [105]</li> </ul>

<b>Chronic Kidney Disease (Secondary Hyperparathyroidism)</b>	<ul style="list-style-type: none"> <li>• Increased cortical bone perfusion [106]</li> <li>• Decreased marrow perfusion [106]</li> <li>• Decreased marrow VEGF [107]</li> </ul>
<b>Sickle Cell Anemia (and other anemias)</b>	<ul style="list-style-type: none"> <li>• Decreased oxygen delivery to bone [108]</li> </ul>
<b>Chronic Obstructive Pulmonary Diseases</b>	<ul style="list-style-type: none"> <li>• Decreased oxygen delivery to bone [109]</li> </ul>
<b><u>Therapy</u></b>	
<b>Teraperatide (Anabolic Therapy)</b>	<ul style="list-style-type: none"> <li>• Increased vascular volume and increased perfusion [110]</li> <li>• Increased VEGF and increased vasodilatory principal nutrient artery of the femur [90]</li> </ul>
<b>Bisphosphonate</b>	<ul style="list-style-type: none"> <li>• Treatment with pamidronate or zoledronate has been reported to reduce vascular endothelial growth factor (VEGF) levels [111] and bone blood flow in rats [112]</li> </ul>
<b><u>Skeletal Tumors</u></b>	<ul style="list-style-type: none"> <li>• Increased vascularity [113]</li> </ul>
<b><u>Aging</u></b>	Decreased perfusion due to vascular rarefaction, reduced angiogenesis, diminished vasodilator capacity, vascular calcification, arteriosclerosis, and atherosclerosis in humans [86,87,114]
<b><u>Substance Abuse</u></b>	
<b>Smoking</b>	<ul style="list-style-type: none"> <li>• Possible link between vasoconstriction due to nicotine and epidemiological evidence linking smoking to osteoporosis [115]</li> </ul>
<b>Alcohol</b>	<ul style="list-style-type: none"> <li>• Possible link between vascular disease (increased BP and triglycerides) and osteopenia leading to skeletal fractures [116,117]</li> </ul>
<b><u>Fracture</u></b>	<ul style="list-style-type: none"> <li>• Short term vasodilation of existing/remaining intact vasculature following injury [118]</li> <li>• Angiogenesis around and within fracture callus [76-78]</li> </ul>
<b><u>Unloading</u></b>	<ul style="list-style-type: none"> <li>• Decreased blood flow and increased vascular resistance [83]</li> </ul>

Preclinical assessment of bone perfusion allows the exploration of relationships between bone health/disease and bone perfusion. Radioactive microspheres were long considered the experimental gold standard for the determination of skeletal perfusion [80] due to their accuracy and ease of analysis [119]. Upon injection into the animal, microspheres lodge in tissue capillaries in direct proportion to the fraction of cardiac output perfusing the tissue [80]. Tissue analysis is relatively straightforward, even for mineralized tissue, in that once tissues of interest are harvested, blood flow is estimated via a gamma spectrometer with minimal tissue processing [83,85,120,121]. Various limitations of radioactive microspheres, including cost, health risks, and the necessity for precautions with use and disposal [122], have resulted in exploration of alternative methods. Alternative methods of preclinical perfusion measurements are laser doppler flowmetry and positive emission tomography (PET). Microsphere injection is a static measurement, while Laser Doppler and PET are continuous measurements. Laser Doppler does not provide anatomical data and is not likely to be useful as a measure of blood flow because the size of the vessels could be different and would not be measurable. Different size vessels would affect flow and thus potentially unknowingly confound the measure.

Fluorescent microspheres, which work on the same principal as radioactive spheres in that they become entrapped within capillaries, have been shown to allow measurement of organ perfusion as effectively as radioactive microspheres [122]. Analysis of fluorescent microspheres requires degradation and filtration of the tissues of interest before the samples can be analyzed and

has been effectively used in numerous soft tissue across multiple species [119,122-125]. Processing of skeletal tissue presents more challenges for fluorescent microspheres compared to soft tissue, perhaps helping to explain why the fluorescent microsphere method has only been performed in two models: mice [126] and rabbits [119]. The current series of studies will utilize fluorescent microspheres to measure bone perfusion in rats with CKD.

The functional anatomy of long bone blood supply is crucial in understanding the potential role of bone perfusion in CKD bone disease. Long bones have four main arterial inputs: nutrient arteries that penetrate the diaphysis, periosteal arteries that are on the bone surface within the periosteum, metaphyseal arteries, and epiphyseal arteries [127]. Cortical bone in the diaphysis is perfused by arterial blood originating from 1) the main nutrient arteries as well as 2) smaller periosteal arteries [81] (**Figure 1-3**). The main blood supply of the marrow originates from the nutrient artery, which originates from large arteries of the extremities (i.e. femoral/tibial and brachial/radial arteries), penetrates the cortex and divides into ascending and descending branching running along the length of the bone within the medullary cavity [128]. The main nutrient artery running longitudinally through the medullary cavity will supply the medullary sinuses in the marrow along with cortical branches directed back toward the endosteum. The cortical branches of the nutrient artery pass through endosteal canals and supply arterial blood to fenestrated intracortical capillaries in the Haversian canal system. Intracortical capillaries anastomose with periosteal plexuses formed by arteries from neighboring connective tissue.

Thus, perfusion of cortical bone in long bones is centrifugal, originating from the nutrient artery in the marrow cavity and anastomosing with periosteal plexuses in the periosteum [128] [81]. Perfusion of the bone can be compromised with either disrupted vascular supply or altered vascular network within the cortex and medullary cavity.



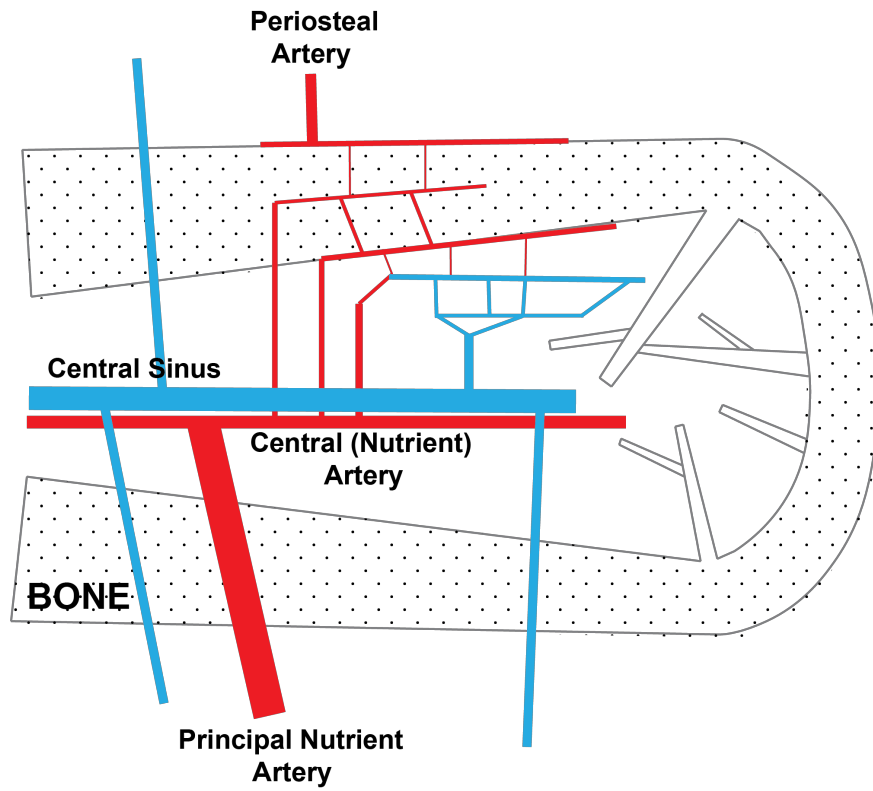


**Figure 1-3:** Diaphyseal bone perfusion.

Chronic kidney disease has negative effects on vascular reactivity and end-organ perfusion. In the setting of CKD, decreased cardiac output [129], vascular calcification [130], and endothelial dysfunction [131-133] could all contribute to altered end-organ perfusion. Hypoperfusion, in CKD patients, that causes ischemia has been illustrated in the myocardium [134], brain [135,136], and mesentery [137]. However, studies that elucidate the effect of individual cardiovascular pathologies on end-organ perfusion in CKD have yet to be performed. Moreover, CKD-induced elevations in uremic toxins including phosphate [138] and parathyroid hormone (PTH) [110] have long been associated with vascular dysfunction through endothelium-dependent, endothelium-independent and/or vascular remodeling mechanisms [139-142]. Extensive work in CKD has documented vascular changes to coronary vessels [143,144] and aorta [145,146]. Gastrointestinal resistance arteries, which control organ perfusion, have also been shown to be adversely affected in models of CKD [147-150]. Other work has illustrated structural remodeling of resistance arteries manifested as alterations in arteriolar wall thickness and lumen diameter [151,152]. Surprisingly, the effects of uremia, including elevations in PTH and phosphate, on skeletal perfusion and vasculature have not been studied.

Parathyroid hormone (PTH) acts directly on vascular smooth muscle cells and modulates bone vasculature. Cardiomyocytes and vascular smooth muscle cells both have PTH receptors [153]. In cardiomyocytes, PTH activates protein kinase C which increases hypertrophic growth that might contribute to left ventricular hypertrophy. In vascular smooth muscle cells, PTH increases cAMP

levels and inhibits L-type calcium channel, which results in vasorelaxation [153-154]. Early studies illustrated the acute effects of intravenous injection of PTH on bone blood flow [154]. Bone blood flow to the tibia and femur was increased 30 minutes after administration of intravenous PTH. This pointed toward a dilatory effect in bone vasculature that was confirmed more recently in a study that showed that PTH enhanced endothelium-dependent vasodilation of the femoral PNA via augmented nitric oxide production [90]. As is expected given the divergent effects of intermittent and continuous PTH on bone mass, the effect of PTH on bone vasculature is dependent on the time-course of PTH administration. In a recent study, intermittent PTH stimulated bone formation and prevented OVX-induced reduction in bone perfusion and bone vessel density, while continuous PTH resulted in a decrease in vessel size [110]. Another study showed that treatment with teriparatide resulted an increase in bone blood flow, evaluated for up to 18 months [155]. Although secondary hyperparathyroidism is prevalent in CKD and has been implicated as one of the factors that results in skeletal deterioration in CKD, the potential effects of PTH on skeletal blood flow and the consequential deterioration of skeletal health have not been studied in CKD. Chronic elevations in parathyroid hormone (PTH) may drive altered bone vascular properties in CKD. In a rat model of CKD, we and others have shown that sustained elevated PTH contributes to high bone remodeling which drives increases in cortical porosity and ultimately compromised bone mechanics [156,157]. Moreover, the role of PTH in modulating vasculature, including that of the bone, has been well-established in the literature [91,110,158,159]. Based on

this, and the above established scientific premise, the goal of the present series of studies is to test the hypothesis that chronic elevations in PTH drive maladaptive changes to the skeletal vasculature that contribute to the skeletal manifestations in CKD.

CKD is a systemic disease that is known to detrimentally alter both the vascular and skeletal systems, and potentially also the bone vascular system. **Figure 1-4** illustrates the potential relationships between systemic disease, vascular disease, skeletal disease, and alterations to the bone vascular network. Understanding the underlying mechanisms of bone vascular alterations due to the sequelae of reduced kidney function, including mechanisms that overlap with cardiovascular and skeletal alterations, is crucial to developing novel ways to reduce mortality in CKD patients.

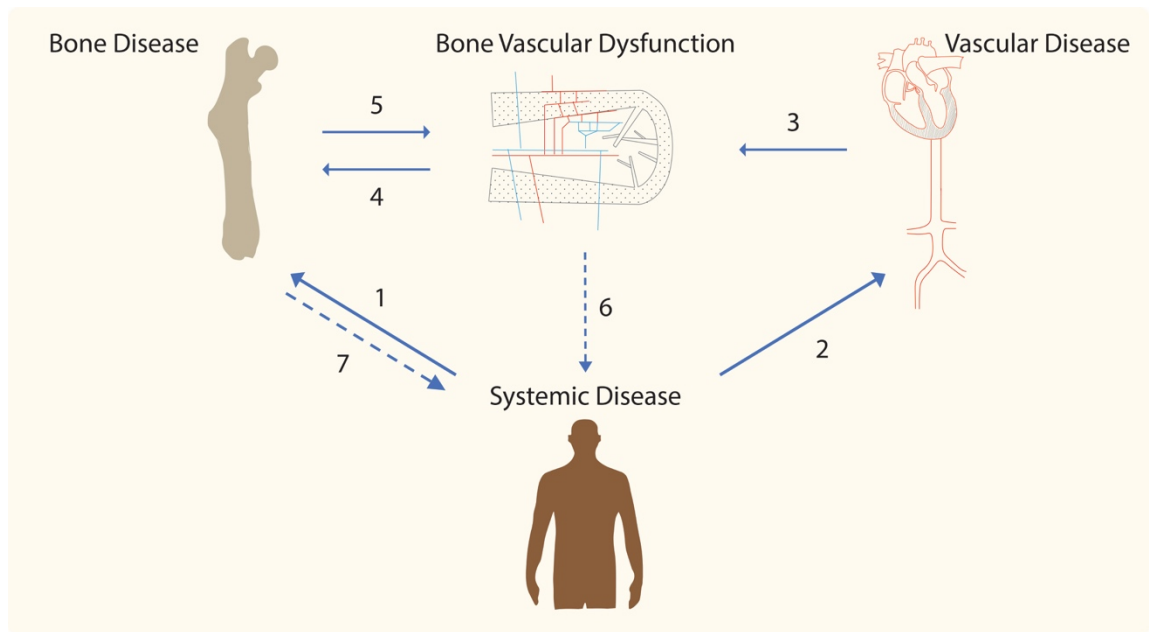


**Figure 1-4:** Bone vascular dysfunction and bone disease.

1. Systemic diseases can affect bone health, structure, and function
2. Systemic diseases can affect vascular health, structure, and function
3. Vascular disease/dysfunction/disturbances can result in bone vascular disease/dysfunction/disturbances
4. Bone vascular disease/dysfunction/disturbances can cause/play a role in bone disease
5. Bone disease can cause bone vascular alterations (that can then play a role in bone disease - 4)
6. Disturbances to bone vascular network can result in altered marrow health that can contribute to systemic pathophysiology
7. Bone diseases can cause mineral disorders that can contribute to systemic pathophysiology

## CHAPTER 2

### ASSESSMENT OF REGIONAL BONE TISSUE PERFUSION IN RATS USING FLOURESCENT MICROSPHERES

#### **Introduction**

Bone blood flow plays a crucial role in bone growth [75], fracture repair [76-78], and bone homeostasis [79,80]. Disturbances to bone blood flow have been shown to have deleterious effects on bone health and function [79,83-85,87] yet there remain many unanswered questions about skeletal perfusion in health and disease, partially due to the complexity of measurement methodologies [80].

Radioactive microspheres were long considered the experimental gold standard for the determination of skeletal perfusion [80] due to their accuracy and ease of analysis [119]. Upon injection into the animal, microspheres lodge in tissue capillaries in direct proportion to the fraction of cardiac output perfusing the tissue [80]. Tissue analysis is relatively straightforward, even for mineralized tissue, in that once tissues of interest are harvested, blood flow is estimated via a gamma spectrometer with minimal tissue processing [83,85,120,121]. Various limitations of radioactive microspheres, including cost, health risks, and the necessity for precautions with use and disposal [122], have resulted in exploration of alternative methods.

Fluorescent microspheres, which work on the same principal as radioactive spheres in that they become entrapped within capillaries, have been shown to allow measurement of organ perfusion as effectively as radioactive

microspheres [122]. Analysis of fluorescent microspheres requires degradation and filtration of the tissues of interest before the samples can be analyzed and has been effectively used in numerous soft tissue across multiple species [119,122-125]. Processing of skeletal tissue presents more challenges for fluorescent microspheres compared to soft tissue, perhaps helping to explain why fluorescent sphere data exists only for mice [126] and rabbits [119].

In the present study, we sought to use fluorescent microspheres in rats to assess regional bone perfusion. The goal was to adapt a fluorescent microsphere protocol used in mice [126] to determine the variability of skeletal perfusion both within and among a set of normal rats, as well as to test various perturbations in experimental methodology.

## **Methods**

### *Microsphere storage and fluorescence decay*

In order to determine characteristics of the microspheres, several perturbations in storage and analyses were carried out prior to animal experiments. The effect of different methods of storage on fluorescence quantification was examined by placing a known amount of microspheres (50,000 beads in 0.05mL) in either phosphate buffered saline (PBS) or ethanol (EtOH). Additional sets of microspheres were placed in PBS and frozen at -4C or -20C. Finally, the stability of fluorescence over time after being released from the microspheres was measured over 10 days.

## *Animals*

Fifteen-week old male Sprague Dawley rats (n=10) were used for this study. All procedures were approved by the Indiana University School of Medicine Animal Care and Use Committee prior to initiating the study.

## *Microsphere injection*

Polystyrene, red fluorescent (580/605), 15  $\mu\text{m}$  microspheres (FluoSpheres, ThermoFisher), were used for blood flow determination. Microsphere injection in half of the rats (n=5) was performed as previously described with minor adaptations for rats [126]. The process is summarized and illustrated in **Figure 2-1**. Briefly, under isoflurane anesthesia, the chest cavity was opened to allow visualization of the heart. A 2.5 mL solution of microspheres (containing one million spheres/mL) was injected in the apex of the left ventricle of the beating heart. The spheres were allowed to circulate for 60 seconds before the animal was euthanized and tissues collected. The number of microspheres injected was based, on a mg/kg basis, off of using  $2 \times 10^5$  microspheres for a 43g mouse which works out to  $4.65 \times 10^6$  spheres/kg; we rounded up to  $5.0 \times 10^6$  spheres/kg for ease [126]. A pilot study was done to verify that the number of spheres entrapped in bone vasculature using a 2.5 million sphere injection was within the generated standard curve used to estimate microsphere number. Due to the potential variability of cardiac function after opening the chest cavity, another five rats were administered a similar number of microspheres (2.5



million) via a tail vein catheter. For these animals, microspheres were allowed to circulate for 5 minutes before the rats were euthanized and tissues collected.

## Bone Blood Flow Measurement using Fluorescent Microspheres

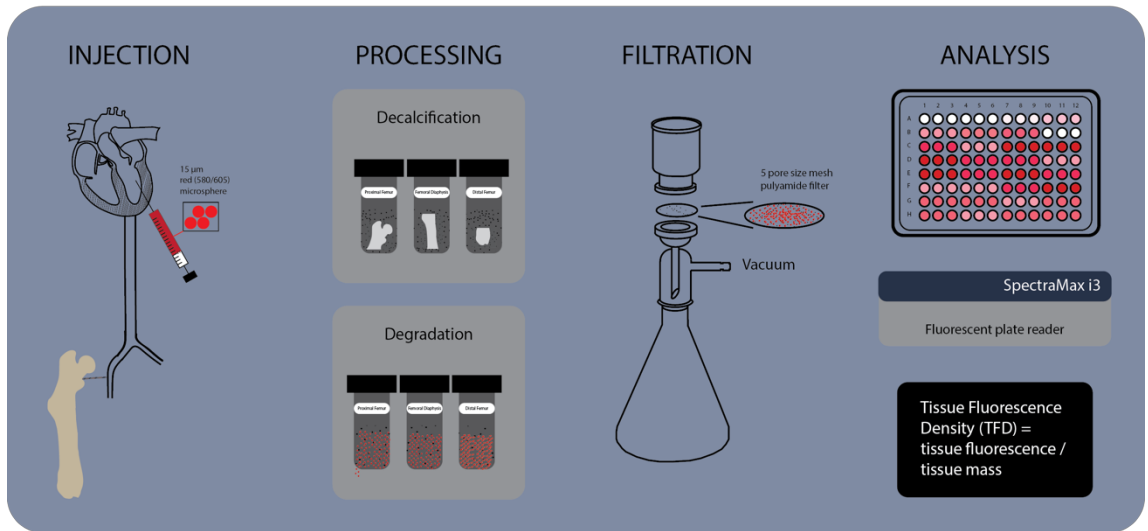


**Figure 2-1:** Graphical depiction of microsphere protocol including microsphere injection, tissue processing and fluorescence quantification.

### *Sample Processing*

Femur and tibia samples were divided into proximal, middle (diaphysis), and distal segments as previously described [83]. Marrow was left intact in all bone specimens. Bone samples were placed in individual amber vials with 15mL of Cal-Ex Decalcifier solution. After 4 days, decalcified bone samples were placed in 5% ethanolic potassium hydroxide for degradation. Samples were vortexed every 24 hours to ensure complete degradation. After 96 hours of degradation, samples were filtered through polyamide mesh filters (5  $\mu\text{m}$  pore size). 1mL of Cellosolve acetate (2-ethoxyethyl acetate, 98%, Sigma, cat. no. 109967) was added to each of the filtered samples to break the microspheres open and expose the fluorescence.

### *Fluorescence quantification*

All fluorescence measurements were made using the SpectraMax i3x microplate reader (Molecular Devices, CA). Three 100 $\mu\text{L}$  aliquots from each sample were placed in a 96-well microplate for fluorescence quantification. Red fluorescence was measured using an excitation of 580nm and an emission of 620nm. Standard curves of serial dilutions with known amounts of microspheres were generated on the day of analysis. Standard curves generated were used to approximate the number of spheres in a given sample. All data is presented as tissue fluorescence density (TFD) as AU/g and scaled by  $10^6$ .

### *Statistical Analysis*

All analyses were performed using the Statistics Toolbox in MATLAB software. Paired student t-tests were utilized to compare right and left TFD measurements of the femora and tibiae. *A priori*  $\alpha$ -levels were set at 0.05 to determine significance. Coefficients of variation (CV) were calculated within each bone segment (using data from both right and left limbs; n=10).

### **Results**

Neither storage of intact microspheres in EtOH or freezing temperatures for 24 hours altered fluorescence of the spheres compared to recommended storage in PBS (**Figure 2-2A**). Furthermore, measurement of fluorescence showed no decay after 4 or 10 days relative to measures taken immediately after fluorescence release (**Figure 2-2B**).

Tissue fluorescence density (TFD) data for the various regions of femora and tibia from animals administered microspheres through the left ventricle are presented in **Table 2-1**. Right and left total femoral TFD ( $2.77 \pm 0.38$  and  $2.70 \pm 0.24$ , respectively) from animals with microspheres injected in the left ventricle were not significantly different ( $p=0.75$ ). Right and left tibial TFD ( $1.11 \pm 0.26$  and  $1.08 \pm 0.34$ , respectively) were also not different ( $p=0.59$ ). The coefficient of variation (CV) of TFDs among the five animals was 10.95% and 26.06% for the femur and tibia, respectively. Partitioning of the tissue perfusion into three segments along the length of the bone showed the proximal femur received  $27.30 \pm 4.04\%$ , the distal femur  $51.34 \pm 7.97\%$ , and the femoral diaphysis  $21.36$

$\pm 6.68\%$  of total femoral perfusion (**Figure 2-3**). The tibia partitioning showed proximal tibia received  $68.77 \pm 5.86\%$ , the distal tibia  $10.68 \pm 4.18\%$ , and the tibial diaphysis  $20.55 \pm 5.86\%$  of total tibial perfusion. Bone segment masses are presented in Supplementary Table 1.

Tail vein injection resulted in unacceptably low levels of tibia perfusion (TFD) in the tibia from 4 of the 5 animals (**Table 2-2**). Analyses of femora from these animals was not undertaken.

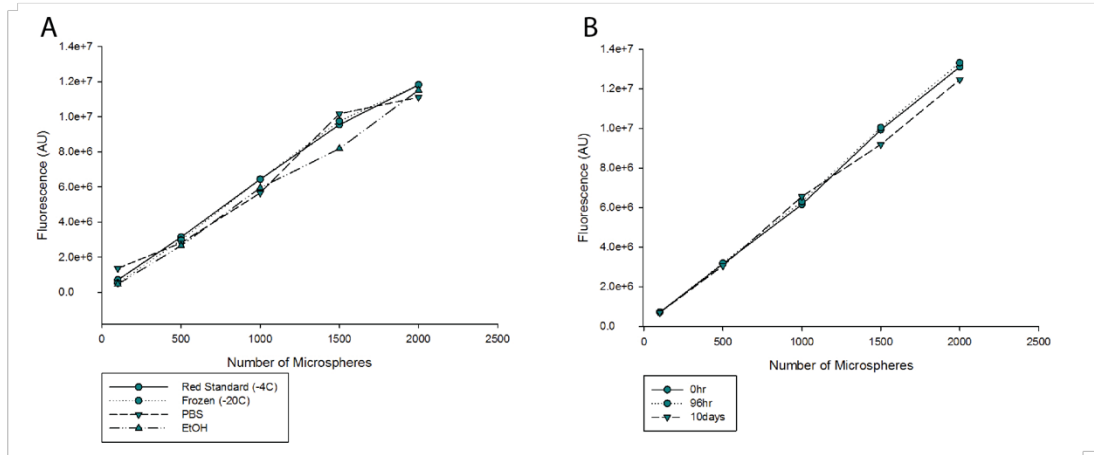


**Figure 2-2:** Microsphere standard curves displayed as bead quantity and fluorescence. (A) Effects of storage conditions. (B) Effects of time.

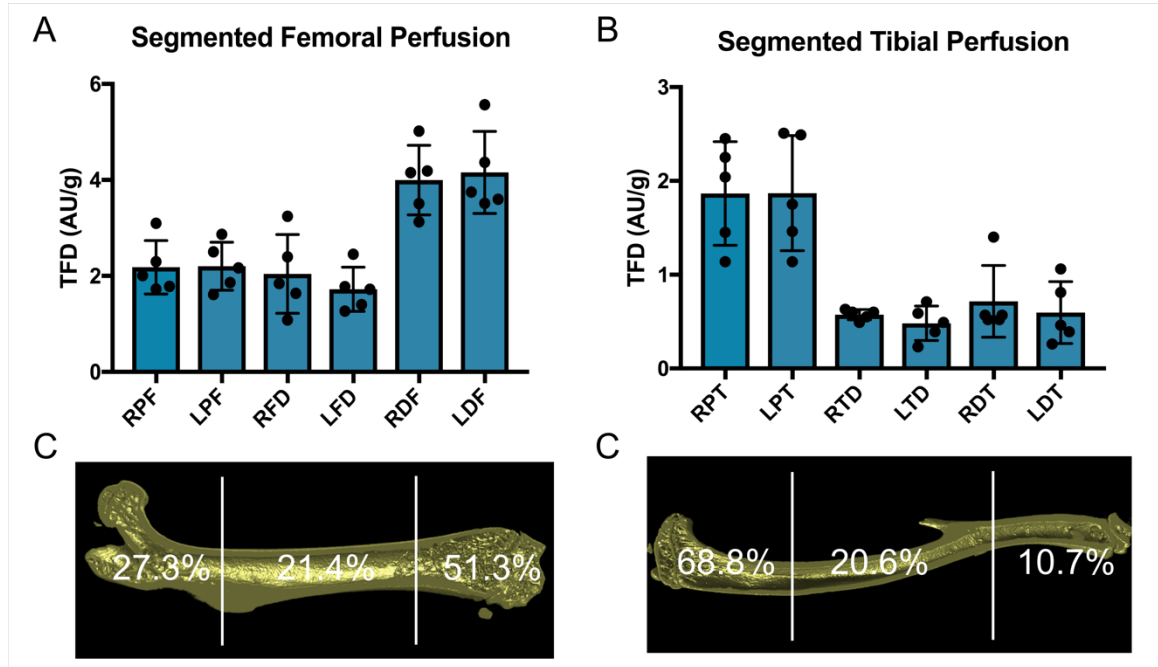


**Figure 2-3:** Tissue fluorescent density (TFD) of segmented femur (A,C) and tibia (B,D). RPF, Right proximal femur; LPF, Left proximal femur; RFD, Right femoral diaphysis; LFD, Left femoral diaphysis; RDF, Right distal femur; LDF, Left distal femur; RPT, Right proximal tibia; LPT, Left proximal tibia; RTD, Right tibial diaphysis; LTD, Left tibial diaphysis; RDT, Right distal tibia; LDT, Left distal tibia.. Data presented as means and standard deviations.

## **Discussion**

The importance of bone blood flow in skeletal health, and its role in disease has been established through several preclinical experiments. Although, the gold standard for bone blood flow measurement has been the injection of radioactive microspheres, fluorescent microspheres have been established as a safer and equally effective technique for non-skeletal tissues (such as lung, kidney, and brain). Measures of bone blood flow using fluorescent microspheres presents challenges due to the difficulty of imaging through mineralized tissue and the technical difficulty of current microsphere assays, especially in small animals. The current work extends the use of fluorescent microspheres, described in detail for mice [126], to assess bone perfusion in rats.

Although the use of fluorescent microspheres has been well detailed in mice [126], some protocol adaptations were needed to measure fluorescent microspheres in rat. A larger absolute number of microspheres was used based on the recommendation of approximately 5 million spheres per kg of body weight used successfully in mice [126]. Due to larger volume of tissue in rat compared to mouse, larger volumes of ethanolic KOH were needed to degrade the tissue. Segments of bone were placed in 15mL of 10% ethanolic KOH (vs 8mL of 3% ethanolic KOH in mice). Also due to the larger tissue volume, a larger vacuum filtration apparatus was necessary to filter the degraded samples. Degraded samples were filtered through 47mm polyamide filters (versus 25mm filters used in mice).



Our results on tibia and femoral perfusion match closely with previous reports examining values across these two bones as well as regionally within each bone. The ratio of femoral to tibial perfusion reported in the current work matches the results of previous studies performed using microspheres in rats [160] [112] and dogs [161]. The percentage of tissue perfusion to the different segments of the femur and tibia reported in our work also match values using radioactive microspheres showing highest flow in distal femur and proximal tibia [162]. This congruence with previous work lends support to the viability of the fluorescent microsphere technique for assessing bone perfusion in rats.

Many regional organ perfusion protocols using microspheres require technically challenging surgical techniques including catheter placement into the left ventricle to inject microspheres, and another catheter placement in the carotid artery or the tail artery to collect a reference blood sample. These techniques are further complicated when performed in rodents, given the smaller size of vessels. Because of potential variability in several steps of the sphere administration process, it is worthwhile to find an alternative way to assure adequate spheres are administered. The use of blood as a reference tissue has been used extensively, but other protocols have used organs as the reference tissue [126]. The advantage of using an organ as a reference tissue is it eliminates the need for catheter placement in vessels while the animal is alive. While this will work for interventions that are isolated (such as limb cooling used in the mouse protocol [126]), our end-goal of this work is to study skeletal

perfusion in the context of systemic disease which will likely affect blood flow systemically (and potentially differently across skeletal sites).

In the current study, microspheres were injection into the left ventricle after opening the chest cavity while the animal was under anesthesia as a terminal procedure. Variability in cardiac function before the animal is euthanized due to invasion of the chest cavity was not assessed in the present study and could account for variability among animals. In an attempt to reduce this variability, injections were performed in the tail vein for a subset of animals in order to allow the animal to maintain normal cardiac function to distribute the spheres systemically. Although it was assumed that spheres would be entrapped in the pulmonary capillaries, if enough microspheres passed through to the arterial system, bone perfusion could be measured while also preserving cardiac function. Our results clearly showed that microsphere entrapment in bone was insufficient for reliable measure and thus this is not a viable method of administration.

In the present study, we have shown that the injection of fluorescent microspheres in the left ventricle of rats is an effective method for the estimation of bone perfusion. However, there are a number of limitations to this study. Due to the fact that we did not collect a blood sample during injection, we are unable to calculate an estimated flow rate to bone. Although a flow rate provides an easily interpretable value (mLs per minute per tissue weight), it is worth noting that collection of reference blood from the tail artery, as many do [163] [164], likely underestimates the concentration of spheres in organs since it is distal to a

majority of the arterial tree including highly vascularized tissue including the brain and kidneys. Another limitation to our study is the lack of hemodynamic stability during the microsphere injection procedure and microsphere circulation. The animals are anesthetized using isoflurane, which is known to affect organ perfusion [165] and cardiovascular dynamics [166]. Finally, without the use of assisted ventilation, this is a terminal procedure and does not allow for the serial injection of microspheres for the evaluation of longitudinal change in skeletal perfusion. This could be overcome by administration of spheres via prolonged or repeated catheterization if longitudinal measures are of interest.

Although the use of fluorescent microspheres is emerging as an accepted alternative to radioactive microspheres as a method for the measurement of blood flow, and some papers have used the technique to examine bone, there has yet to be a study to assess these techniques in rats. The current work fills this void by showing the viability of injection and analysis of fluorescent microspheres to assess regional bone tissue perfusion in rats.

**Tables**

**Table 2-1:** Tissue fluorescence density in the femur and tibia following intra-cardiac injection of microspheres

Femur								
	Proximal		Diaphysis		Distal		Total	
Animal	Right	Left	Right	Left	Right	Left	Right	Left
1	2.01	2.17	1.08	1.27	5.02	5.57	2.73	2.80
2	1.78	1.86	2.40	1.40	4.19	4.37	2.77	2.63
3	2.30	2.87	1.64	1.72	4.15	3.75	2.84	2.90
4	3.10	2.50	3.24	2.45	3.51	3.51	3.28	2.83
5	1.73	1.61	1.84	1.78	3.13	3.60	2.22	2.31
Mean	2.18	2.20	2.04	1.72	4.00	4.16	2.77	2.70
Stdev	0.56	0.50	0.82	0.46	0.72	0.86	0.38	0.24
CV	0.23		0.34		0.18		0.11	
Tibia								
	Proximal		Diaphysis		Distal		Total	
Animal	Right	Left	Right	Left	Right	Left	Right	Left
1	2.45	2.51	0.63	0.39	1.40	1.06	1.51	1.37
2	2.25	2.49	0.49	0.59	0.57	0.81	1.13	1.44
3	1.14	1.46	0.60	0.49	0.52	0.46	0.81	0.87
4	2.04	1.14	0.55	0.23	0.52	0.26	1.12	0.63
5	1.45	1.75	0.60	0.71	0.57	0.39	0.96	1.10
Mean	1.87	1.87	0.57	0.48	0.72	0.60	1.11	1.08
Stdev	0.55	0.61	0.06	0.19	0.38	0.33	0.26	0.34
CV	0.29		0.26		0.52		0.26	

Tissue fluorescence density (TFD) data presented as AU/g and scaled by  $10^6$ . CV = coefficient of variation among right and left (combined together so n=10 specimens per CV) bone segments across all five animals.

**Table 2-2:** Tibia tissue fluorescence density following cardiac versus tail vein microsphere injection

Animal	Cardiac injection		Animal	Tail injection	
	Right tibia	Left tibia		Right tibia	Left tibia
1	1.51	1.37	6	1.04	1.34
2	1.13	1.44	7	0.04	0.02
3	0.81	0.87	8	0.03	0.01
4	1.12	0.63	9	0.02	0.01
5	0.96	1.10	10	0.03	0.02
Mean	1.11	1.08		0.23	0.28
Stdev	0.26	0.34		0.45	0.59

Tissue fluorescence density (TFD) data presented as AU/g and scaled by  $10^6$

## Supplemental Tables

**Supplemental Table 2-1: Femur and tibia mass data (in grams)**

Femur								
	Proximal		Diaphysis		Distal		Total	
Animal	Right	Left	Right	Left	Right	Left	Right	Left
1	0.32	0.38	0.32	0.33	0.33	0.27	0.98	0.98
2	0.54	0.46	0.42	0.52	0.49	0.57	1.45	1.55
3	0.61	0.46	0.37	0.41	0.6	0.59	1.59	1.46
4	0.51	0.48	0.46	0.48	0.51	0.5	1.49	1.46
5	0.53	0.47	0.46	0.51	0.48	0.47	1.47	1.44
Tibia								
	Proximal		Diaphysis		Distal		Total	
Animal	Right	Left	Right	Left	Right	Left	Right	Left
1	0.27	0.28	0.27	0.28	0.15	0.15	0.69	0.72
2	0.23	0.3	0.29	0.28	0.13	0.12	0.65	0.71
3	0.37	0.36	0.4	0.39	0.13	0.16	0.91	0.91
4	0.32	0.39	0.36	0.34	0.15	0.16	0.83	0.9
5	0.44	0.42	0.42	0.36	0.16	0.19	1.02	0.97

Mass data presented in grams.

## CHAPTER 3

### SKELETAL VASCULAR PERFUSION IS ALTERED IN CHRONIC KIDNEY DISEASE

#### **Introduction**

Patients with chronic kidney disease (CKD) have accelerated bone loss, vascular calcification and abnormal biochemistries. Together, these factors contribute to patients being at an alarming risk of cardiovascular disease and fracture-associated mortality [167]. In CKD patients, the risk of cardiovascular disease is increased 3 to 100-fold [168] and the risk of fracture 4 to 14-fold [169] compared to the normal population. These risks rise progressively as kidney function deteriorates. More striking, cardiovascular disease accounts for nearly 60% of deaths in those with CKD (compared to 28% in the normal population); similarly over 60% of CKD patients that sustain a hip fracture die within a year (compared to 20% in the normal population) [2]. These striking statistics emphasize the critical need to better understand the underlying mechanism driving altered cardiovascular and skeletal homeostasis, as well as any potential connection between the two.

Bone is a highly vascularized tissue and bone perfusion plays a crucial role in bone growth [75], fracture repair [76-78], and bone homeostasis [79,80]. Disturbances to bone blood flow have been shown to have associated effects on bone health and function [79,82-85]. Conditions that alter bone remodeling (diabetes, disuse, aging, estrogen withdrawal, anabolic drug treatment) have all been associated with changes in bone blood flow [82,83,86-91]. Moreover,

disturbances to bone vasculature, due to any of a number of causes, result in alterations in tissue perfusion [92] and often bone loss [93]. CKD-induced elevations in uremic toxins have long been associated with vascular dysfunction of multiple arterial beds through endothelium-dependent, endothelium-independent and/or vascular remodeling mechanisms [139-142]. In patients with CKD, decreased cardiac output [129], vascular calcification [130], and endothelial dysfunction [131-133] could all contribute to altered end-organ perfusion. Surprisingly data describing alterations in skeletal vascular perfusion in the setting of CKD are lacking.

The goal of the present study was to test the hypothesis that skeletal perfusion is altered in the setting of CKD. To accomplish this goal, we utilized fluorescent microspheres, which lodge in tissue capillaries in direct proportion to the fraction of cardiac output perfusing the tissue. This technique has been shown to allow measurement of organ perfusion as effectively as radioactive microspheres [122], the experimental gold standard [80], and has recently been applied to study skeletal perfusion in rats [170].

## **Methods**

### *Animals*

Male Cy/+ rats, Han:SPRD rats (n=12) with autosomal dominant polycystic kidney disease [171], and their unaffected (normal) littermates (n=12) were used for this study. Male heterozygous rats (Cy/ +) develop characteristics of CKD around 10 weeks of age that progress to terminal uremia by about 40



weeks. Our laboratory has demonstrated that this animal model recapitulates all three manifestations of CKD-Mineral and Bone Disorder (CKD-MBD) - biochemical abnormalities, extraskeletal calcification, and abnormal bone [72,73,171]. There are many other animal models of the systemic repercussions of kidney disease, but unlike the Cy/+ model, most animal models of CKD are either acute injury or developmental/growth alterations and do not model the effect of the progressive nature of CKD on mineral metabolism. The model utilized in the current study (the Cy/+ rat) avoids this drawback. All animals were fed a casein diet (Purina AIN-76A, Purina Animal Nutrition, Shreevport, LA, USA); 0.53% Ca and 0.56% P) from 24 weeks on during the experiment, which has been shown to produce a more consistent kidney disease in this model [171]. Blood was collected ~24 hours prior to the end of the study for measurement of plasma biochemistries. All procedures were reviewed and approved by the Indiana University School of Medicine Institutional Animal Care and Use Committee prior to study initiation.

### *Experiments*

CKD animals and their normal littermates were used in two separate studies, designed to assess alterations in two distinct time points along the progression of disease in the Cy/+ model:

Experiment 1 – 30 week time point (~25% normal kidney function). Normal (NL) and Cy/+ (CKD) animals (n=6/group) were assessed for serum biochemistries ~

one day before undergoing *in vivo* microsphere injection to assess bone tissue perfusion.

Experiment 2 – 35 week time point (~15% normal kidney function). Normal (NL) and Cy/+ (CKD) animals (n=6/group) were assessed for serum biochemistries ~ one day before undergoing *in vivo* microsphere injection to assess bone tissue perfusion.

These two separate experiments aimed to describe skeletal perfusion at 30 and 35 weeks were designed based on previous work demonstrating significant progression of skeletal disease in this timeframe [156,157]. While elevations in blood urea nitrogen (BUN) are noted by 25 weeks, progressive hyperphosphatemia, hyperparathyroidism, and skeletal abnormalities become evident by 30 weeks. Between 30 and 35 weeks there is marked progression of all of the end organ manifestations of CKD-MBD, including left ventricular hypertrophy, cardiac and vascular calcification, and severe high turnover bone disease evident by severe cortical porosity, high turnover and compromised mechanical properties [156,157,172,173].

#### *Bone perfusion measurement*

Microsphere injection was performed as previously described [170]. Briefly, under isoflurane anesthesia, polystyrene red fluorescent (580/605), 15 µm microspheres (FluoSpheres, ThermoFisher) were injected into the apex of the beating left ventricle after opening the chest cavity. The spheres were allowed to circulate for 60 seconds before the animal was euthanized by cardiac

dissection. A total of  $5.0 \times 10^6$  spheres/kg were injected, a number sufficient to assess perfusion in skeletal tissue [170].

Tibiae, femora, humeri, vertebrae (L4 body), kidneys and testes were collected and weighed. Testes were used as a positive control for assessing adequacy of microsphere delivery within each animal. Microsphere mixing and injection was considered adequate for an animal when right and left testicle perfusions were within 25% of each other. On the basis of this criterion, no animals were excluded from the study. Femur samples were divided into proximal, middle (diaphysis), and distal segments as previously described [83], and weighed separately. Right femoral diaphysis marrow was left intact in bone while left femoral diaphysis marrow was thoroughly flushed and femoral cortex was weighed. Marrow was extracted from the tibial diaphysis by centrifugation; both marrow and tibial cortex were weighed. Marrow was left intact in the remainder of all specimens.

Bone samples were placed in individual amber vials with 15mL of Cal-Ex Decalcifier solution. After 7 days, decalcified bone samples were placed in 10% ethanolic potassium hydroxide (KOH) for degradation. Soft tissue samples (kidney and testes) were placed in KOH directly. After 24 hours of degradation, samples were vortexed to complete the degradation process and then filtered through polyamide mesh filters (5  $\mu\text{m}$  pore size). 1mL of Cellosolve acetate (2-ethoxyethyl acetate, 98%, Sigma) was added to each of the filtered samples to dissolve the microspheres and expose the fluorescence. The 24 hour KOH degradation step differed from the original protocol [170], where samples were

degraded in KOH for 48 hours. This slight alteration was made based on developmental work in our lab showing 24 hours was sufficient for degradation with longer durations causing progressive decline in fluorescence.

All fluorescence measurements were made using the SpectraMax i3x microplate reader (Molecular Devices, CA). Three 100 $\mu$ L aliquots from each sample were placed in a 96-well V-bottom polypropylene microplate for fluorescence quantification. The readings from the three aliquots were averaged to produce a single fluorescence measurement per sample. Red fluorescence was measured using an excitation of 580nm and an emission of 620nm. Standard curves of serial dilutions with known amounts of microspheres were generated on the day of analysis. Fluorescent measurements of samples found to be outside the standard curve (kidneys) were serially diluted and measured in order to detect any potential quenching effects. All data is presented as tissue fluorescence density (TFD) with units of Arbitrary Units per gram of tissue (AU/g) and scaled by  $10^6$ .

### *Biochemistries*

Blood plasma was analyzed for blood urea nitrogen (BUN) and calcium using colorimetric assays (BioAssy System, DIUR-100). Intact PTH was determined by ELISA (Immutopics, REF-60-2500).

## *Statistical Analysis*

All analyses were performed using GraphPad Prism software. Student's t-tests were used to compare CKD and NL groups within each experiment. Pearson product correlations were used to assess relationships between BUN, PTH and tissue perfusion. *A priori*  $\alpha$ -levels were set at 0.05 to determine statistical significance.

## **Results**

### *Experiment 1: 30 week data*

There was no significant difference in body or bone mass between the two groups of animals (**Supplemental Tables 3-1** and **3-2**). Kidney mass was significantly higher in CKD due to cystic disease compared to age-matched normal littermates (NL) (**Supplemental Tables 3-2**). Plasma BUN, but not PTH, was significantly higher in CKD compared to age-matched normal littermates (NL), the former being consistent with reduced kidney function (**Table 3-1**). TFD was significantly higher in the femoral cortex (+259%,  $p < 0.05$ ) (**Figure 3-1A**) but not the tibial cortex (+140%,  $p = 0.11$ ) (**Figure 3-1B**) of CKD animals relative to NL. Isolated tibial marrow perfusion showed a trend toward being higher (+183%,  $p = 0.08$ ) in CKD compared to NL (**Figure 3-1C**). Vertebral body TFD was significantly higher in CKD animals (+116%,  $p < 0.05$ ) while neither distal femur (+109%,  $p = 0.18$ ) or humerus (+136%,  $p = 0.08$ ), significantly differed between groups (**Figure 3-1E-G**). These three bone sites all had intact marrow. Kidney perfusion was not significantly different in CKD animals when compared to their

normal littermates at 30 weeks ( $p=0.06$ ) (**Supplemental Table 3-3**). There were no scientifically significant correlations between PTH and TFD for either NL or CKD animals (data not shown).

**Table 3-1:** Serum biochemistries

Experiment 1 – 30 Weeks		
	NL	CKD
BUN, (mg/dL)	19.1 ± 1.7	39.7 ± 6.0*
PTH, (pg/mL)	376 ± 298	420 ± 378
Experiment 2 – 35 Weeks		
	NL	CKD
BUN, (mg/dL)	17.8 ± 1.9	50.4 ± 8.0*
PTH, (pg/mL)	123 ± 49	1305 ± 237*

Data presented as mean and standard deviation. \*p<0.05

*Experiment 2: 35 week data*

Animal body mass was significantly lower in CKD (-15%) compared to NL animals (**Supplemental Table 3-1**). Kidney mass was significantly higher and femoral diaphysis (with marrow) mass was significantly lower in CKD compared to age-matched normal littermates (NL) (**Supplemental Table 3-2**). Plasma BUN and PTH were both significantly higher in CKD compared to NL (**Table 3-1**). TFD in CKD animals was significantly higher in both the femoral cortex (+173%,  $p < 0.05$ ) (**Figure 3-2A**) and the tibial cortex (+241%,  $p < 0.05$ ) (**Figure 3-2B**) relative to NL. Isolated tibial marrow TFD was significantly lower (-57%,  $p < 0.05$ ) in CKD animals when compared to age-matched normal littermates (**Figure 3-2C**). Vertebral body perfusion (-71%,  $p < 0.05$ ) was significantly lower in CKD animals compared to NL while neither distal femur (-27%,  $p = 0.17$ ) or humerus (-10%,  $p = 0.95$ ) perfusions, both with marrow intact, were significantly different between groups (**Figure 3-2E-G**). Kidney perfusion was significantly lower in CKD animals when compared to their normal littermates ( $p < 0.05$ ) (**Supplemental Table 3-3**). There was no significant correlation between PTH and TFD for any site in the NL animals while 4 of the 6 sites assessed for TFD had significant negative relationships with PTH values (**Table 3-2**).



**Table 3-2:** 35 week correlations between PTH and tissue fluorescence density

	Femoral Cortex TFD	Tibial Cortex TFD	Tibial marrow TFD	Distal femur TFD	L4 TFD	Humerus TFD
PTH (NL)	0.337	-0.264	-0.617	0.294	0.465	0.465
PTH (CKD)	<b>-0.764</b>	<b>-0.772</b>	0.338	<b>-0.888</b>	0.653	<b>-0.724</b>

Data presented at r values with bolded values indicating  $p < 0.05$ .

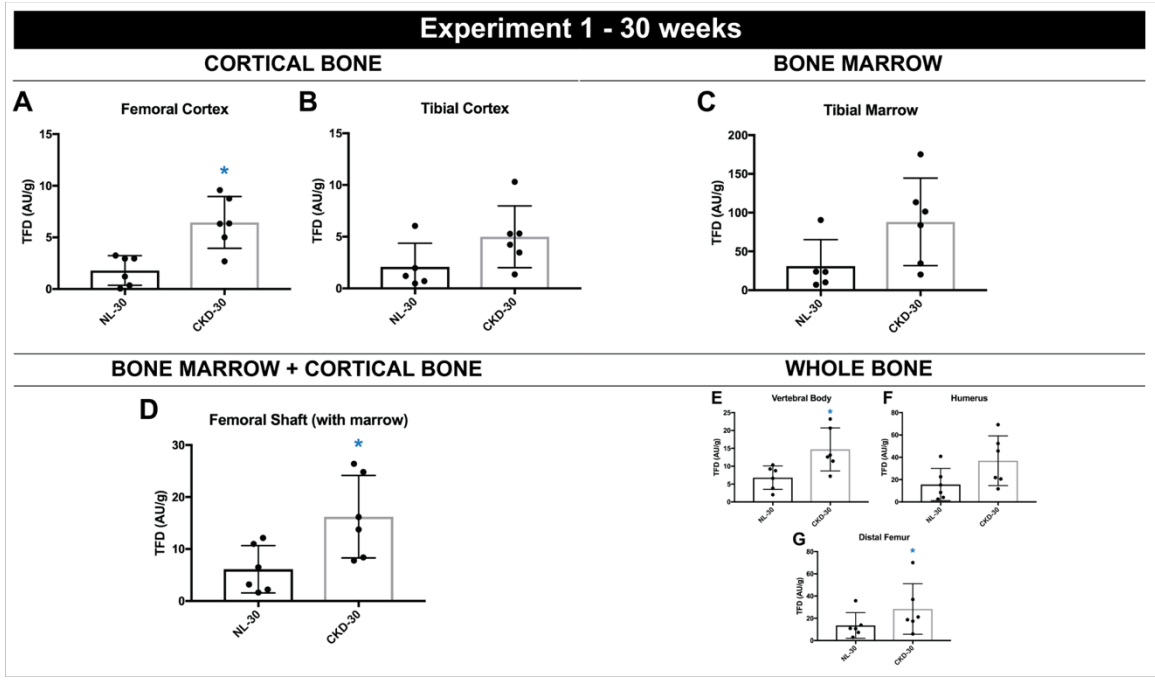


**Figure 3-1:** 30 week time point bone perfusion data (n=6/group). Tissue fluorescence density (TFD) of (A) femoral cortical bone (p<0.05) (B) tibial cortical bone (p=0.11) (C) tibial bone marrow (p=0.08) (D) femoral diaphysis including marrow (p<0.05) (E) L4 vertebral body (p<0.05) (F) humerus (p=0.08) and (G) distal femur (p=0.18). Dots represent data points, and error bars represent standard deviation.

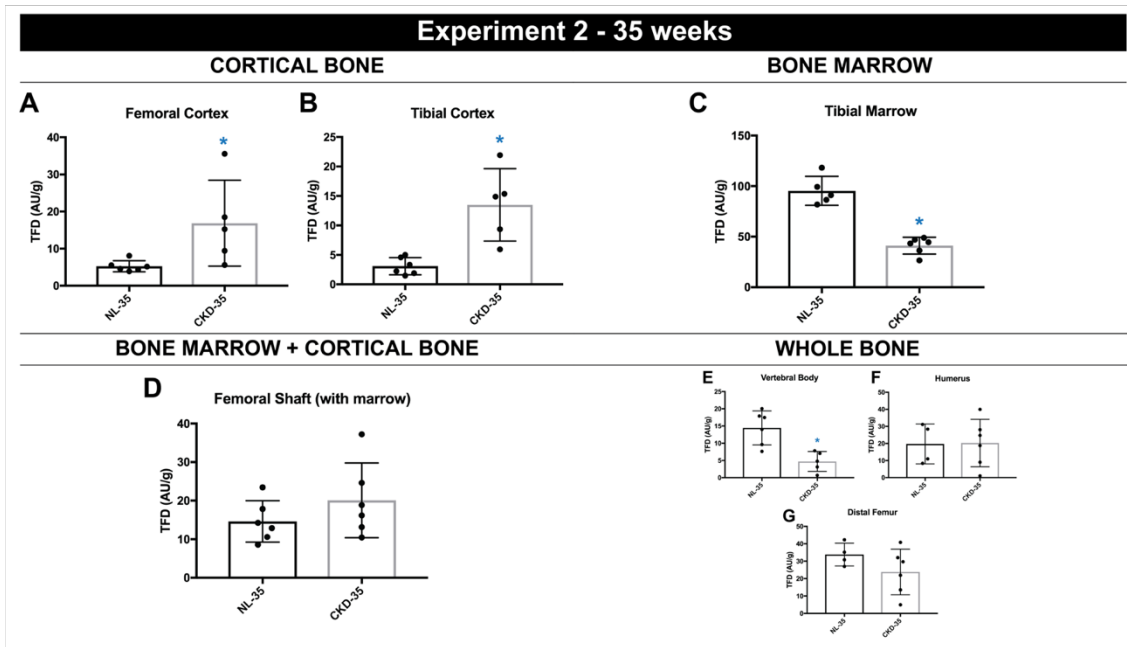


**Figure 3-2:** 35 week time point bone perfusion data (n=6/group). Tissue fluorescence density (TFD) of (A) femoral cortical bone (p<0.05) (B) tibial cortical bone (p<0.05) (C) tibial bone marrow (p<0.05) (D) femoral diaphysis including marrow (p<0.05) (E) L4 vertebral body (p<0.05) (F) humerus (p=0.95) and (G) distal femur (p=0.17). Dots represent data points, and error bars represent standard deviation.

## **Discussion**

Deterioration of both bone and cardiovascular properties have been well documented during the progression of CKD. Bone is a highly vascularized tissue that depends on regulated perfusion for growth, repair, and homeostasis [81] . Since CKD is known to be associated with both cardiac and vascular abnormalities, the investigation of skeletal perfusion in the setting of CKD could provide insights into the pathophysiology of abnormal bone in CKD. The current study demonstrates two findings regarding bone perfusion in an animal model of high turnover CKD. First, cortical bone perfusion is higher than it is in animals with normal kidney function. Second, changes in bone marrow perfusion are more complex than those of bone, with higher perfusion early in disease and lower levels with prolonged/late stage disease. The differential changes in bone and marrow perfusion likely account for the more modest differences between CKD and NL in bone segments containing both tissues (**Figures 3-1 and 3-2**). The opposite trends of cortical bone and bone marrow and the proportional amount and type of marrow in each of the tested whole bones may play a role in the unclear trend observed in whole bone at 35 weeks.

Using fluorescent microspheres to measure regional bone perfusion, we show that animals with high turnover CKD have higher cortical bone perfusion at both 30 and 35 weeks compared to normal. Despite evidence of vascular pathologies in the current model [171-173] and known vascular dysfunction in CKD [15,144,145], we show that cortical bone perfusion in isolated femoral and tibia cortical bone diaphyses is nonetheless higher. We hypothesize that this

elevated cortical perfusion is due to one, or a combination, of two separate mechanisms. Cortical perfusion may be increased in response to increased metabolic needs of high turnover CKD bone, necessitating endothelial cells to express vasoactive substances that increase tissue blood flow [174].

Alternatively, PTH has been shown to have direct effects on the endothelial expression of vascular endothelial growth factor [175] such that worsening secondary hyperparathyroidism could be driving increased perfusion.

Conditions that alter bone remodeling (diabetes, disuse, aging, estrogen withdrawal, anabolic drug treatment) have all been associated with changes in bone blood flow [82,83,86-91]. Previous work has demonstrated that changes in perfusion can precede alterations to bone structure and function in these models. Increased perfusion occurs prior to fatigue loading-induced addition of bone mass [176]. By 30 weeks in this model Cy/+ rats have significant elevations in bone remodeling on trabecular bone surfaces whereas by 35 weeks they not only have high remodeling but also significant increases in intracortical remodeling and peritrabecular fibrosis. Previous work from our group suggests the escalation of skeletal deterioration in terms of increased turnover, impaired mechanics, cortical porosity, loss of cortical mass, and increased marrow fibrosis in the Cy/+ rat model between the two time points evaluated in this study – 30 and 35 weeks [157,177]. Further investigations will be needed to determine whether blood flow changes are driven by metabolic demands in CKD and whether these drive the skeletal phenotype (cortical porosity) or whether the bone and/or marrow changes alter the vascular perfusion.

In the setting of CKD, we and others have shown that sustained elevated PTH contributes to high bone remodeling which drives increases in cortical porosity and ultimately compromised bone mechanics [156,157] but its contribution in vascular perfusion in CKD is unknown. The direct role of PTH in modulating vasculature, including that of the bone, has been well-established in the literature [91,110,158,159]. Early studies illustrated the acute effects of intravenous injection of PTH to increase tibial and femoral perfusion within 30 minutes after administration of intravenous PTH [178]. This suggested a vasodilatory effect that was confirmed in a recent study that showed PTH enhanced endothelium-dependent vasodilation of the femoral principal nutrient artery via augmented nitric oxide production [90]. Both of these studies represent acute PTH, and the effects of chronic elevation of PTH as seen in CKD may be different, given the divergent effects of intermittent and continuous PTH on bone mass. Roche et al found intermittent PTH stimulated bone formation and prevented OVX-induced reduction in bone perfusion and bone vessel density, while continuous PTH resulted in a decrease in vessel size [110]. Another study showed that treatment with teriparatide resulted an increase in bone blood flow, evaluated for up to 18 months [155]. Our correlation analysis of PTH and tissue perfusion resulted in an unexpected strong negative relationship between PTH and tissue perfusion across multiple bones. While these data cannot speak to cause/effect, they provide a basis for future hypotheses that can fuel studies aimed at dissecting the role of PTH levels in CKD-related skeletal perfusion changes.

Patterns of marrow perfusion (marrow having been extracted from the diaphyseal region only) in CKD animals diverged from those of cortical bone in late-stage high turnover disease. Although CKD animals show no change to marrow perfusion (trending towards higher) in the 30 week time point there was significantly lower perfusion at 35-weeks compared to NL animals. This is in contrast to cortical bone perfusion which was significantly higher in CKD animals at both of the time points. Previous work from our group has demonstrated lower levels of VEGF-A expression in bone marrow of 35-week old CKD animals compared to their normal littermates [107]. These suggest there may either be a dramatic shift in marrow VEGF signaling or marrow content during the later-stage manifestation of CKD. Given the known fibrosis that occurs with the severe hyperparathyroid bone disease osteitis fibrosis cystica this may have decreased the overall non-fibrotic marrow in the 35 weeks animals. An alternative explanation is that more severe cardiac dysfunction due to heart calcification or aorta calcification may limit the ability to perfuse distal organs such as bone at late stage CKD [173].

Our results should be interpreted in the context of various assumptions and limitations. Injection of microspheres in the left ventricle to assess perfusion is based on a set of assumptions, including: microspheres are homogeneously distributed in the left ventricle, trapped in capillaries on first passage with no shunting or dislodging, and do not themselves alter the hemodynamics upon injection. This is the same set of assumptions made in any blood flow measurement using microspheres, the current experimental gold standard for the

determination of skeletal perfusion. A recovery standard was not utilized in order to ensure that sample is not lost during processing. The animals are anesthetized using isoflurane, which is known to affect organ perfusion [165] and cardiovascular dynamics [166]. Without the use of assisted ventilation, the open-chest cardiac injection of microspheres is performed under diminishing physiologic hemodynamic, as well as hypoxic, conditions. Given that the time from anesthesia to injection is consistent in experiments at each time point, and the injected spheres are fully circulated within the 60 seconds between injection and euthanasia, declining kidney function is not a major factor in the differences detected by our perfusion measurements.

In conclusion, we have shown that bone perfusion is altered in an animal model of progressive high turnover chronic kidney disease. Determining whether these changes in bone perfusion are drivers, propagators, or consequences of skeletal deterioration in CKD will necessitate further work.



## Supplemental Tables

**Supplemental Table 3-1: Body Masses**

	30 weeks		35 weeks	
	NL	CKD	NL	CKD
Body Mass (grams)	541.3 ± 34.7	531.8 ± 15.1	590.2 ± 34.1	500.5 ± 68.5*

Data presented as mean and standard deviation. \*p<0.05

**Supplemental Table 3-2: Tissue Masses**

	Tissue Mass			
	30 weeks		35 weeks	
	NL	CKD	NL	CKD
Kidney (grams)	1.95 ± 0.10	3.27 ± 0.22*	1.79 ± 0.31	3.69 ± 1.07*
Tibial Cortex (grams)	0.19 ± 0.01	0.19 ± 0.02	0.21 ± 0.02	1.79 ± 0.31
Tibial Marrow (grams)	0.029 ± 0.01	0.031 ± 0.01	0.039 ± 0.01	0.038 ± 0.01
Femoral Cortex (grams)	0.34 ± 0.03	0.32 ± 0.04	0.28 ± 0.04	0.31 ± 0.02
Femoral Diaphysis (with marrow) (grams)	0.36 ± 0.02	0.35 ± 0.02	0.36 ± 0.02	0.31 ± 0.03*
Distal Femur (grams)	0.62 ± 0.03	0.63 ± 0.04	0.69 ± 0.04	0.65 ± 0.07
L4 – Vertebral Body (grams)	0.28 ± 0.04	0.25 ± 0.02	0.23 ± 0.05	0.23 ± 0.02
Humerus (grams)	0.72 ± 0.03	0.71 ± 0.04	0.73 ± 0.05	0.71 ± 0.23

Data presented as mean and standard deviation. \*p<0.05

**Supplemental Table 3-3: Kidney Perfusion**

	30 weeks		35 weeks	
	NL	CKD	NL	CKD
Kidney Perfusion (TFD)	562.5 ± 424.8	178.2 ± 106.0	1039.7 ± 259.3	66.1 ± 32.3*

Data presented as mean and standard deviation. \*p<0.05; TFD = tissue fluorescent density (AU/grams)

## CHAPTER 4

# SUPPRESSION OF PARATHYROID HORMONE NORMALIZES CHRONIC KIDNEY DISEASE-INDUCED ELEVATIONS IN CORTICAL BONE VASCULAR PERFUSION

### **Introduction**

Chronic kidney disease–mineral and bone disorder (CKD-MBD), consisting of accelerated bone loss, vascular calcification, and abnormal biochemistries [179], contributes to an increased risk of premature death due to cardiovascular disease and fracture-associated mortality [167]. Understanding the underlying mechanisms of cardiovascular and skeletal alterations due to the sequelae of reduced kidney function, including mechanisms that overlap between cardiovascular and skeletal alterations, is crucial to developing novel ways to reduce mortality in CKD patients.

Patients with CKD have vascular dysfunction through endothelium-dependent, endothelium-independent, and/or vascular remodeling mechanisms [139-142], along with decreased cardiac output [129], and vascular calcification [130], suggesting that altered skeletal perfusion can be expected in CKD. Bone health and homeostasis are dependent on regulated skeletal perfusion [81] and conditions that result in altered bone perfusion have been shown to be associated with bone loss [93]. Data from our lab have shown that cortical bone perfusion is elevated in a rat model of chronically high parathyroid hormone (PTH), high remodeling CKD [106]. However, whether vascular dysfunction and the bone abnormalities are related in CKD is not known.

Sustained elevation of serum PTH in the setting of CKD has been shown, by our group and others, to contribute to compromised bone quantity and quality via elevated bone turnover and increased cortical porosity [156,157]. Currently, the primary goal of CKD-MBD therapy is the suppression of elevated levels of PTH [180] utilizing calcitriol (and its analogues) and calcimimetics. Our group has previously shown that the suppression of PTH levels with calcium supplementation in drinking water in rodents substantially mitigates the deleterious effects of CKD on bone parameters, essentially normalizing bone turnover and mass [181,182]. Despite the consistent suppression of PTH levels and the positive skeletal effects, calcium supplementation has been shown to increase vascular calcification [157] and, therefore, is not a viable therapeutic option. Calcimimetics, such as the recently FDA-approved etelcalcitide, suppress PTH without contributing to increased vascular calcification in rodents [183]. For this reason, the present study utilizes both calcium supplementation and a calcimimetic to evaluate the effect of PTH suppression on cortical bone perfusion. We hypothesized that suppression of PTH would normalize CKD-induced elevations in cortical bone perfusion.

## **Methods**

### *Animals*

Male Cy/+ (CKD) rats, Han:SPRD rats are characterized with a spontaneous and slowly progressive kidney disease [171]. Blood urea nitrogen (BUN) and creatinine are elevated by 10 weeks of age. With progression of CKD,

hyperphosphatemia, hyperparathyroidism, and skeletal abnormalities develop and ultimately progress to dramatic manifestations of cardiac and vascular calcification as well as severe cortical porosity and compromised bone mechanical properties [72,73].

### *Experimental Design*

#### Experiment 1:

CKD animals (n=12) and their normal littermates (NL, n=6) were used to assess alterations in skeletal perfusion at 35 weeks of age (~15% normal kidney function in the Cy/+ model). The CKD treatment animals were divided into two groups (n=6/group) at 25 weeks of age: half were administered normal deionized drinking water (CKD) and the other half administered calcium gluconate (3% Ca) in the drinking water (CKD+Ca). The calcium gluconate was used as a phosphate binder with the goal of PTH suppression as shown previously [157]. Age-matched normal (NL) littermate animals (n=6) were used as a comparator group to determine if treatment normalized skeletal perfusion. All animals were fed a casein diet (Purina AIN-76A, Purina Animal Nutrition, Shreevport, LA, USA); 0.53% Ca and 0.56% P) during the experimental period (weeks 25-35), which has been shown to produce a more consistent kidney disease in this model [171]. At 35 weeks, all animals were assessed for serum biochemistries approximately 24 hours before undergoing *in vivo* microsphere injection to assess bone tissue perfusion. Tibiae, femora, and testes were collected for analyses.

## Experiment 2:

In order to differentiate the effects of PTH lowering from that of increased calcium intake, CKD animals (n=6) and their normal littermates (n=4) were used to assess the effect of KP-2326 (KP), an active metabolite of the calcimimetic etalcalcitide, on CKD-induced alterations in skeletal perfusion. The CKD treatment groups (n=3/group) were administered either vehicle injections thrice weekly or KP injection thrice weekly (i.p. 1mg/kg) from age 25 to 35 weeks. At 35 weeks, all animals were assessed for serum biochemistries approximately 24 hours before undergoing *in vivo* microsphere injection to assess bone tissue perfusion. Tibiae were collected for analysis.

### *Plasma Biochemistries*

Blood plasma was analyzed for blood urea nitrogen (BUN), calcium, phosphorus, and creatinine using colorimetric assays (Point Scientific, Canton, MI, USA; or Sigma kits; Sigma, St. Louis, MO, USA). Intact PTH was determined by ELISA (Alpco, Salem, NH, USA).

### *Bone perfusion measurement*

Microsphere injection was performed as we previously described [170]. Briefly, under isoflurane anesthesia, polystyrene red fluorescent (580/605), 15  $\mu\text{m}$  microspheres (FluoSpheres, ThermoFisher) were injected into the apex of the beating left ventricle. The animal was euthanized by cardiac dissection 60 seconds after the completion of the injection, allowing for the circulation of

spheres. A total of  $5.0 \times 10^6$  spheres/kg were injected, a number sufficient to assess perfusion in skeletal tissue [170].

Tibiae, femora, and testes were collected and weighed. Microsphere mixing, injecting, and delivery of microspheres were considered adequate for an animal when right and left testicle perfusions were within 25% of each other. On the basis of this criterion, no animals were excluded from experiment 1 and testes collection/analyses were deemed unnecessary for experiment 2. Femoral diaphyses were isolated, thoroughly flushed of marrow, and weighed. Marrow was extracted from the tibial diaphysis by centrifugation; both marrow and tibial cortex were weighed. In Experiment 2, only the tibia was collected for perfusion analysis. The tibial cortex was isolated and marrow was separated by centrifugation.

Samples isolated for tissue perfusion measures were processed as previously described [170]. Briefly, bone samples were placed in a Cal-Ex Decalcifier solution for 7 days. Decalcified bone samples were degraded in 10% ethanolic potassium hydroxide (KOH) for 24 hours. Soft tissue samples (testes) were placed in KOH directly. Degraded samples were filtered through polyamide mesh filters (5  $\mu\text{m}$  pore size) and placed into microcentrifuge vials along with 1 mL of Cellosolve acetate (2-ethoxyethyl acetate, 98%, Sigma) to dissolve the microspheres and distribute the fluorescence into solution.

Fluorescence measurements were performed as previously described [170]. Briefly, three 100  $\mu\text{L}$  aliquots from each sample were placed in a 96-well V-bottom polypropylene microplate for fluorescence quantification using the



SpectraMax i3x microplate reader (Molecular Devices, CA). The readings from the three aliquots were averaged to produce a single fluorescence measurement per sample. Red fluorescence was measured using an excitation of 580nm and an emission of 620nm. All data is presented as tissue fluorescence density (TFD) with units of Arbitrary Units per gram of tissue (AU/g) and scaled by  $10^6$ .

### *$\mu$ CT Imaging*

Tibiae were scanned (Skyscan 1172, 6 micron resolution) to obtain cortical morphology at a standardized location (~2.5mm distal to the proximal growth plate). Cortical parameters included total cross-sectional area, bone area, marrow area, cortical thickness, and cortical porosity. Porosity was calculated as the percent of void area within the total cross sectional area ( $100 - BA/TA*100$ ). Nomenclature is reported in accordance with ASBMR guidelines [184].

### *Statistics*

All analyses were performed using GraphPad Prism software. Comparisons among groups were assessed by Kruskal-Wallis analysis of ranks with Dunn's multiple comparisons post-hoc tests when appropriate. A priori  $\alpha$ -levels were set at  $p \leq 0.05$  to determine statistical significance.

## **Results**

### *Plasma Biochemistries*

#### Experiment 1:

Animals with CKD had serum blood urea nitrogen (BUN) and PTH levels that were significantly higher than NL (+182% and +958%;  $p < 0.05$ ) (**Table 4-1**). CKD+Ca animals had BUN levels that were not different from CKD ( $p = 0.7922$ ), while PTH levels were significantly lower than CKD alone ( $p = 0.004$ ) and not different from NL (**Table 4-1**).

#### Experiment 2:

Animals with CKD had elevated serum blood urea nitrogen (BUN) and PTH levels compared to NL (+119% and +2700%), although due to variability and low sample size, the results did not reach statistical significance (**Table 4-1**). CKD+KP animals had BUN levels that were not different from CKD, while PTH levels were lower than CKD alone and not different from NL (**Table 4-1**).

**Table 4-1:** Serum biochemistries at end point (35 weeks)

Experiment 1			
	Normal	CKD	CKD+Ca
BUN (mg/dL)	17.8 ± 1.9*	50.4 ± 8.0	49.1 ± 9.4
PTH (mg/dL)	123 ± 49	2105 ± 139*	33 ± 42
Experiment 2			
	Normal	CKD	CKD+KP
BUN (mg/dL)	20.8 ± 1.8	45.7 ± 2.6	51.2 ± 8.7
PTH (mg/dL)	263 ± 66	6840 ± 6935	403 ± 265

Data presented as mean and standard deviation. \*p<0.05, different from all other groups

## *Bone geometry*

### Experiment 1:

Cortical mean cross-sectional area ( $p=0.002$ ) was significantly lower in CKD animals when compared to NL animals, while the calcium supplementation (CKD+Ca) group was not different from NL (**Table 4-2**). MicroCT analysis of the proximal tibia cortical porosity was higher in CKD (+401% vs. NL;  $p=0.017$ ) and not different in CKD+Ca (+111% relative to NL;  $p = 0.38$ ) (**Table 4-2**).

### Experiment 2:

MicroCT analysis of the proximal tibia demonstrated cortical porosity was significantly higher in CKD (+925%;  $p=0.05$ ) vs. NL, but not different in CKD+KP (+42%;  $p = 0.86$ ) animals relative to NL (**Figure 4-1**). Cortical mean cross-sectional area (ANOVA,  $p=0.09$ ) showed a trend toward lower values in CKD (-20%;  $p=0.078$ ) compared to NL while CKD+KP (-8%;  $p = 0.70$ ) animals were not different compared to NL (**Table 4-2**).

**Table 4-2:** Proximal tibia cortical geometry

Experiment 1			
	Normal	CKD	CKD+Ca
Cortical Area (mm <sup>2</sup> )	7.3 ± 0.2	6.1 ± 0.7*	7.1 ± 0.3
Cortical Porosity (%)	1.1 ± 2.0	5.7 ± 4.7	2.4 ± 2.3
Experiment 2			
	Normal	CKD	CKD+KP
Cortical Area (mm <sup>2</sup> )	6.0 ± 0.3	4.8 ± 1.1	5.5 ± 0.1
Cortical Porosity (%)	2.8 ± 0.5	28.3 ± 22.25*	3.9 ± 2.2

Data presented as mean and standard deviation. \*p<0.05, compared to Normal group

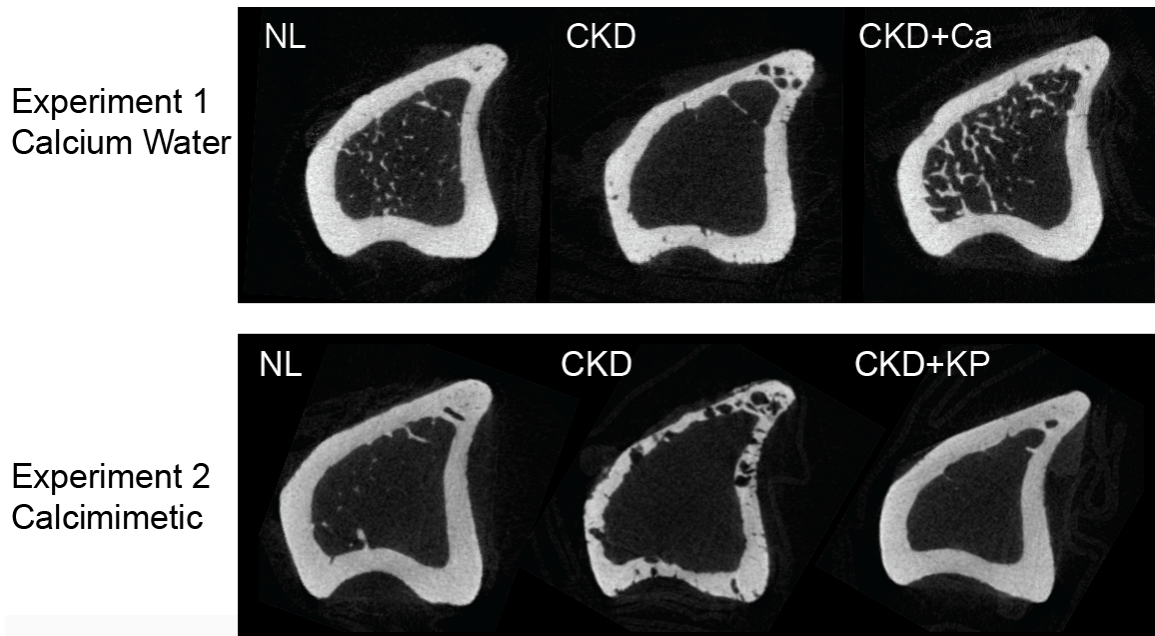


**Figure 4-1:** MicroCT of proximal tibia 2.5mm distal to the proximal growth plate

### *Bone perfusion measurement*

#### Experiment 1:

Femoral cortex ( $p=0.003$ ) and tibial cortex ( $p=0.005$ ) tissue perfusion were both significantly higher in CKD animals when compared to NL animals (**Figure 4-2A&B**). PTH suppression via calcium supplementation resulted in femoral and tibial cortical perfusion that was not different than normal. Isolated marrow perfusion ( $p=0.005$ ) was significantly lower in CKD animals when compared to NL animals (**Figure 4-2C**). PTH suppression via calcium supplementation resulted in isolated marrow perfusion with values not different from CKD animals receiving no treatment.

#### Experiment 2:

Tibial cortex ( $p=0.05$ ) tissue perfusion was significantly higher in CKD animals when compared to NL animals (**Figure 4-2D**). PTH suppression via KP treatment resulted in tibial cortical perfusion that was not different than normal. Isolated marrow perfusion showed a trend toward lower values in CKD (-63%;  $p=0.11$ ) vs. NL, while CKD+KP were not different from NL (-26%;  $p = 0.40$ ) (**Figure 4-2E**).

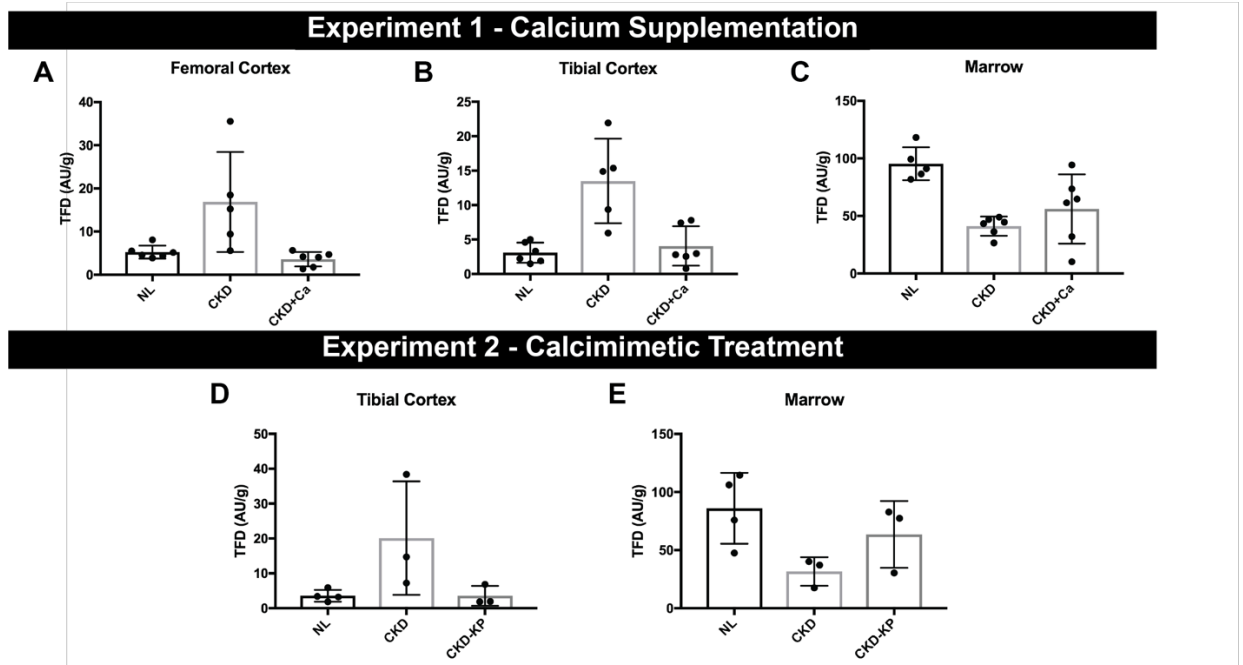


**Figure 4-2:** Bone perfusion data. Experiment 1: Tissue fluorescence density (TFD) of (A) femoral cortical bone (Kruskal-Willis,  $p=0.0030$ ) (B) tibial cortical bone (Kruskal-Willis,  $p=0.0051$ ) (C) tibial bone marrow (Kruskal-Willis,  $p=0.0047$ ). Experiment 2: Tissue fluorescence density (TFD) of (A) tibial cortical bone (Kruskal-Willis,  $p=0.0505$ ) (B) tibial bone marrow (Kruskal-Willis,  $p=0.0780$ ). Dots represent data points, and error bars represent standard deviation. \* $p<0.05$ , different from all other groups



## **Discussion**

CKD causes progressive damage to bone. Bone deterioration in CKD can be characterized by changes in turnover, mineralization, and volume [179], where, most commonly, high turnover drives bone loss. Altered bone turnover/remodeling has been associated with changes in bone perfusion in a number of conditions including diabetes, disuse, aging, and estrogen withdrawal [82,83,86-91]. In turn, reduced bone perfusion has also been associated with bone loss in a number of conditions [93]. Since CKD is known to be associated with both cardiac and vascular abnormalities, we investigated skeletal perfusion in the setting of CKD to provide insights into the pathophysiology of skeletal changes in CKD.

Previous studies, by our group and others, have shown that sustained elevation of serum PTH in the setting of CKD contributes to compromised bone quantity and quality [156,157]. In the present study, with the use of fluorescent microspheres to measure regional perfusion in bone, we show that PTH suppression, using two different approaches, normalizes CKD-induced elevations in cortical bone perfusion. CKD animals with calcium supplementation and calcimimetic treatment had PTH levels that were suppressed by 98% and 94% relative to untreated CKD animals, respectively, yielding PTH levels that were not significantly different than normal animals. Our group has previously shown that the suppression of PTH levels with calcium supplementation in drinking water has substantial positive skeletal effects, essentially normalizing bone turnover and volume [181,182]. In the present study, PTH suppression via calcium

supplementation or calcimimetic treatment resulted in higher cortical bone area along with normalized cortical bone perfusion (**Figure 4-3A-B**). It is unclear whether normalization of CKD-induced elevations in cortical bone perfusion via PTH suppression is secondary to normalized CKD-induced structural changes in bone, directly due to the effect of low PTH/low remodeling CKD on vasculature, or more likely, a combination of both (**Figure 4-4**). In other words, the normalization of cortical bone perfusion via PTH suppression suggests that perfusion elevations are either dependent on PTH, or dependent on a factor secondary to elevated PTH, such as increased cell metabolism. PTH suppression can reduce the direct effects of PTH on the endothelial expression of vascular endothelial growth factor [175] and consequently normalize CKD-induced elevation in cortical bone perfusion. On the other hand, PTH suppression can result in the attenuation of the increased metabolic demands [174] of high turnover CKD secondary to elevated PTH levels.

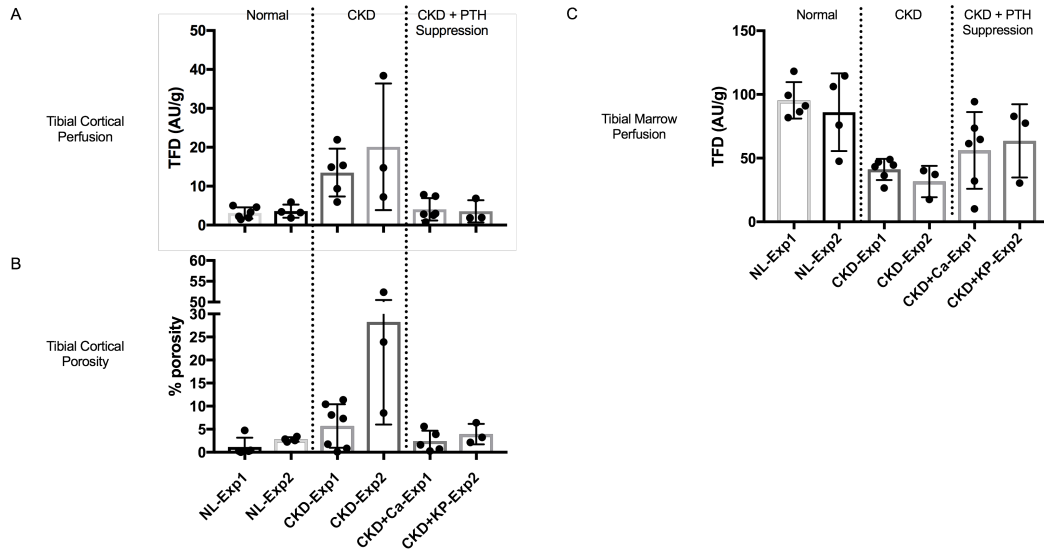


**Figure 4-3:** Combined graphs with data from Experiments 1 & 2: (A) tibial cortical perfusion, (B) tibial cortical porosity, (C) tibial marrow perfusion

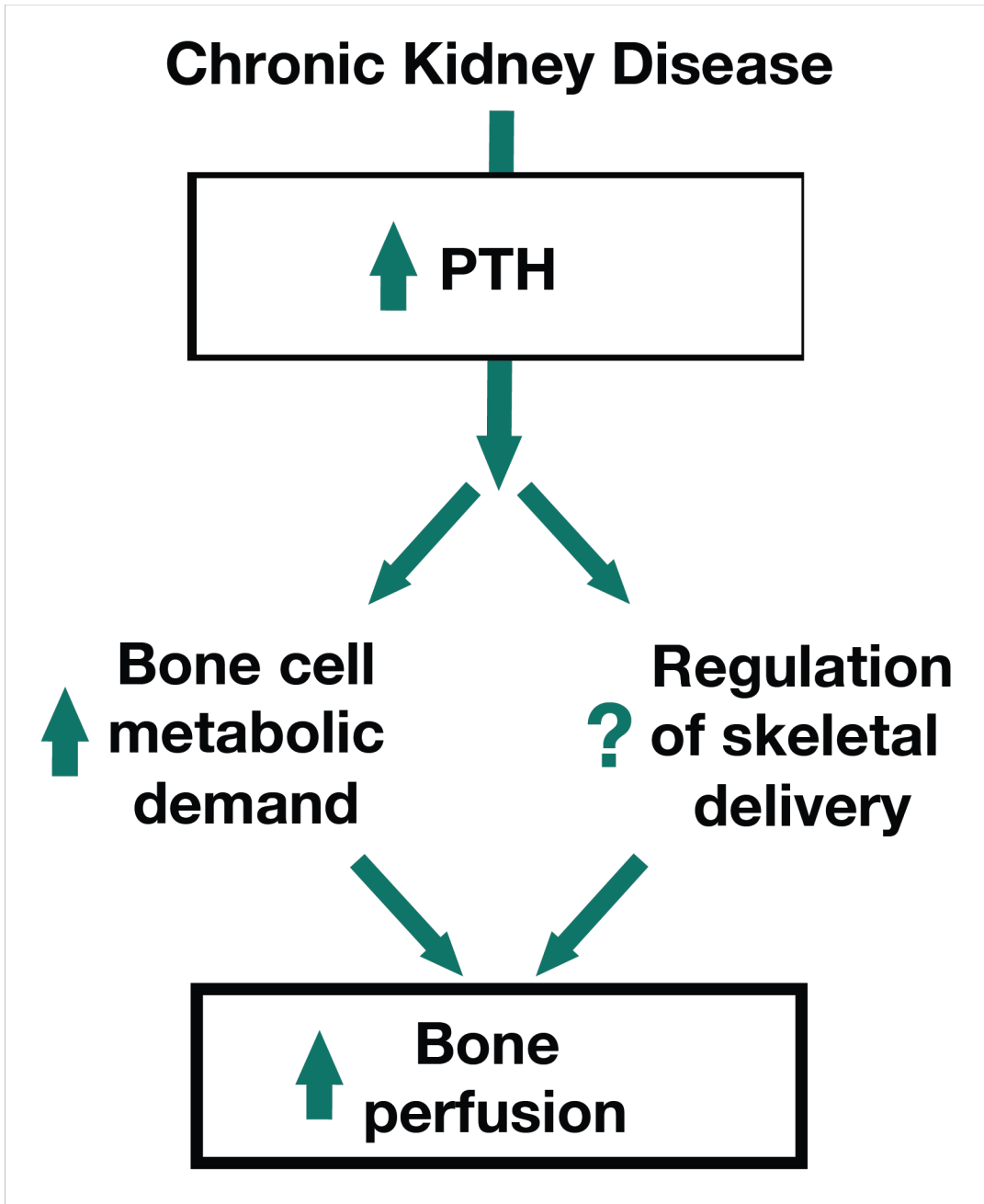


Figure 4-4: Potential mechanism of elevated PTH effect on cortical perfusion

The current study demonstrates lower marrow perfusion in the setting of high PTH/high remodeling CKD in two separate experiments that is not completely normalized with PTH suppression (**Figure 3C**). In addition to well-described mineral disturbances and hormonal factors that influence osteoclast differentiation in CKD, osteoclast differentiation and activity may be further exacerbated by decreased marrow perfusion resulting in medullary hypoxia. Medullary hypoxia has been shown to induce osteoclast and inhibit osteoblast differentiation [81]. The lack of normalization of CKD-induced lowering of marrow perfusion in the low PTH/low remodeling CKD state suggests that marrow perfusion is not dependent on the high remodeling state in the setting of CKD. Other factors including arterial perfusion pressures, myogenic, endothelial, neural and hormonal disturbances may explain alterations of marrow perfusion in the setting of CKD. Marrow hypoxia may also explain the relative suppression hypoxia inducible factor-1 (Hif-1) with suppression of PTH in the Cy/+ rats [107].

Characterizations of bone circulation have confirmed that principal relationships of regulatory factors in the circulation of other tissues also apply to the vascular tissue in bone [128]. Thus regulation of cortical bone perfusion is dictated by a balance between oxygen delivery to cortical bone (supply) and metabolism of bone cells (demand). Mechanisms that help maintain this balance are arterial perfusion pressures, myogenic, local metabolic, endothelial, neural and hormonal influences. Despite the well-established evidence of vascular dysfunction in CKD [15,144,145], along with evidence of vascular pathologies in the Cy/+ rat model [171-173], data from our lab have shown that cortical bone

perfusion is elevated in the setting of high parathyroid hormone (PTH), high remodeling CKD [106], in combination with lower marrow perfusion. Our working hypothesis is that increased cortical bone perfusion, in the setting of decreased delivery due to the known vascular dysfunction of CKD, is likely indicative of increased metabolism of cortical bone cells. The decrease of marrow perfusion in the setting of the increased metabolism due to increased bone turnover in CKD is likely indicative of decreased delivery to the marrow.

Our results should be interpreted in the context of various assumptions and limitations. Injection of microspheres in the left ventricle to assess perfusion is based on a set of assumptions and has multiple limitations as discussed in our previous work [170] [106]. While these limitations are important to consider from a technical standpoint, we have now consistently shown in several studies that in CKD in the setting of high PTH there is higher cortical perfusion. Another limitation of our current work is the low number of animals in Experiment 2. Although we did not have as many animals in Experiment 2, the results of PTH suppression due to calcimimetic treatment paralleled that observed with calcium induced suppression of PTH in that both treatments normalize cortical bone perfusion, without effect on marrow perfusion (**Figure 2A-C**), thus confirming that the effects are due to PTH suppression rather than the calcium treatment.

The effect of CKD-induced perfusion elevations in cortical bone are normalized by reductions in PTH. The normalization of cortical bone perfusion via PTH suppression suggests that perfusion elevations are PTH dependent, either direct or indirectly mediated via another factor. Determining the mechanisms of

these bone perfusion alterations and whether they are drivers, propagators, or consequences of skeletal deterioration in CKD will necessitate further work but will help untangle a key player in CKD-induced bone quality alterations.

## CHAPTER 5

### EFFECTS OF CKD ON ISOLATED VESSEL PROPERTIES: PRELIMINARY INVESTIGATION

#### **Introduction**

Chronic kidney disease has negative effects on vascular reactivity and end-organ perfusion. In the setting of CKD, decreased cardiac output [129], vascular calcification [130], and endothelial dysfunction [131-133] could all contribute to altered end-organ perfusion. Hypoperfusion, in the setting of CKD, that causes ischemia has been illustrated in the myocardium [134], brain [135,136], and mesentery [137]. However, studies that elucidate the effect of individual cardiovascular pathologies on end-organ perfusion in CKD have yet to be performed. Moreover, CKD-induced elevations in uremic toxins including phosphate [138] and parathyroid hormone (PTH) [110] have long been associated with vascular dysfunction through endothelium-dependent, endothelium-independent and/or vascular remodeling mechanisms [139-142]. Extensive work in CKD has documented vascular changes to coronary vessels [143,144] and aorta [145,146]. Gastrointestinal resistance arteries, which control organ perfusion, have also been shown to be adversely affected in models of CKD [147-150]. Other work has illustrated structural remodeling of resistance arteries manifested as alterations in arteriolar wall thickness and lumen diameter [151,152]. Surprisingly, the effects of uremia, including elevations in PTH and phosphate, on skeletal vascular reactivity have not been studied.

In vitro isolated vessel preparations can be used to characterize functional reactivity of vessels in settings of disease and in response to vasoactive agents.



Myography is an in vitro vessel preparation method that enables the characterization of the functional reactivity of vessels through the measurement of tension induced in isometric conditions (Wire Myography), or the measurement of changes in diameter under isobaric conditions (Pressure Myography). In the current studies we isolate vessels from CKD animals and utilize wire myography to test vascular reactivity. The objective of these pilot studies is to work out methods and begin generating data to address the hypothesis that vascular reactivity is altered in the setting of chronic kidney disease.

## **Methods**

### *Animals*

Male Cy/+ rats, Han:SPRD rats (n=4) with autosomal dominant polycystic kidney disease [171], and their unaffected (normal) littermates (n=4) were used for this study. Male heterozygous rats (Cy/+) develop characteristics of CKD around 10 weeks of age that progress to terminal uremia by about 40 weeks. Our laboratory has demonstrated that this animal model recapitulates all three manifestations of CKD-Mineral and Bone Disorder (CKD-MBD) - biochemical abnormalities, extraskelatal calcification, and abnormal bone [72,73,171]. Arteries (aorta and femoral artery) were harvested at 35 weeks after animals were euthanized. All procedures were reviewed and approved by the Indiana University School of Medicine Institutional Animal Care and Use Committee prior to study initiation.

### *Aortic wire myography*

Immediately following euthanasia (n=2) via aortic rupture under isoflurane, the abdominal aorta was removed and dissected into two 3-mm aortic rings. The aortic rings were then suspended and hooked to a force transducer in a warmed organ bath ( $37 \pm 0.5^\circ\text{C}$ ) containing gassed (95%  $\text{O}_2$  and 5%  $\text{CO}_2$ ) physiological solution (in mM: NaCl 136.9, KCl 5.4,  $\text{MgCl}_2$  1.05,  $\text{NaH}_2\text{PO}_4$  0.42,  $\text{NaHCO}_3$  22.6,  $\text{CaCl}_2$  1.8, glucose 5.5, ascorbic acid 0.28 and  $\text{Na}_2\text{EDTA}$  0.05). Smooth muscle cell contractile function was determined by a cumulative concentration-response curve to increasing concentrations of KCl (concentration 10mM to 60mM). Endothelial control of vascular relaxation (endothelium-dependent) was determined by adding the muscarinic agonist acetylcholine (concentration  $10^{-9}$  to  $10^{-5}$  M) following a 70% submaximal pre-contraction to noradrenaline. The change in isometric force was measured using Grass FT03 force transducers (Grass, MA, USA) connected to a PowerLab chart recording system using Chart 4.0 recording software (AD Instruments, Sydney, NSW, Australia). Two aortic rings were tested per animal and average values were calculated resulting in one set of values per animal. Main outcomes of vascular reactivity were active tension (in grams) in response to potassium chloride and active relaxation (measured as % relaxation following 70% submaximal pre-contraction to noradrenaline) in response to acetylcholine by measuring contraction and relaxation with the force transducer of the wire myograph.

### *Femoral artery wire myography*

Immediately following euthanasia (n=2) via aortic rupture under isoflurane, the right femoral artery was removed, dissected, and divided into two 3-mm femoral artery segments. The femoral artery segments were mounted on two 40  $\mu\text{m}$  stainless steel wires in a myograph chamber (620M; Danish Myo Technology; Aarhus, Denmark) and kept in Krebs' PSS at 37C (pH 7.4) with continuous aeration by a mixture of 95% O<sub>2</sub> and 5% CO<sub>2</sub>. The distance between the wires was adjustable to set the passive force of the femoral artery segment before testing. One wire was connected to an isometric force transducer while the other was connected to a screw micrometer used for adjustment of passive force. Measurement of vascular contractile force was recorded on a computer using LabChart 7 software (AD Instruments, Pty. Ltd, Bella Vista, NSW, Australia). Smooth muscle cell contractile function was determined by a cumulative concentration-response curve to increasing concentrations of KPSS (concentration 10mM to 60mM). Endothelial control of vascular relaxation (endothelium-dependent) was determined by adding the muscarinic agonist acetylcholine (concentration  $10^{-9}$  to  $10^{-5}$  M) following a 70% submaximal pre-contraction to KPSS. Main outcomes of vascular reactivity were active tension (in mN) in response to potassium chloride and active relaxation (measured as % relaxation following 70% submaximal pre-contraction to KPSS) in response to acetylcholine by measuring contraction and relaxation with the force transducer of the wire myograph.

### *Statistical analysis*

All data presented as mean  $\pm$  SD. Active tension and active relaxation of NL and CKD arteries were compared statistically using unpaired t tests at each concentration of vasoactive agent. All statistical analysis was performed using GraphPad Prism 8.0 (GraphPad software, San Diego, CA, USA). *A priori*  $\alpha$ -levels were set at 0.05 to determine significance.

### **Results and Discussion**

KPSS (femoral wire myography) induced concentration-dependent contractile effects of CKD arteries that were attenuated at higher concentrations when compared to NL arteries (**Figure 1A and 1C**). Although a similar trend was observed in aortic wire myography, there was not statistical difference of CKD aorta active tension when compared to NL aortas. Acetylcholine induced a concentration-dependent relaxation of pre-contracted rat aortic rings and femoral arteries. While ACh-induced relaxation of CKD arteries was attenuated in the aorta (**Figure 5-1B**), ACh-induced relaxation of the femoral artery (**Figure 5-1D**) was not statistically different when compared to NL arteries. Altered mineral metabolism, inflammation, and oxidative stress have been identified as causative factors of vascular dysfunction in CKD [185]. Functional and morphological changes to vascular smooth muscle and endothelium impair vascular function [196]. One of these impairments of vascular function in CKD is the loss of contractile elements due to alterations of the vascular smooth muscle cell phenotype due to the uremia of CKD [196]. In the present study, we demonstrate

diminished active tension in both the aorta and the femoral artery in the setting of CKD, along with altered endothelial dependent relaxation.

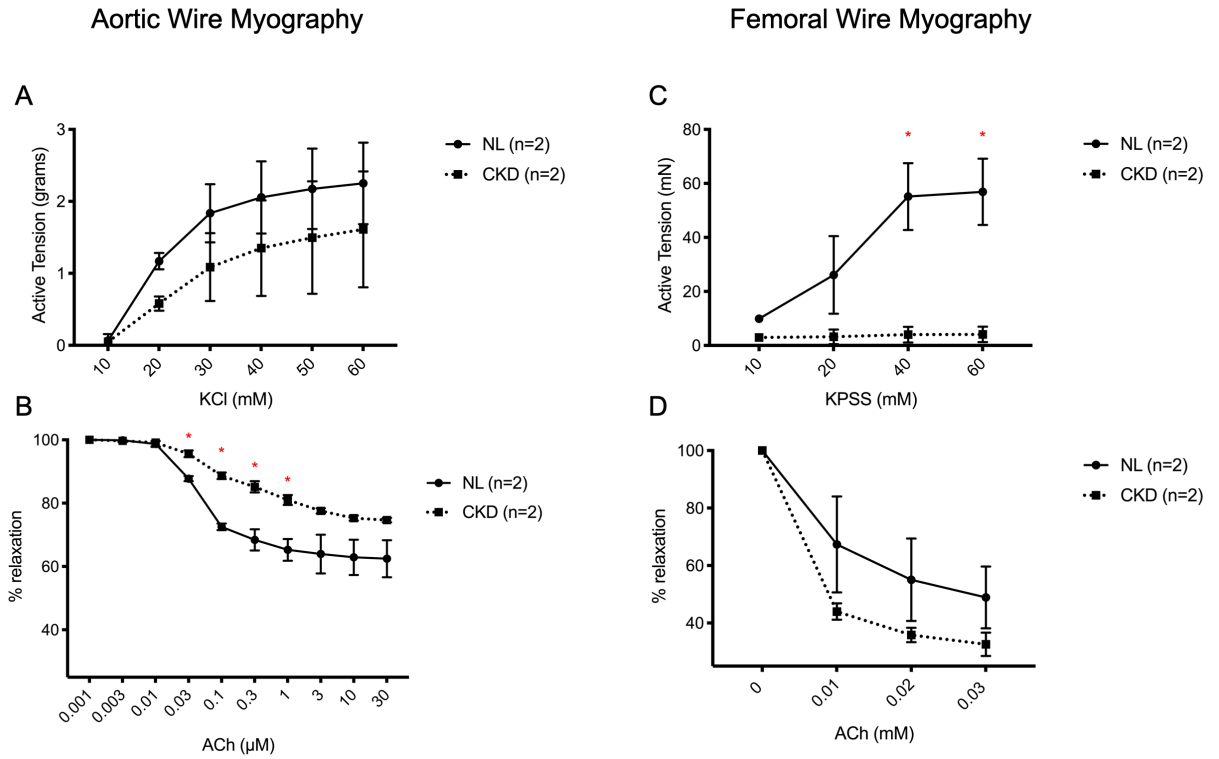
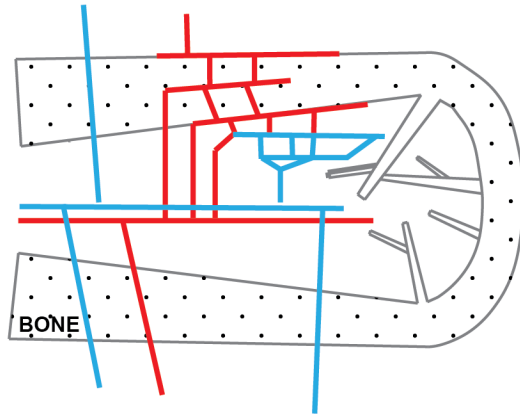


**Figure 5-1:** Aortic and femoral wire myography. Aortic wire myography (n=2) A) aortic active tension B) aortic endothelial-dependent relaxation. Femoral artery wire myography (n=2) C) aortic active tension D) aortic endothelial-dependent relaxation. Data presented as mean + SD.

In three separate experiments, we show lower bone marrow perfusion in CKD tibiae when compared to their normal littermates (**Chapters 3&4**). Altered perfusion can be a result of any one, or a combination of, disturbances to supply (vascular delivery or vascular volume), disturbances to demand (metabolic activity), or dysregulated signaling/pathology that affects the bone vascular network. Diminished marrow perfusion in the setting of CKD is likely due to a combination of disrupted vascular delivery secondary to vascular dysfunctions of CKD along with decreased metabolic demand due to decreased marrow cellularity and marrow cell function (**Figure 5-2**). This decreased marrow perfusion may result in diminished marrow cell function that may then further decrease metabolic demand and further decrease marrow perfusion. In other words, decreased marrow function as a consequence of decreased marrow perfusion may itself perpetuate decreased marrow perfusion. In the current pilot studies, we show that vascular reactivity is altered in both the aorta and the femoral artery in animals with progressive kidney disease, suggesting that diminished marrow perfusion may occur, at least partly, due to altered vascular reactivity and ultimately decreased blood supply.



## Decreased Marrow Perfusion

### potential causes

- disrupted supply
- decreased metabolic activity due to decreased marrow cellularity or cell function

### potential consequences

- disrupted osteoprogenitor differentiation
- diminished marrow cell function (i.e. anemia)

**Figure 5-2:** Potential causes and consequences of decreased marrow perfusion.

The next steps in investigating the impact of altered vascular reactivity in the setting of CKD on bone perfusion are expanding the sample size in large vessel wire myography studies, quantifying alterations to bone vascular reactivity in CKD via isolated vessel experiments utilizing the principal nutrient artery of the femur, and performing isolated vessel wire myography experiments incorporating in vivo and ex vivo elevations of PTH to test the direct effects of high levels of PTH on vascular reactivity. Chronic elevations in parathyroid hormone (PTH) may drive altered bone vascular properties in CKD. In the setting of CKD, we and others have shown that sustained elevated PTH contributes to high bone remodeling which drives increases in cortical porosity and ultimately compromised bone mechanics [156,157]. Moreover, the role of PTH in modulating vasculature, including that of the bone, has been well-established in the literature [91,110,158,159]. The present study presents preliminary data utilizing the wire myography method to perform isolated vessel experiments that will enable the testing of our working hypothesis: elevated PTH drives maladaptive changes to the skeletal vasculature that contribute to the skeletal deterioration in CKD.

The major limitation of the wire myograph method is that the function of these vessels was studied under conditions that remove myogenic, neural, hormonal, and metabolic factors, which are significant contributors to the regulation of vascular reactivity. However, wire myography is a well-accepted method in the field to test vascular reactivity. Further studies can utilize pressure



myography in order to test myogenic responses, but removing neural, hormonal and metabolic factors is characteristic to isolated vessel experiments.

In health, the main blood supply of the marrow originates from the nutrient artery, which originates from large arteries of the extremities (i.e femoral/tibial and brachial/radial arteries), penetrates the cortex and divides into ascending and descending branching running along the length of the bone within the medullary cavity [128]. The main nutrient artery running longitudinally through the medullary cavity will supply the medullary sinuses in the marrow along with cortical branches directed back toward the endosteum. Any disturbances to the vascular supply to the nutrient artery (including decreased vascular reactivity of large arteries) will result in decreased perfusion to the marrow. The current study presents preliminary data that demonstrates altered vascular reactivity in both the aorta and the femoral artery in the setting of CKD, which may play a role in altered bone perfusion in CKD.

## CHAPTER 6

### DISCUSSION

#### **Summary**

The objective of the current series of studies was to better understand the effects of CKD on maladaptive changes to skeletal perfusion that may contribute to the skeletal deterioration in CKD. Gaining a better understanding of the multiple factors that lead to bone structural and material deterioration in CKD is crucial to finding novel and effective therapy targets.

Disturbances to bone perfusion have been shown to play a role in skeletal dysfunction in systemic and skeletal diseases [79,83-85,87] yet there remain many unanswered questions, due in part to the complexity of measurement methodologies [80]. In **Chapter 2**, we fill this void by showing the viability of injection and analysis of fluorescent microspheres to assess regional bone tissue perfusion in rats. Although this technique has been documented with radioactive microspheres in rats, and using these fluorescent microsphere in mice, there necessitated significant technique development to apply fluorescent sphere measures in rats. In **Chapter 3**, we utilize animals with progressive kidney disease and their normal littermates to assess alterations in skeletal perfusion at two different time points. Using the fluorescent microsphere protocol established in Chapter 1, we show that animals with high turnover CKD have higher cortical bone perfusion at both 30 and 35 weeks compared to non-diseased animals. Despite evidence of vascular pathologies in the current model [171-173] and known vascular dysfunction in CKD [15,144,145], we show for the first time that cortical bone perfusion in isolated femoral and tibia cortical bone diaphyses is

nonetheless higher. Also, most interestingly, in **Chapter 3**, we show that patterns of marrow perfusion in CKD animals diverged from those of cortical bone in late-stage high turnover disease. Although CKD animals show no change to marrow perfusion (trending towards higher) in the 30 week time point there was significantly lower perfusion at 35-weeks compared to NL animals. In **Chapter 4**, with the goal of showing proof of principle that treatments could normalize tissue perfusion, we show that PTH suppression, using two different approaches, normalizes CKD-induced elevations in cortical bone perfusion. We also demonstrate that the lower marrow perfusion in high PTH/high remodeling CKD is not completely normalized with PTH suppression.

Past literature has documented that regulation of bone perfusion is dictated by a balance between oxygen delivery to the bone (supply) and metabolism of cells in bone (demand). Altered perfusion can be a result of disturbances to supply (vascular delivery or vascular volume), demand (metabolic activity), or dysregulated signaling/pathology that affects the bone vascular network. In **Chapter 5**, we undertook preliminary investigation of blood delivery to bone upstream of cortex through measures of vascular reactivity of the aorta and the femoral artery. Using *ex vivo* wire myography, we were able to generate preliminary data to show that vascular reactivity is altered in both the aorta and the femoral artery in animals with progressive CKD.

In summary, the novel findings of this work are: 1) cortical bone perfusion is elevated and bone marrow perfusion is lower in the setting of high PTH/high remodeling CKD; and 2) PTH suppression, using two different approaches,

normalizes CKD-induced elevations in cortical bone perfusion but not CKD-induced depression in bone marrow perfusion.

#### *Understanding CKD-induced elevations in cortical bone perfusion*

Despite evidence of vascular pathologies in the current model [171-173] and known vascular dysfunction in CKD [15,144,145], we show that cortical bone perfusion in isolated femoral and tibia cortical bone diaphyses is nonetheless higher (**Chapter 2**). We hypothesize that this elevated cortical perfusion is due to one, or a combination, of two separate mechanisms. Cortical perfusion may be increased in response to increased metabolic needs of high turnover CKD bone, necessitating endothelial cells to express vasoactive substances that increase tissue blood flow [174]. Alternatively, PTH has been shown to have direct effects on the endothelial expression of vascular endothelial growth factor [175] such that worsening secondary hyperparathyroidism with sustained elevations in PTH could be driving increased perfusion.

PTH suppression via calcium supplementation or calcimimetic treatment resulted in higher cortical bone area along with normalized cortical bone perfusion (**Chapter 4**). It is unclear whether normalization of CKD-induced elevations in cortical bone perfusion via PTH suppression is secondary to normalized CKD-induced structural changes in bone, directly due to the effect of low PTH/low remodeling CKD on vasculature, or more likely, a combination of both. In other words, the normalization of cortical bone perfusion via PTH suppression suggests that perfusion elevations are either dependent on PTH, or

dependent on a factor secondary to elevated PTH, such as increased cell metabolism. PTH suppression can reduce the direct effects of PTH on the endothelial expression of vascular endothelial growth factor [175] and consequently normalize CKD-induced elevation in cortical bone perfusion. On the other hand, PTH suppression can result in the attenuation of the increased metabolic demands [174] of high turnover CKD secondary to elevated PTH levels. In order to uncouple the effects of PTH and bone turnover on altered perfusion, future investigation will utilize a bisphosphonate to suppress only turnover and not PTH, and calcium supplementation to suppress both turnover and PTH (see **Table 6-2** section 3a for more details).

Previous studies have established the relationship between bone metabolic demand and bone remodeling rates. Sim and Kelly performed a study of vascular aspects of endocrinopathies and showed a weak but present relationship between oxygen consumption and bone remodeling in mature beagle bone [190]. Similarly, with the increased bone remodeling rates observed in high PTH/high remodeling CKD, there is also expected to be elevated oxygen consumption in the bone, and thus, increased metabolic demand, which would signal for increased perfusion to the bone. Concurrently, it is important to understand that hypoxia has been shown to stimulate bone resorption by accelerating the formation of osteoclasts and ultimately increasing osteoclast number [95], and bone resorption. In addition to well-described mineral disturbances and hormonal factors that promote osteoclast differentiation in CKD, marrow hypoxia may contribute to increased osteoclast differentiation,

ultimately resulting in increased cortical bone turnover and increased metabolic demand [81][191].

**Table 6-1:** Bone perfusion, bone formation rate, and bone volume in different conditions

Condition	Bone perfusion	BFR	Bone remodeling balance	Bone volume
Aging [87]	Decreased (bone) Decreased (marrow)	-	Net negative	Bone loss
Diabetes [84]	Decreased (marrow) Not measured (bone)	-/low	-	-
CKD [106]	Increased (bone) Decreased (marrow)	high	Net negative	Bone loss
Unloading [83]	Decreased (bone) Decreased (marrow)	high	Net negative	Bone loss
Intermittent PTH [186]	Increased (bone) Increased (marrow)	high	Net positive	Bone gain
Continuous PTH [110]	No change (marrow)* Not measured (bone)	high	Net negative	Bone loss

\*only 14 days of continuous PTH therapy

Aging Diabetes CKD [106] Unloading Intermittent PTH Continuous PTH

**Table 6-1** summarizes the relationship between bone perfusion, bone remodeling rate, and bone volume in a number of conditions, including CKD. Net negative remodeling balance does not appear to directionally correspond to increased or decreased perfusion, but decreased marrow perfusion seems to directionally match with bone loss. So although increased metabolic demand secondary to increased cortical bone resorption may drive increased cortical bone perfusion, medullary hypoxia secondary to CKD-induced vascular dysfunction may contribute to the increased availability of active osteoclasts in the marrow.

#### *Understanding CKD-induced lowering of marrow perfusion*

In three separate experiments, we show marrow perfusion to be lower in CKD animals when compared to their normal littermates (**Chapters 3&4**). This is in contrast to cortical bone perfusion which was significantly higher in CKD animals at both of the time points. CKD-induced alterations to marrow perfusion were not corrected by PTH suppression, in contrast to CKD-induced elevation in cortical bone perfusion (**Chapter 4**). The lack of normalization of CKD-induced lowering of marrow perfusion in the low PTH/low remodeling CKD state suggests that marrow perfusion is not dependent on the high remodeling state in the setting of CKD. In addition to well-described mineral disturbances and hormonal factors that influence osteoclast differentiation in CKD, osteoclast differentiation and activity may be further exacerbated by decreased marrow perfusion resulting



in medullary hypoxia. Medullary hypoxia has been shown to induce osteoclast and inhibit osteoblast differentiation [81].

Reductions in marrow perfusion in the setting of CKD suggest either a dramatic shift in marrow VEGF signaling or marrow content during the later-stage manifestation of CKD. Previous work from our group has demonstrated lower levels of VEGF-A expression in bone marrow of 35-week old CKD animals compared to their normal littermates [107]. Concurrently, there is evidence of decreased marrow cellularity, increased marrow adiposity and increased marrow fibrosis [187]. Further investigation will require the determination of the relationship between these various factors. Do reductions in perfusion begin a cascade of marrow content alteration that results in lower levels of VEGF expression? Does VEGF expression occur first, resulting in reductions in marrow perfusion that then drives the changes in marrow content? Or are both reductions of VEGF expression and reductions in perfusion secondary to a change in marrow content that is occurring through another mechanism altogether? (see **Table 6-2** sections 2a-b, 6a).

A likely alternative explanation is that more severe vascular dysfunction with progressive renal failure may limit the ability to perfuse distal organs such as bone at late stage CKD [173]. Our work in **Chapter 5** shows that in our CKD model, rats with progressive kidney disease have dysfunctions of vascular reactivity in large vessels, which could compromise end-organ perfusion including that of bone. In health, the main blood supply of the marrow originates from the nutrient artery, which originates from large arteries of the extremities (i.e.

femoral/tibial and brachial/radial arteries), penetrates the cortex and divides into ascending and descending branching running along the length of the bone within the medullary cavity [128]. The main nutrient artery running longitudinally through the medullary cavity will supply the medullary sinuses in the marrow along with cortical branches directed back toward the endosteum. Any disturbances to the vascular supply to the nutrient artery (including decreased vascular reactivity of large arteries) will result in decreased perfusion to the marrow.

The lack of normalization of CKD-induced lowering of marrow perfusion in the low PTH/low remodeling CKD state suggests that marrow perfusion is less dependent on the high remodeling state in the setting of CKD and more dependent on vascular dysfunction of CKD. Likely, the CKD-induced lowering of marrow perfusion observed in high PTH/high remodeling CKD is due to compromised blood supply (vascular delivery or vascular volume) or dysregulated signaling/pathology that affects the bone vascular network.

### **Clinical Implications**

The clinical importance of the bone vascular system lies mainly in its ability/permmissiveness to deliver 1) nutrients/oxygen, 2) cells with cancerous potential, and 3) therapies to bone and marrow tissue. The bone vascular system is paramount to the delivery of nutrients/oxygen to bone. The delivery of nutrients/oxygen to bone becomes clinically relevant, broadly, in two categories: altered vasculature that affects bone health and function, or altered bone metabolism requires an increased delivery of nutrients/oxygen to bone. The

delivery of cells with cancerous potential to bone is obviously of clinical importance. Bone is the third most common site of cancer metastasis after the lung and the liver, potentially due to marrow vascularity and permeability of marrow sinusoids [197]. The delivery of therapies to bone is dependent on the viability and activity of the bone vascular system. As the conduit of nutrients necessary for health and function, cells that have cancerous potential, and therapies that can fix or poison bone tissue, the bone vascular network is clinically important. In the following sections, the clinical implications of our findings will be discussed.

#### *Clinical implications of CKD-induced elevations in cortical bone perfusion*

Elevated perfusion to the cortical bone in chronic kidney disease results in relatively increased delivery of nutrients/oxygen, presumably, as detailed in above sections, in response to increased metabolic demand. Although delivery of nutrients/oxygen is increased in cortical bone in CKD, the supply may not be increased in proportion to the increased metabolic demand (see [Future Studies](#) section 2b for elaboration on the potential for mismatched supply and demand with regards to cortical bone perfusion).

A major implication of increased cortical bone perfusion is increased delivery of systemic therapies. This discussion will focus mostly on bone-targeted therapy, however, increased delivery of all systemic therapies may also be of clinical importance given that CKD patients often have many comorbidities

requiring a variety of therapies and increased exposure of bone to drugs with various toxicities may have a detrimental effect on bone health and function.

Increased bisphosphonate accumulation in CKD may occur due to increased cortical bone perfusion. Bisphosphonates are a class of antiresorptive drugs that are effective in decreasing fracture risk in situations of bone loss. Secondary hyperparathyroidism in the setting of CKD can result in dramatically increased osteoclast differentiation and activity. Bisphosphonates would be advantageous in counteracting this increased osteoclast activity, and thus work to reverse the bone loss of CKD. Bisphosphonate use in CKD is approved as an acceptable method of treatment of high turnover renal osteodystrophy in early CKD stages, and contraindicated in later stage CKD (stages 3-5), according to recommendations by the Kidney Disease Improving Global Outcomes committee (KDIGO). In a study performed to characterize how alterations in kidney function affect the distribution and accumulation of zoledronate, our group found that animals with early stage CKD (about 50% of normal kidney function) accumulate significantly higher amounts of zoledronate [188]. Although the field has hypothesized increased accumulation of bisphosphonate due to decreased filtration of bisphosphonates (which are renally cleared), the present work presents another potential and convincing explanation. Bisphosphonates are transported to bone surfaces via bone nutrient arteries and the bone vascular system where they bind hydroxyapatite in the bone matrix. Although decreased filtration has been cited as the reason for increased skeletal accumulation of bisphosphonate in CKD, increased cortical perfusion is likely to also play a role.

Bisphosphonates can be effective in attenuating bone loss in early stages of CKD, however, the increased cortical bone perfusion has the potential to alter the amount of drug delivered to bone surfaces and increase skeletal accumulation of bisphosphonate. Although the physiologic implications of the skeletal accumulation of bisphosphonates are not clear, in vitro studies indicate its potential cytotoxic effects in high doses [192][193].

In light of the findings of the present work (increased cortical bone perfusion in the setting of CKD) and increased skeletal accumulation of zoledronate in CKD [188], further investigation is necessary to better understand the relationship of regional bone perfusion and skeletal accumulation of bisphosphonate (see **Table 6-2** section 4).

#### *Clinical implications of CKD-induced lowering of marrow perfusion*

Decreased bone marrow perfusion in the setting of CKD may contribute to marrow dysfunction and alterations, including anemia, along the course of CKD. Marrow function and cellularity are dependent on an intact medullary vascular network. Decreased marrow cellularity is paired with decreased marrow function [199], both corresponding with decreased perfusion to the marrow [198]. Reductions of marrow perfusion in the setting of CKD are accompanied by, albeit with no evidence of causation, decreased marrow cellularity, increased marrow adiposity [187] and increased marrow fibrosis. Despite the overwhelming impact of anemia on CKD dialysis patients, along with the crucial nature of the bone vascular network in the health and function of bone marrow, marrow perfusion

has not been studied as a potential culprit for disease or target for therapy. The major challenge in the clinical relevance of marrow perfusion is the inability/challenge in modulating levels of marrow perfusion. However, with further investigation, marrow perfusion can be identified as a clinical target for anemia therapy in end-stage renal disease patients (see **Table 6-2** sections 2a-b, 6a).

#### *Clinical measurement of bone perfusion*

Measurement of bone perfusion can serve as a biomarker for bone turnover in CKD with the potential to guide treatment course. The ability to measure bone perfusion in a noninvasive and serial manner has the potential of providing novel information with clinical utility in the longitudinal tracking of diagnosis and treatment of bone pathologies (e.g.  $^{18}\text{F}$ -Fluoride positron emission tomography in fracture healing and osteoarthritis [195]). A parallel can be drawn here with a field more advanced in utilizing perfusion measurements to gather clinically relevant information – oncology. The assessment of tumor perfusion has been used in diagnosis (i.e. angiogenic progression of the lesion) along with treatment efficacy (i.e. estimating adequate drug delivery along with longitudinal tracking)[194] and ultimately led to the development of anti-angiogenic drugs that are currently in use today [200]. Similarly, the noninvasive and serial measurement of bone perfusion in CKD can serve as a biomarker of bone turnover, and thus be of clinical utility in diagnoses and treatment efficacy tracking of renal osteodystrophy. Currently, serum PTH and serum BSAP are used as biomarkers

for serial tracking of bone turnover in CKD patients, even though it is known that they are poor markers [189]. The alternative is an invasive iliac crest bone biopsy for histological measure of bone turnover, but is not ideal as a longitudinal measure. Bone perfusion measurement presents a potential solution as a noninvasive and serial assessment of bone activity. Further studies will need to be performed to establish the relationship between clinically measured bone perfusion with histologically measured bone turnover (See **Table 6-2** sections 5a-b).

### **Future Studies**

The current series of studies answers several important question with regards to skeletal perfusion in the setting of CKD, however, these results also lead to several more questions. **Table 6-2** summarizes some potential experiments based on the results of this work.

**Table 6-2:** Description of future studies

<b>EXPERIMENT</b>	<b>DESCRIPTION</b>
<i>1 - Reproducing results of CKD-induced elevations in cortical bone perfusion</i>	
a) Cortical bone perfusion elevation in CKD bone with intracortical remodeling	Utilizing higher order animal models (rabbit/dog/pig) of CKD that have intracortical remodeling to confirm the results presented in current work
b) Translatability to CKD patients	Clinical study to assess bone perfusion in patients with known CKD bone disease
<i>2 - Understanding the relationship between altered bone perfusion and bone deterioration in CKD</i>	
a) Temporal relationship of bone deterioration and altered perfusion	<p>Utilizing an animal model of CKD-MBD to establish the temporal relationship of increased bone perfusion, increased bone turnover, and increased cortical porosity via longitudinal measures (animals euthanized at different ages). This will also allow the assessment of the temporal relationship of reductions in marrow perfusion and changes in marrow content:</p> <ul style="list-style-type: none"> <li>• Do reductions in perfusion begin a cascade of marrow content alteration that results in lower levels of VEGF expression? Does VEGF expression occur first, resulting in reductions in marrow perfusion that then drives the changes in marrow content? Or are both reductions of VEGF expression and reductions in perfusion secondary to a change in marrow content that is occurring through another mechanism altogether?</li> </ul>
b) Functional measures of altered perfusion	<p>Utilizing an animal model of CKD-MBD to perform functional assessments (e.g. measures of hypoxia, metabolic activity, oxygen consumption etc.) of altered bone perfusion. This will allow the testing of these hypotheses:</p> <ul style="list-style-type: none"> <li>• Increased cortical perfusion is a compensatory mechanism for increased metabolic demand</li> <li>• Even in the presence of increased cortical perfusion, hypoxia still plays</li> </ul>



	<p>an active role in cortical bone deterioration</p> <ul style="list-style-type: none"> <li>• Marrow dysfunction in CKD is paired with decreased marrow perfusion, decreased marrow oxygen consumption, and increased marrow hypoxia.</li> </ul>
<p><i>3- Uncoupling hyperparathyroidism and bone remodeling as drivers of altered bone perfusion in CKD</i></p>	
<p>a) Uncoupling the effects PTH and bone turnover on altered perfusion</p>	<p>Utilizing an animal model of CKD-MBD to uncouple the effects of secondary hyperparathyroidism and resulting elevated bone turnover on the increased cortical bone perfusion. To accomplish this, at least 4 groups will be necessary:</p> <ul style="list-style-type: none"> <li>• Normal</li> <li>• CKD – high PTH/high turnover</li> <li>• CKD – low PTH/low turnover</li> <li>• CKD – high PTH/low turnover</li> </ul>
<p>b) Uncoupling the effects of continuous PTH and CKD on altered perfusion</p>	<p>Utilizing normal animals and PTH therapy to uncouple the effects of high serum PTH levels and CKD on the increased cortical bone perfusion observed in CKD. To accomplish this, at least 3 groups will be necessary:</p> <ul style="list-style-type: none"> <li>• Normal</li> <li>• Normal + continuous PTH</li> <li>• CKD – high PTH/high turnover</li> </ul>
<p><i>4- Understanding the relationship between regional bone perfusion and bisphosphonate accumulation</i></p>	
<p>a) Regional bone perfusion, bisphosphonate accumulation, and regional bone turnover</p>	<p>Utilizing normal animals and fluorescently-tagged bisphosphonate agents to measure bone perfusion, bisphosphonate accumulation and regional bone turnover in the same skeletal region at various bone sites. This study would test the hypothesis that regional perfusion dictates bisphosphonate accumulation at a specific skeletal site, and that the areas of accumulation will also have turnover suppression (whereas regions without bisphosphonate accumulation will not have turnover suppression)</p>
<p>b) Bone perfusion imaging to measure</p>	<p>Clinical study utilizing PET imaging in bisphosphonate-treated individuals to better understand the effect of bisphosphonates on</p>

efficacy of zoledronate	bone perfusion and bone metabolic demand. This allows the investigation of the potential that some skeletal regions prone to fracture do not receive the anti-resorptive effect of bisphosphonates due to dysfunctional vascular network or other factors of drug distribution
<i>5 - Understanding the relationship between regional bone perfusion and bone turnover to utilize bone perfusion as a biomarker of bone turnover in the treatment of renal osteodystrophy in CKD</i>	
a) Regional bone turnover and regional perfusion	Utilizing an animal model of CKD-MBD to investigate the relationship between regional bone turnover and regional bone perfusion at multiple bone sites
b) Bone turnover and bone perfusion imaging	Clinical study with matched bone biopsies and bone perfusion imaging
<i>6 - Understanding the effect of altered marrow perfusion on marrow health</i>	
a) Nutrient artery ligation and anemia	Utilizing normal animals and ligation of the principal nutrient artery of the femur to study the effects of disrupted perfusion on marrow health, and anemia specifically. This will also allow the investigation of the relationship between marrow perfusion, marrow VEGF, and marrow content.

## **Conclusion**

Assessment of skeletal perfusion in an animal model of progressive CKD demonstrated elevations in cortical bone perfusion in the setting of high parathyroid hormone (PTH)/high remodeling CKD, in combination with lower marrow perfusion. The elevation of cortical bone perfusion occurs despite the well-established evidence of vascular dysfunction in CKD. These data uncover a novel player in CKD-induced bone alterations. Currently, the primary goal of CKD-MBD therapy is the suppression of elevated levels of PTH utilizing calcitriol (and its analogues) and calcimimetics. In the present series of studies, we show that PTH suppression, utilizing both calcium supplementation and calcimimetic therapy, normalizes CKD-induced elevations in cortical bone perfusion. These data demonstrate that the combination of bone remodeling suppression and serum PTH reduction normalizes cortical bone perfusion in the setting of CKD. While the relationship of altered bone perfusion and bone deterioration in CKD necessitates further work, these results indicate that determining the mechanisms of bone perfusion alterations and whether they are drivers, propagators, or consequences of skeletal deterioration in CKD could help untangle a key player in CKD-induced bone alterations.

## REFERENCES

- [1] Centers for Disease Control and Prevention (CDC). (2014). National Chronic Kidney Disease Fact Sheet: General Information and National Estimates on Chronic Kidney Disease in the United States, 2014. Atlanta, GA: US Department of Health and Human Services, Centers for Disease Control and Prevention.
- [2] M. Coco, H. Rush, Increased incidence of hip fractures in dialysis patients with low serum parathyroid hormone, *American Journal of Kidney Diseases*. 36 (2000) 1115–1121. doi:10.1053/ajkd.2000.19812.
- [3] A.S. Levey, K.-U. Eckardt, Y. Tsukamoto, A. Levin, J. Coresh, J. Rossert, et al., Definition and classification of chronic kidney disease: A position statement from Kidney Disease: Improving Global Outcomes (KDIGO), *Kidney Int*. 67 (2005) 2089–2100. doi:10.1111/j.1523-1755.2005.00365.x.
- [4] A. Levin, G.L. Bakris, M. Molitch, M. Smulders, J. Tian, Prevalence of abnormal serum vitamin D, PTH, calcium, and phosphorus in patients with chronic kidney disease: results of the study to evaluate early kidney ..., *Kidney Int*. 71 (2007) 31–38. doi:10.1038/sj.ki.5002009.
- [5] A.C. Dooley, N.S. Weiss, B. Kestenbaum, Increased Risk of Hip Fracture Among Men With CKD, *American Journal of Kidney Diseases*. 51 (2008) 38–44. doi:10.1053/j.ajkd.2007.08.019.
- [6] L.F. Fried, M.L. Biggs, M.G. Shlipak, S. Seliger, B. Kestenbaum, C. Stehman-Breen, et al., Association of kidney function with incident hip fracture in older adults, *Journal of the American Society of Nephrology*. 18 (2007) 282–286. doi:10.1681/ASN.2006050546.
- [7] T.L. Nickolas, D.J. McMahon, E. Shane, Relationship between moderate to severe kidney disease and hip fracture in the United States, *Journal of the American Society of Nephrology*. 17 (2006) 3223–3232. doi:10.1681/ASN.2005111194.
- [8] D. Nitsch, A. Mylne, P.J. Roderick, L. Smeeth, R. Hubbard, A. Fletcher, Chronic kidney disease and hip fracture-related mortality in older people in the UK, *Nephrol. Dial. Transplant*. 24 (2009) 1539–1544. doi:10.1093/ndt/gfn678.
- [9] A.M. Ball, D.L. Gillen, D. Sherrard, N.S. Weiss, S.S. Emerson, S.L. Seliger, et al., Risk of Hip Fracture Among Dialysis and Renal Transplant Recipients, *Jama*. 288 (2002) 3014–3018. doi:10.1001/jama.288.23.3014.
- [10] A. Mittalhenkle, D.L. Gillen, C.O. Stehman-Breen, Increased risk of mortality associated with hip fracture in the dialysis population, *American Journal of Kidney Diseases*. 44 (2004) 672–679. doi:10.1053/j.ajkd.2004.07.001.
- [11] S. Kansal, L. Fried, Bone Disease in Elderly Individuals With CKD, *Advances in Chronic Kidney Disease*. 17 (2010) e41–e51. doi:10.1053/j.ackd.2010.05.001.

- [12] S.M. Moe, CHRONIC KIDNEY DISEASE – MINERAL BONE DISORDER, *Perit Dial Int.* 28 (2008) S5–S10.
- [13] F. Zannad, Co-morbidities in Heart Failure, *An Issue of Heart Failure Clinics*, Elsevier Health Sciences, 2014.
- [14] F.G. Hage, R. Venkataraman, G.J. Zoghbi, The scope of coronary heart disease in patients with chronic kidney disease, *Journal of the ...*, 2009.
- [15] R.T. Gansevoort, R. Correa-Rotter, B.R. Hemmelgarn, T.H. Jafar, H.J.L. Heerspink, J.F. Mann, et al., Chronic kidney disease and cardiovascular risk: epidemiology, mechanisms, and prevention, *The Lancet.* 382 (2013) 339–352. doi:10.1016/S0140-6736(13)60595-4.
- [16] F. Tentori, M.J. Blayney, J.M. Albert, B.W. Gillespie, P.G. Kerr, J. Bommer, et al., Mortality Risk for Dialysis Patients With Different Levels of Serum Calcium, Phosphorus, and PTH: The Dialysis Outcomes and Practice Patterns Study (DOPPS), *American Journal of Kidney Diseases.* 52 (2008) 519–530. doi:10.1053/j.ajkd.2008.03.020.
- [17] N.S. Bricker, P.A.F. Morrin, S.W. Kime, The pathologic physiology of chronic bright's disease: An exposition of the 'intact nephron hypothesis', *The American Journal of Medicine.* 28 (1960) 77–98. doi:10.1016/0002-9343(60)90225-4.
- [18] N.S. Bricker, On the pathogenesis of the uremic state: An exposition of the trade-off hypothesis, *N Engl J Med.* (1972).
- [19] C. Faul, A.P. Amaral, B. Oskouei, M.-C. Hu, A. Sloan, T. Isakova, et al., FGF23 induces left ventricular hypertrophy, *J. Clin. Invest.* 121 (2011) 4393–4408. doi:10.1172/JCI46122.
- [20] M.A.I. Mirza, A. Larsson, H. Melhus, L. Lind, T.E. Larsson, Serum intact FGF23 associate with left ventricular mass, hypertrophy and geometry in an elderly population, *Atherosclerosis.* 207 (2009) 546–551. doi:10.1016/j.atherosclerosis.2009.05.013.
- [21] H.J. Hsu, M.S. Wu, Fibroblast growth factor 23: a possible cause of left ventricular hypertrophy in hemodialysis patients, *The American Journal of the Medical Sciences.* (2009).
- [22] D. Levy, R.J. Garrison, D.D. Savage, Prognostic implications of echocardiographically determined left ventricular mass in the Framingham Heart Study, ... *England Journal of ....* (1990).
- [23] V. Shalhoub, E.M. Shatzen, S.C. Ward, J. Davis, J. Stevens, V. Bi, et al., FGF23 neutralization improves chronic kidney disease–associated hyperparathyroidism yet increases mortality, *J. Clin. Invest.* 122 (2012) 2543–2553. doi:10.1172/JCI61405.
- [24] C.D. Touchberry, T.M. Green, V. Tchikrizov, J.E. Mannix, T.F. Mao, B.W. Carney, et al., FGF23 is a novel regulator of intracellular calcium and cardiac contractility in addition to cardiac hypertrophy, *American Journal of Physiology - Endocrinology and Metabolism.* 304 (2013) E863–E873. doi:10.1152/ajpendo.00596.2012.
- [25] J. Ärnlöv, A.C. Carlsson, J. Sundström, E. Ingelsson, A. Larsson, L. Lind, et al., Serum FGF23 and risk of cardiovascular events in relation

- to mineral metabolism and cardiovascular pathology, *Clin J Am Soc Nephrol.* 8 (2013) 781–786. doi:10.2215/CJN.09570912.
- [26] J. Bernheim, S. Benchetrit, The potential roles of FGF23 and Klotho in the prognosis of renal and cardiovascular diseases, *Nephrology Dialysis Transplantation.* 26 (2011) gfr208–2438. doi:10.1093/ndt/gfr208.
- [27] D. Gruson, T. Lepoutre, J.-M. Ketelslegers, J. Cumps, S.A. Ahn, M.F. Rousseau, C-terminal FGF23 is a strong predictor of survival in systolic heart failure, *Peptides.* 37 (2012) 258–262. doi:10.1016/j.peptides.2012.08.003.
- [28] A. Jovanovich, J.H. Ix, J. Gottdiener, K. McFann, R. Katz, B. Kestenbaum, et al., Fibroblast growth factor 23, left ventricular mass, and left ventricular hypertrophy in community-dwelling older adults, *Atherosclerosis.* 231 (2013) 114–119.
- [29] K. Lindberg, H. Olauson, R. Amin, A. Ponnusamy, R. Goetz, R.F. Taylor, et al., Arterial Klotho Expression and FGF23 Effects on Vascular Calcification and Function, *PLoS ONE.* 8 (2013) e60658. doi:10.1371/journal.pone.0060658.
- [30] L.F. Bonewald, M.J. Wacker, FGF23 production by osteocytes, *Pediatr Nephrol.* 28 (2013) 563–568. doi:10.1007/s00467-012-2309-3.
- [31] K. Shibata, S.-I. Fujita, H. Morita, Y. Okamoto, K. Sohmiya, M. Hoshiga, et al., Association between Circulating Fibroblast Growth Factor 23,  $\alpha$ -Klotho, and the Left Ventricular Ejection Fraction and Left Ventricular Mass in Cardiology Inpatients, *PLoS ONE.* 8 (2013) e73184. doi:10.1371/journal.pone.0073184.
- [32] S. Investigators, Effect of enalapril on survival in patients with reduced left ventricular ejection fractions and congestive heart failure, *N Engl J Med.* (1991).
- [33] Y. Okamoto, S.-I. Fujita, H. Morita, S. Kizawa, T. Ito, K. Sakane, et al., Association between circulating FGF23,  $\alpha$ -Klotho, and left ventricular diastolic dysfunction among patients with preserved ejection fraction, *Heart Vessels.* 31 (2016) 66–73. doi:10.1007/s00380-014-0581-9.
- [34] M. Rodríguez, I. López, J. Muñoz, E. Aguilera-Tejero, Y. Almaden, FGF23 and mineral metabolism, implications in CKD-MBD, *Nefrología (Madrid).* 32 (2012) 275–278.
- [35] A. Unsal, S. Kose Budak, Y. Koc, T. Basturk, T. Sakaci, E. Ahbap, et al., Relationship of fibroblast growth factor 23 with left ventricle mass index and coronary calcification in chronic renal disease, *Kidney Blood Press. Res.* 36 (2012) 55–64. doi:10.1159/000339026.
- [36] M. Ketteler, P.H. Biggar, O. Liangos, FGF23 antagonism: the thin line between adaptation and maladaptation in chronic kidney disease, *Nephrol. Dial. Transplant.* 28 (2013) 821–825. doi:10.1093/ndt/gfs557.
- [37] W. Seeherunvong, C.L. Abitbol, J. Chandar, P. Rusconi, G.E. Zilleruelo, M. Freundlich, Fibroblast growth factor 23 and left ventricular hypertrophy in children on dialysis, *Pediatr Nephrol.* 27 (2012) 2129–2136. doi:10.1007/s00467-012-2224-7.

- [38] I.Z. Ben-Dov, H. Galitzer, V. Lavi-Moshayoff, R. Goetz, M. Kuro-o, M. Mohammadi, et al., The parathyroid is a target organ for FGF23 in rats, *J. Clin. Invest.* 117 (2007) 4003–4008. doi:10.1172/JCI32409.
- [39] T. Krajisnik, P. Björklund, R. Marsell, Ö. Ljunggren, G. Åkerström, K.B. Jonsson, et al., Fibroblast growth factor-23 regulates parathyroid hormone and 1 $\alpha$ -hydroxylase expression in cultured bovine parathyroid cells, *Journal of Endocrinology.* 195 (2007) 125–131. doi:10.1677/JOE-07-0267.
- [40] A. Kottgen, S.D. Russell, L.R. Loehr, Reduced kidney function as a risk factor for incident heart failure: the atherosclerosis risk in communities (ARIC) study, *Journal of the ...*, 2007.
- [41] K. Wattanakit, A.R. Folsom, E. Selvin, J. Coresh, A.T. Hirsch, B.D. Weatherley, Kidney function and risk of peripheral arterial disease: results from the Atherosclerosis Risk in Communities (ARIC) Study, *Journal of the American Society of Nephrology.* 18 (2007) 629–636. doi:10.1681/ASN.2005111204.
- [42] B.C. Astor, J. Coresh, G. Heiss, D. Pettitt, M.J. Sarnak, Kidney function and anemia as risk factors for coronary heart disease and mortality: The Atherosclerosis Risk in Communities (ARIC) Study, *American Heart Journal.* 151 (2006) 492–500. doi:10.1016/j.ahj.2005.03.055.
- [43] M.I. Aguilar, E.S. O'Meara, S. Seliger, W.T. Longstreth, R.G. Hart, P.E. Pergola, et al., Albuminuria and the risk of incident stroke and stroke types in older adults, *Neurology.* 75 (2010) 1343–1350. doi:10.1212/WNL.0b013e3181f73638.
- [44] S.I. Hallan, K. Matsushita, Y. Sang, B.K. Mahmoodi, C. Black, A. Ishani, et al., Age and Association of Kidney Measures With Mortality and End-stage Renal Disease, *Jama.* 308 (2012) 2349–2360. doi:10.1001/jama.2012.16817.
- [45] C.E. McCulloch, C. Hsu, Chronic Kidney Disease and the Risks of Death, Cardiovascular Events, and Hospitalization, (2004).
- [46] S. Hallan, B. Astor, S. Romundstad, K. Aasarød, K. Kvenild, J. Coresh, Association of Kidney Function and Albuminuria With Cardiovascular Mortality in Older vs Younger Individuals: The HUNT II Study, *Arch Intern Med.* 167 (2007) 2490–2496. doi:10.1001/archinte.167.22.2490.
- [47] M.P. Marco, L. Craver, A. Betriu, M. Belart, J. Fibla, Higher impact of mineral metabolism on cardiovascular mortality in a European hemodialysis population, *Kidney ....* (2003).
- [48] S. Schwarz, B.K. Trivedi, K. Kalantar-Zadeh, Association of disorders in mineral metabolism with progression of chronic kidney disease, *Clinical Journal of the ...*, 2006.
- [49] M. Noordzij, J.C. Korevaar, W.J. Bos, E.W. Boeschoten, F.W. Dekker, P.M. Bossuyt, et al., Mineral metabolism and cardiovascular morbidity and mortality risk: peritoneal dialysis patients compared with haemodialysis patients, *Nephrology Dialysis Transplantation.* 21 (2006) 2513–2520. doi:10.1093/ndt/gfl257.

- [50] N. Kimata, J.M. Albert, T. Akiba, S. Yamazaki, Y. Kawaguchi, S. Fukuhara, et al., Association of mineral metabolism factors with all-cause and cardiovascular mortality in hemodialysis patients: The Japan dialysis outcomes and practice patterns study, *Hemodialysis International*. 11 (2007) 340–348. doi:10.1111/j.1542-4758.2007.00190.x.
- [51] H. Dobnig, S. Pilz, H. Scharnagl, W. Renner, U. Seelhorst, B. Wellnitz, et al., Independent Association of Low Serum 25-Hydroxyvitamin D and 1,25-Dihydroxyvitamin D Levels With All-Cause and Cardiovascular Mortality, *Arch Intern Med*. 168 (2008) 1340–1349. doi:10.1001/archinte.168.12.1340.
- [52] A. Covic, P. Kothawala, M. Bernal, S. Robbins, A. Chalian, D. Goldsmith, Systematic review of the evidence underlying the association between mineral metabolism disturbances and risk of all-cause mortality, cardiovascular mortality and cardiovascular events in chronic kidney disease, *Nephrology Dialysis Transplantation*. 24 (2009) 1506–1523. doi:10.1093/ndt/gfn613.
- [53] M. Noordzij, E.M. Cranenburg, L.F. Engelsman, M.M. Hermans, E.W. Boeschoten, V.M. Brandenburg, et al., Progression of aortic calcification is associated with disorders of mineral metabolism and mortality in chronic dialysis patients, *Nephrol. Dial. Transplant*. 26 (2011) 1662–1669. doi:10.1093/ndt/gfq582.
- [54] R. Baczynski, S.G. Massry, R. Kohan, M. Magott, Y. Saglikes, N. Brautbar, Effect of parathyroid hormone on myocardial energy metabolism in the rat, *Kidney Int*. 27 (1985) 718–725. doi:10.1038/ki.1985.71.
- [55] S.G. Massry, M. Smogorzewski, Mechanisms through which parathyroid hormone mediates its deleterious effects on organ function in uremia, *Semin Nephrol*. 14 (1994) 219–231.
- [56] K. Amann, E. Ritz, Cardiac disease in chronic uremia: pathophysiology, *Advances in renal replacement ...*, 1997.
- [57] S. Mazzaferro, G. Coen, S. Bandini, P.P. Borgatti, M. Ciaccheri, D. Diacinti, et al., Role of ageing, chronic renal failure and dialysis in the calcification of mitral annulus, *Nephrology Dialysis Transplantation*. 8 (1993) 335–340.
- [58] M. Kosch, M. Hausberg, K. Vormbrock, K. Kisters, G. Gabriels, K.H. Rahn, et al., Impaired flow-mediated vasodilation of the brachial artery in patients with primary hyperparathyroidism improves after parathyroidectomy, *Cardiovascular Research*. 47 (2000) 813–818. doi:10.1016/S0008-6363(00)00130-9.
- [59] K. Amann, J. Törnig, C. Flechtenmacher, A. Nabokov, G. Mall, E. Ritz, Blood-pressure-independent wall thickening of intramyocardial arterioles in experimental uraemia: evidence for a permissive action of PTH, *Nephrology Dialysis Transplantation*. 10 (1995) 2043–2048.
- [60] T.L. Nickolas, E. Stein, A. Cohen, V. Thomas, R.B. Staron, D.J. McMahon, et al., Bone mass and microarchitecture in CKD patients with



- fracture, *J. Am. Soc. Nephrol.* 21 (2010) 1371–1380.  
doi:10.1681/ASN.2009121208.
- [61] T.D.T. Vu, X.F. Wang, Q. Wang, N.E. Cusano, D. Irani, B.C. Silva, et al., New insights into the effects of primary hyperparathyroidism on the cortical and trabecular compartments of bone, *Bone*. 55 (2013) 57–63.
- [62] D. Cejka, J.M. Patsch, M. Weber, D. Diarra, M. Riegersperger, Z. Kikic, et al., Bone Microarchitecture in Hemodialysis Patients Assessed by HR-pQCT, *Clinical Journal of the American Society of Nephrology*. 6 (2011) 2264–2271. doi:10.2215/CJN.09711010.
- [63] J.M. Bargman, K. Skorecki, Chapter 280. Chronic kidney disease, *Harrison's Principles of Internal Medicine*. 18th ed. New ... , 2012.
- [64] N. Shobeiri, M.A. Adams, R.M. Holden, Vascular calcification in animal models of CKD: A review, *Am J Nephrol*. 31 (2010) 471–481.  
doi:10.1159/000299794.
- [65] T.D. Hewitson, S.G. Holt, E.R. Smith, Animal models to study links between cardiovascular disease and renal failure and their relevance to human pathology, *Frontiers in Immunology*. (2015).  
doi:10.3389/fimmu.2015.00465.
- [66] M. Rambausek, E. Ritz, G. Mall, O. Mehls, H. Katus, Myocardial hypertrophy in rats with renal insufficiency, *Kidney Int.* 28 (1985) 775–782. doi:10.1038/ki.1985.197.
- [67] S. Lekawanvijit, A.R. Kompa, M. Manabe, B.H. Wang, Chronic kidney disease-induced cardiac fibrosis is ameliorated by reducing circulating levels of a non-dialysable uremic toxin, indoxyl sulfate, *PLoS ....* (2012).  
doi:10.1371/journal.pone.0041281.
- [68] K. Amann, G. Wiest, G. Zimmer, N. Gretz, E. Ritz, G. Mall, Reduced capillary density in the myocardium of uremic rats—A stereological study, *Kidney Int.* 42 (1992) 1079–1085. doi:10.1038/ki.1992.390.
- [69] S. Kadokawa, T. Matsumoto, H. Naito, Assessment of trabecular bone architecture and intrinsic properties of cortical bone tissue in a mouse model of chronic kidney disease, *Journal of Hard Tissue ....* (2011).
- [70] Y. Iwasaki, J.J. Kazama, H. Yamato, H. Shimoda, M. Fukagawa, Accumulated uremic toxins attenuate bone mechanical properties in rats with chronic kidney disease, *Bone*. 57 (2013) 477–483.  
doi:10.1016/j.bone.2013.07.037.
- [71] S. Nagao, M. Kugita, D. Yoshihara, T. Yamaguchi, Animal models for human polycystic kidney disease, *Experimental Animals*. (2012).
- [72] S.M. Moe, N.X. Chen, M.F. Seifert, R.M. Sinders, D. Duan, X. Chen, et al., A rat model of chronic kidney disease-mineral bone disorder, *Kidney Int.* 75 (2008) 176–184. doi:10.1038/ki.2008.456.
- [73] M.R. Allen, N.X. Chen, V.H. Gattone, X. Chen, A.J. Carr, P. LeBlanc, et al., Skeletal effects of zoledronic acid in an animal model of chronic kidney disease, *Osteoporos Int.* 24 (2012) 1471–1481.  
doi:10.1007/s00198-012-2103-x.
- [74] M.R. Allen, C.L. Newman, N. Chen, M. Granke, J.S. Nyman, S.M. Moe, Changes in skeletal collagen cross-links and matrix hydration in high-

- and low-turnover chronic kidney disease, *Osteoporos Int.* 26 (2014) 977–985. doi:10.1007/s00198-014-2978-9.
- [75] J.T. Fleming, M.T. Barati, D.J. Beck, J.C. Dodds, Bone blood flow and vascular reactivity, *Cells Tissues ....* 169 (2001) 279–284. doi:10.1159/000047892.
- [76] R.E. Tomlinson, M.J. Silva, Skeletal Blood Flow in Bone Repair and Maintenance, Nature Publishing Group. 1 (2014) 311–322. doi:10.4248/BR201304002.
- [77] C. Maes, T. Kobayashi, M.K. Selig, S. Torrekens, S.I. Roth, S. Mackem, et al., Osteoblast Precursors, but Not Mature Osteoblasts, Move into Developing and Fractured Bones along with Invading Blood Vessels, *Developmental Cell.* 19 (2010) 329–344. doi:10.1016/j.devcel.2010.07.010.
- [78] O. Grundnes, O. Reikerås, Blood flow and mechanical properties of healing bone, *Acta Orthopaedica Scandinavica.* 63 (2009) 487–491. doi:10.3109/17453679209154720.
- [79] C. Carulli, M. Innocenti, M.L. Brandi, Bone vascularization in normal and disease conditions, *Frontiers in Endocrinology.* (2013). doi:10.3389/fendo.2013.00106/abstract.
- [80] I. McCarthy, The Physiology of Bone Blood Flow: A Review, *J Bone Joint Surg Am.* 88 (2006) 1–6. doi:10.2106/jbjs.f.00890.
- [81] M. Marenzana, T.R. Arnett, The Key Role of the Blood Supply to Bone, *Bone Res.* 1 (2013) 203–215. doi:10.4248/BR201303001.
- [82] R.D. Prisby, J.M. Swift, S.A. Bloomfield, H.A. Hogan, M.D. Delp, Altered bone mass, geometry and mechanical properties during the development and progression of type 2 diabetes in the Zucker diabetic fatty rat, *J. Endocrinol.* 199 (2008) 379–388. doi:10.1677/JOE-08-0046.
- [83] P.N. Colleran, M.K. Wilkerson, S.A. Bloomfield, L.J. Suva, R.T. Turner, M.D. Delp, Alterations in skeletal perfusion with simulated microgravity: a possible mechanism for bone remodeling, *J. Appl. Physiol.* 89 (2000) 1046–1054.
- [84] J.N. Stabley, R.D. Prisby, B.J. Behnke, M.D. Delp, Type 2 diabetes alters bone and marrow blood flow and vascular control mechanisms in the ZDF rat, *Journal of Endocrinology.* 225 (2015) 47–58. doi:10.1530/JOE-14-0514.
- [85] J.N. Stabley, R.D. Prisby, B.J. Behnke, M.D. Delp, Chronic skeletal unloading of the rat femur: mechanisms and functional consequences of vascular remodeling, *Bone.* 57 (2013) 355–360. doi:10.1016/j.bone.2013.09.003.
- [86] R.D. Prisby, J.M. Dominguez, J. Muller-Delp, M.R. Allen, M.D. Delp, Aging and estrogen status: a possible endothelium-dependent vascular coupling mechanism in bone remodeling, *PLoS ONE.* 7 (2012) e48564. doi:10.1371/journal.pone.0048564.
- [87] R.D. Prisby, M.W. Ramsey, B.J. Behnke, J.M. Dominguez II, A.J. Donato, M.R. Allen, et al., Aging Reduces Skeletal Blood Flow,

- Endothelium-Dependent Vasodilation, and NO Bioavailability in Rats, *J Bone Miner Res.* 22 (2007) 1280–1288. doi:10.1359/jbmr.070415.
- [88] R.Y. Kwon, D.R. Meays, W.J. Tang, J.A. Frangos, Microfluidic enhancement of intramedullary pressure increases interstitial fluid flow and inhibits bone loss in hindlimb suspended mice, *J Bone Miner Res.* 25 (2010) 1798–1807. doi:10.1002/jbmr.74.
- [89] A.P. Bergula, W. Huang, J.A. Frangos, Femoral vein ligation increases bone mass in the hindlimb suspended rat, *Bone.* 24 (1999) 171–177.
- [90] R. Prisby, T. Menezes, J. Campbell, Vasodilation to PTH (1-84) in bone arteries is dependent upon the vascular endothelium and is mediated partially via VEGF signaling, *Bone.* 54 (2013) 68–75. doi:10.1016/j.bone.2013.01.028.
- [91] R. Prisby, A. Guignandon, Intermittent PTH (1–84) is osteoanabolic but not osteoangiogenic and relocates bone marrow blood vessels closer to bone-forming sites, *Journal of Bone and ...* (2011). doi:10.1002/jbmr.523).
- [92] E. Schipani, C. Maes, G. Carmeliet, G.L. Semenza, Regulation of osteogenesis-angiogenesis coupling by HIFs and VEGF, *J Bone Miner Res.* 24 (2009) 1347–1353. doi:10.1359/jbmr.090602.
- [93] T.R. Arnett, Acidosis, hypoxia and bone, *Arch. Biochem. Biophys.* 503 (2010) 103–109. doi:10.1016/j.abb.2010.07.021.
- [94] M. Laroche, Intraosseous circulation from physiology to disease, *Joint Bone Spine.* 69 (2002) 262–269.
- [95] T.R. Arnett, D.C. Gibbons, J.C. Utting, I.R. Orriss, A. Hoebertz, M. Rosendaal, et al., Hypoxia is a major stimulator of osteoclast formation and bone resorption, *J. Cell. Physiol.* 196 (2003) 2–8. doi:10.1002/jcp.10321.
- [96] J.C. Utting, A.M. Flanagan, A. Brandao-Burch, I.R. Orriss, T.R. Arnett, Hypoxia stimulates osteoclast formation from human peripheral blood, *Cell Biochem Funct.* 28 (2010) 374–380. doi:10.1002/cbf.1660.
- [97] T.C. Dandajena, M.A. Ihnat, B. Disch, Hypoxia triggers a HIF-mediated differentiation of peripheral blood mononuclear cells into osteoclasts, *Orthodontics & ...* (2012). doi:10.1111/j.1601-6343.2011.01530.x.
- [98] J.C. Utting, S.P. Robins, A. Brandao-Burch, I.R. Orriss, J. Behar, T.R. Arnett, Hypoxia inhibits the growth, differentiation and bone-forming capacity of rat osteoblasts, *Exp. Cell Res.* 312 (2006) 1693–1702. doi:10.1016/j.yexcr.2006.02.007.
- [99] Q. Zhao, X. Shen, W. Zhang, G. Zhu, J. Qi, L. Deng, Mice with increased angiogenesis and osteogenesis due to conditional activation of HIF pathway in osteoblasts are protected from ovariectomy induced bone loss, *Bone.* 50 (2012) 763–770. doi:10.1016/j.bone.2011.12.003.
- [100] K.N. Shah, J. Racine, L.C. JONES, R.K. Aaron, Pathophysiology and risk factors for osteonecrosis, *Curr Rev Musculoskelet Med.* 8 (2015) 201–209. doi:10.1007/s12178-015-9277-8.
- [101] Y. Feng, S.-H. Yang, B.-J. Xiao, W.-H. Xu, S.-N. Ye, T. Xia, et al., Decreased in the number and function of circulation endothelial

- progenitor cells in patients with avascular necrosis of the femoral head, *Bone*. 46 (2010) 32–40. doi:10.1016/j.bone.2009.09.001.
- [102] Z. Stark, R. Savarirayan, Osteopetrosis, *Orphanet J Rare Dis*. 4 (2009) 5–12. doi:10.1186/1750-1172-4-5.
- [103] J. Filipowska, K.A. Tomaszewski, Ł. Niedźwiedzki, J.A. Walocha, T. Niedźwiedzki, The role of vasculature in bone development, regeneration and proper systemic functioning, *Angiogenesis*. 20 (2017) 291–302. doi:10.1007/s10456-017-9541-1.
- [104] A. Oikawa, M. Siragusa, F. Quaini, G. Mangialardi, R.G. Katare, A. Caporali, et al., Diabetes mellitus induces bone marrow microangiopathy, *Arteriosclerosis, Thrombosis, and Vascular Biology*. 30 (2010) 498–508. doi:10.1161/ATVBAHA.109.200154.
- [105] S. Portal-Núñez, J.A. Ardura, D. Lozano, O.H. Bolívar, A. López-Herradón, I. Gutiérrez-Rojas, et al., Adverse Effects of Diabetes Mellitus on the Skeleton of Aging Mice, *J. Gerontol. a Biol. Sci. Med. Sci*. 71 (2016) 290–299. doi:10.1093/gerona/glv160.
- [106] M.W. Aref, E.A. Swallow, N.X. Chen, S.M. Moe, M.R. Allen, Skeletal vascular perfusion is altered in chronic kidney disease, *Bone Reports*. 8 (2018) 215–220. doi:10.1016/j.bonr.2018.05.001.
- [107] N.X. Chen, K.D. O’Neill, M.R. Allen, C.L. Newman, S.M. Moe, Low Bone Turnover in Chronic Kidney Disease Is Associated with Decreased VEGF-A Expression and Osteoblast Differentiation, *Am J Nephrol*. 41 (2015) 464–473. doi:10.1159/000438461.
- [108] R. Burkhardt, G. Kettner, W. Böhm, M. Schmidmeier, R. Schlag, B. Frisch, et al., Changes in trabecular bone, hematopoiesis and bone marrow vessels in aplastic anemia, primary osteoporosis, and old age: a comparative histomorphometric study, *Bone*. 8 (1987) 157–164.
- [109] E. Regan, J. Jaramillo, It's the fracture that matters -bone disease in COPD patients, *Copd*. 9 (2012) 319–321. doi:10.3109/15412555.2012.708544.
- [110] B. Roche, A. Vanden-Bossche, L. Malaval, M. Normand, M. Jannot, R. Chaux, et al., Parathyroid Hormone 1-84 Targets Bone Vascular Structure and Perfusion in Mice: Impacts of Its Administration Regimen and of Ovariectomy, *J Bone Miner Res*. 29 (2014) 1608–1618. doi:10.1002/jbmr.2191.
- [111] D. Santini, B. Vincenzi, G. Avvisati, Pamidronate Induces Modifications of Circulating Angiogenetic Factors in Cancer Patients, *Clinical Cancer Research*. Vol. 8, 1080–1084, May 2002 (2002).
- [112] J. Kapitola, J. Zák, Effect of pamidronate on bone blood flow in oophorectomized rats, *Physiol Res*. 47 (1998) 237–240.
- [113] L.J. Suva, C. Washam, R.W. Nicholas, R.J. Griffin, Bone metastasis: mechanisms and therapeutic opportunities, *Nat Rev Endocrinol*. 7 (2011) 208–218. doi:10.1038/nrendo.2010.227.
- [114] G. Bridgeman, M. Brookes, Blood supply to the human femoral diaphysis in youth and senescence, *Journal of Anatomy*. 188 ( Pt 3) (1996) 611–621.

- [115] V. Yoon, N.M. Maalouf, K. Sakhaee, The effects of smoking on bone metabolism, *Osteoporos Int.* 23 (2012) 2081–2092. doi:10.1007/s00198-012-1940-y.
- [116] R.F. Klein, K.A. Fausti, A.S. Carlos, Ethanol inhibits human osteoblastic cell proliferation, *Alcohol. Clin. Exp. Res.* 20 (1996) 572–578.
- [117] P.B. Rapuri, J.C. Gallagher, K.E. Balhorn, K.L. Ryschon, Alcohol intake and bone metabolism in elderly women, *The American Journal of Clinical Nutrition.* 72 (2000) 1206–1213. doi:10.1093/ajcn/72.5.1206.
- [118] G.P. Ashcroft, N.T. Evans, D. Roeda, M. Dodd, J.R. Mallard, R.W. Porter, et al., Measurement of blood flow in tibial fracture patients using positron emission tomography, *J Bone Joint Surg Br.* 74 (1992) 673–677. doi:10.1016/S0925-8388(16)30699-5.
- [119] H. Anetzberger, E. Thein, M. Becker, B. Zwissler, K. Messmer, Microspheres Accurately Predict Regional Bone Blood Flow, *Clinical Orthopaedics and Related Research.* 424 (2004) 253–265. doi:10.1097/01.blo.0000128281.67589.b4.
- [120] O.J. Kirkeby, T. Berg-Larsen, Regional blood flow and strontium-85 incorporation rate in the rat hindlimb skeleton, *J. Orthop. Res.* 9 (1991) 862–868. doi:10.1002/jor.1100090612.
- [121] C. Schimmel, D. Frazer, S.R. Huckins, R.W. Glenny, Validation of automated spectrofluorimetry for measurement of regional organ perfusion using fluorescent microspheres, *Computer Methods and Programs in Biomedicine.* 62 (2000) 115–125. doi:10.1016/S0169-2607(00)00057-2.
- [122] R.W. Glenny, S. Bernard, M. Brinkley, Validation of fluorescent-labeled microspheres for measurement of regional organ perfusion, *J. Appl. Physiol.* 74 (1993) 2585–2597.
- [123] W.A. Altemeier, S. McKinney, R.W. Glenny, Fractal nature of regional ventilation distribution, *Journal of Applied Physiology.* 88 (2000) 1551–1557.
- [124] M.P. Hlastala, S.L. Bernard, H.H. Erickson, M.R. Fedde, E.M. Gaughan, R. McMurphy, et al., Pulmonary blood flow distribution in standing horses is not dominated by gravity, *Journal of Applied Physiology.* 81 (1996) 1051–1061.
- [125] G. De Visscher, M. Haseldonckx, W. Flameng, M. Borgers, R.S. Reneman, K. van Rossem, Development of a novel fluorescent microsphere technique to combine serial cerebral blood flow measurements with histology in the rat, *Journal of Neuroscience Methods.* 122 (2003) 149–156. doi:10.1016/S0165-0270(02)00316-3.
- [126] M.A. Serrat, Measuring bone blood supply in mice using fluorescent microspheres, *Nature Protocols.* 4 (2009) 1779–1758. doi:10.1038/nprot.2009.190.
- [127] E.O. Johnson, K. Sultanis, P.N. Soucacos, Vascular anatomy and microcirculation of skeletal zones vulnerable to osteonecrosis: vascularization of the femoral head, *Orthopedic Clinics of North America.* 35 (2004) 285–291. doi:10.1016/j.ocl.2004.03.002.

- [128] M. Brookes, *The Blood Supply of Bone*, Butterworth-Heinemann, 1971.
- [129] G.B. Bleeker, J.J. Bax, P. Steendijk, M.J. Schalij, E.E. van der Wall, Left ventricular dyssynchrony in patients with heart failure: pathophysiology, diagnosis and treatment, *Nat Clin Pract Cardiovasc Med*. 3 (2006) 213–219. doi:10.1038/ncpcardio0505.
- [130] S.M. Moe, N.X. Chen, Mechanisms of Vascular Calcification in Chronic Kidney Disease, *Journal of the American Society of Nephrology*. 19 (2008) 213–216. doi:10.1681/ASN.2007080854.
- [131] J. Malyszko, Mechanism of endothelial dysfunction in chronic kidney disease, *Clin. Chim. Acta*. 411 (2010) 1412–1420. doi:10.1016/j.cca.2010.06.019.
- [132] M. Le Brocq, S.J. Leslie, P. Milliken, I.L. Megson, Endothelial dysfunction: from molecular mechanisms to measurement, clinical implications, and therapeutic opportunities, *Antioxid. Redox Signal*. 10 (2008) 1631–1674. doi:10.1089/ars.2007.2013.
- [133] S. Vettoretti, P. Ochodnický, H. Buikema, R.H. Henning, C.A. Kluppel, D. de Zeeuw, et al., Altered myogenic constriction and endothelium-derived hyperpolarizing factor-mediated relaxation in small mesenteric arteries of hypertensive subtotaly nephrectomized rats, *J. Hypertens*. 24 (2006) 2215–2223. doi:10.1097/01.hjh.0000249699.04113.36.
- [134] S. Yoda, K. Nakanishi, A. Tano, Y. Kasamaki, S. Kunimoto, N. Matsumoto, et al., Risk stratification of cardiovascular events in patients at all stages of chronic kidney disease using myocardial perfusion SPECT, *J Cardiol*. 60 (2012) 377–382. doi:10.1016/j.jjcc.2012.06.011.
- [135] A.M. Murray, Cognitive impairment in the aging dialysis and chronic kidney disease populations: an occult burden, *Advances in Chronic Kidney Disease*. 15 (2008) 123–132. doi:10.1053/j.ackd.2008.01.010.
- [136] M.S. Fernando, J.E. Simpson, F. Matthews, C. Brayne, C.E. Lewis, R. Barber, et al., White Matter Lesions in an Unselected Cohort of the Elderly, *Stroke*. 37 (2006) 1391–1398. doi:10.1161/01.STR.0000221308.94473.14.
- [137] C.W. McIntyre, L.E.A. Harrison, M.T. Eldehni, H.J. Jefferies, C.C. Szeto, S.G. John, et al., Circulating Endotoxemia: A Novel Factor in Systemic Inflammation and Cardiovascular Disease in Chronic Kidney Disease, *Clinical Journal of the American Society of Nephrology*. 6 (2011) 133–141. doi:10.2215/CJN.04610510.
- [138] P. Gross, I. Six, S. Kamel, Z.A. Massy, Vascular Toxicity of Phosphate in Chronic Kidney Disease, *Circ J*. 78 (2014) 2339–2346. doi:10.1253/circj.CJ-14-0735.
- [139] I.L. Geenen, F.F. Kolk, D.G. Molin, A. Wagenaar, M.G. Compeer, J.H. Tordoir, et al., Nitric Oxide Resistance Reduces Arteriovenous Fistula Maturation in Chronic Kidney Disease in Rats, *PLoS ONE*. 11 (2016) e0146212. doi:10.1371/journal.pone.0146212.
- [140] S.C. Palmer, A. Hayen, P. Macaskill, F. Pellegrini, Serum levels of phosphorus, parathyroid hormone, and calcium and risks of death and

- cardiovascular disease in individuals with chronic kidney disease: a systematic ... , *Jama*. 305 (2011) 1119. doi:10.1001/jama.2011.308.
- [141] N. Dhaun, The Endothelin System and Its Antagonism in Chronic Kidney Disease, *Journal of the American Society of Nephrology*. 17 (2006) 943–955. doi:10.1681/ASN.2005121256.
- [142] V. Costa-Hong, L.A. Bortolotto, V. Jorgetti, F. Consolim-Colombo, E.M. Krieger, J.J.G. de Lima, Oxidative stress and endothelial dysfunction in chronic kidney disease, *Arquivos Brasileiros De Cardiologia*. 92 (2009) 413–418. doi:10.1590/S0066-782X2009000500013.
- [143] B. Afsar, K. Turkmen, A. Covic, M. Kanbay, An update on coronary artery disease and chronic kidney disease, *Int J Nephrol*. 2014 (2014) 767424. doi:10.1155/2014/767424.
- [144] A.A. Haydar, A. Covic, H. Colhoun, M. Rubens, D.J.A. Goldsmith, Coronary artery calcification and aortic pulse wave velocity in chronic kidney disease patients, *Kidney Int*. 65 (2004) 1790–1794. doi:10.1111/j.1523-1755.2004.00581.x.
- [145] O.Z. Ameer, R. Boyd, M. Butlin, A.P. Avolio, J.K. Phillips, Abnormalities associated with progressive aortic vascular dysfunction in chronic kidney disease, *Front. Physiol*. 6 (2015) 1–13. doi:10.3389/fphys.2015.00150.
- [146] F.T. Spradley, J.J. White, W.D. Paulson, D.M. Pollock, J.S. Pollock, Differential regulation of nitric oxide synthase function in aorta and tail artery from 5/6 nephrectomized rats, *Physiol Rep*. 1 (2013) e00145–n/a. doi:10.1002/phy2.145.
- [147] P. Jolma, P. Koobi, J. Kalliovalkama, H. Saha, Treatment of secondary hyperparathyroidism by high calcium diet is associated with enhanced resistance artery relaxation in experimental renal failure, *Nephrology Dialysis ....* 18 (2003) 2560–2569. doi:10.1093/ndt/gfg374.
- [148] C. Aalkjaer, E.B. Pedersen, H. Danielsen, O. Fjeldborg, B. Jespersen, T. Kjaer, et al., Morphological and functional characteristics of isolated resistance vessels in advanced uraemia, *Clin. Sci*. 71 (1986) 657–663.
- [149] C. Aalkjaer, M.J. Mulvany, Functional and morphological properties of human omental resistance vessels, *Blood Vessels*. 18 (1981) 233–244.
- [150] M. Pacurari, D. Xing, R.H.P. Hilgers, Y.Y. Guo, Z. Yang, F.G. Hage, Endothelial cell transfusion ameliorates endothelial dysfunction in 5/6 nephrectomized rats, *Am. J. Physiol. Heart Circ. Physiol*. 305 (2013) H1256–64. doi:10.1152/ajpheart.00132.2013.
- [151] D.I. New, A.M. Chesser, R.C. Thuraingham, M.M. Yaqoob, Structural remodeling of resistance arteries in uremic hypertension, *Kidney Int*. 65 (2004) 1818–1825. doi:10.1111/j.1523-1755.2004.00591.x.
- [152] J. Törnig, K. Amann, E. Ritz, C. Nichols, Arteriolar wall thickening, capillary rarefaction and interstitial fibrosis in the heart of rats with renal failure: the effects of ramipril, nifedipine and moxonidine, *Journal of the ....* (1996).

- [153] K.-D. Schlüter, H.M. Piper, Cardiovascular actions of parathyroid hormone and parathyroid hormone-related peptide, *Cardiovascular Research*. 37 (1998) 34–41. doi:10.1016/S0008-6363(97)00194-6.
- [154] J. Kapitola, J. Zák, Effect of parathormone on bone blood flow in rats-- possible role of NO, *Sb Lek.* (2002).
- [155] A.E. Moore, G.M. Blake, K.A. Taylor, A.E. Rana, M. Wong, P. Chen, et al., Assessment of regional changes in skeletal metabolism following 3 and 18 months of teriparatide treatment, *J Bone Miner Res.* 25 (2010) 960–967. doi:10.1359/jbmr.091108.
- [156] C.L. Newman, S.M. Moe, N.X. Chen, M.A. Hammond, J.M. Wallace, J.S. Nyman, et al., Cortical Bone Mechanical Properties Are Altered in an Animal Model of Progressive Chronic Kidney Disease, *PLoS ONE*. 9 (2014) e99262–8. doi:10.1371/journal.pone.0099262.
- [157] S.M. Moe, N.X. Chen, C.L. Newman, V.H. Gattone II, J.M. Organ, X. Chen, et al., A Comparison of Calcium to Zoledronic Acid for Improvement of Cortical Bone in an Animal Model of CKD, *J Bone Miner Res.* 29 (2014) 902–910. doi:10.1002/jbmr.2089.
- [158] S.G. Rostand, T.B. Drüeke, Parathyroid hormone, vitamin D, and cardiovascular disease in chronic renal failure, *Kidney Int.* 56 (1999) 383–392. doi:10.1046/j.1523-1755.1999.00575.x.
- [159] R. Wang, L. Wu, E. Karpinski, P.K. Pang, The changes in contractile status of single vascular smooth muscle cells and ventricular cells induced by bPTH-(1-34), *Life Sci.* 52 (1993) 793–801.
- [160] J.N. MacPherson, P. Tothill, Bone Blood Flow and Age in the Rat, *Clin. Sci.* 54 (2012) 1–3. doi:10.1042/cs0540111.
- [161] M. Okubo, T. Kinoshita, T. Yukimura, Y. Abe, A. Shimazu, Experimental study of measurement of regional bone blood flow in the adult mongrel dog using radioactive microspheres, *Clinical Orthopaedics and Related Research.* (1979) 263–270.
- [162] A. Schoutens, P. Bergmann, M. Verhas, Bone blood flow measured by <sup>85</sup>Sr microspheres and bone seeker clearances in the rat, *AJP: Heart and Circulatory Physiology.* 236 (1979) H1–H6.
- [163] K.S. McDonald, M.D. Delp, R.H. Fitts, Effect of hindlimb unweighting on tissue blood flow in the rat, *Journal of Applied Physiology.* 72 (1992) 2210–2218.
- [164] S.A. Bloomfield, H.A. Hogan, M.D. Delp, Decreases in bone blood flow and bone material properties in aging Fischer-344 rats, *Clinical Orthopaedics and Related Research.* 396 (2002) 248–257. doi:10.1097/00003086-200203000-00036.
- [165] J.M. Bernard, M.F. Doursout, P. Wouters, C.J. Hartley, M. Cohen, R.G. Merin, et al., Effects of enflurane and isoflurane on hepatic and renal circulations in chronically instrumented dogs, *Anesthesiology.* 74 (1991) 298–302. doi:10.1097/00000542-199102000-00016.
- [166] J.M. Bernard, P.F. Wouters, M.F. Doursout, B. Florence, J.E. Chelly, R.G. Merin, Effects of sevoflurane and isoflurane on cardiac and



- coronary dynamics in chronically instrumented dogs, *Anesthesiology*. 72 (1990) 659–662. doi:10.1097/00000542-199004000-00014.
- [167] L. Demer, Y. Tintut, The bone–vascular axis in chronic kidney disease, *Current Opinion in Nephrology and Hypertension*. 19 (2010) 349–353. doi:10.1097/MNH.0b013e32833a3d67.
- [168] K. Kundhal, C.E. Lok, Clinical epidemiology of cardiovascular disease in chronic kidney disease, *Nephron Clin Pract*. 101 (2005) c47–52. doi:10.1159/000086221.
- [169] A.M. Alem, D.J. Sherrard, D.L. Gillen, N.S. Weiss, S.A. Beresford, S.R. Heckbert, et al., Increased risk of hip fracture among patients with end-stage renal disease, *Kidney Int*. 58 (2000) 396–399. doi:10.1046/j.1523-1755.2000.00178.x.
- [170] M.W. Aref, E. Akans, M.R. Allen, Assessment of regional bone tissue perfusion in rats using fluorescent microspheres, *Bone Reports*. 6 (2017) 140–144.
- [171] S.M. Moe, N.X. Chen, M.F. Seifert, R.M. Sindors, D. Duan, X. Chen, et al., A rat model of chronic kidney disease-mineral bone disorder, *Kidney Int*. 75 (2009) 176–184. doi:10.1038/ki.2008.456.
- [172] C.H. Hsueh, N.X. Chen, S.F. Lin, P.S. Chen, V.H. Gattone, M.R. Allen, et al., Pathogenesis of Arrhythmias in a Model of CKD, *Journal of the American Society of Nephrology*. 25 (2014) 2812–2821. doi:10.1681/ASN.2013121343.
- [173] S.M. Moe, S.M. Moe, M.F. Seifert, M.F. Seifert, N.X. Chen, N.X. Chen, et al., R-568 reduces ectopic calcification in a rat model of chronic kidney disease-mineral bone disorder (CKD-MBD), *Nephrology Dialysis Transplantation*. 24 (2009) 2371–2377. doi:10.1093/ndt/gfp078.
- [174] T.H. Adair, W.J. Gay, J.P. Montani, Growth regulation of the vascular system: evidence for a metabolic hypothesis, *Am. J. Physiol*. 259 (1990) R393–404. doi:10.1152/ajpregu.1990.259.3.R393.
- [175] G. Rashid, J. Bernheim, J. Green, S. Benchetrit, Parathyroid hormone stimulates the endothelial expression of vascular endothelial growth factor, *European Journal of Clinical Investigation*. 38 (2008) 798–803. doi:10.1111/j.1365-2362.2008.02033.x.
- [176] H. Matsuzaki, G.R. Wohl, D.V. Novack, J.A. Lynch, M.J. Silva, Damaging fatigue loading stimulates increases in periosteal vascularity at sites of bone formation in the rat ulna, *Calcif Tissue Int*. 80 (2007) 391–399. doi:10.1007/s00223-007-9031-3.
- [177] M.R. Allen, N.X. Chen, V.H. Gattone, X. Chen, A.J. Carr, P. LeBlanc, et al., Skeletal effects of zoledronic acid in an animal model of chronic kidney disease, *Osteoporos Int*. 24 (2013) 1471–1481. doi:10.1007/s00198-012-2103-x.
- [178] J. Kapitola, J. Zák, [Effect of parathormone on bone blood flow in rats--possible role of NO], *Sb Lek*. 104 (2003) 133–137.
- [179] K.U.W. Group, KDIGO 2017. Clinical Practice Guideline Update for the Diagnosis, Evaluation, Prevention, and Treatment of Chronic Kidney

- Disease — Mineral and Bone Disorder (CKD-MBD), *Kidneys*. 6 (2017) 149–154. doi:10.22141/2307-1257.6.3.2017.109030.
- [180] P. Kandula, M. Dobre, J.D. Schold, M.J. Schreiber, R. Mehrotra, S.D. Navaneethan, Vitamin D supplementation in chronic kidney disease: a systematic review and meta-analysis of observational studies and randomized controlled trials, *Clin J Am Soc Nephrol*. 6 (2011) 50–62. doi:10.2215/CJN.03940510.
- [181] S.M. Moe, N.X. Chen, C.L. Newman, J.M. Organ, M. Kneissel, I. Kramer, et al., Anti-Sclerostin Antibody Treatment in a Rat Model of Progressive Renal Osteodystrophy, *J Bone Miner Res*. 30 (2015) 499–509. doi:10.1002/jbmr.2372.
- [182] C.L. Newman, N.X. Chen, E. Smith, M. Smith, D. Brown, S.M. Moe, et al., Compromised vertebral structural and mechanical properties associated with progressive kidney disease and the effects of traditional pharmacological interventions, *Bone*. 77 (2015) 50–56. doi:10.1016/j.bone.2015.04.021.
- [183] L. Yu, J.E. Tomlinson, S.T. Alexander, K. Hensley, C.-Y. Han, D. Dwyer, et al., Etelcalcetide, A Novel Calcimimetic, Prevents Vascular Calcification in A Rat Model of Renal Insufficiency with Secondary Hyperparathyroidism, *Calcif Tissue Int*. 101 (2017) 641–653. doi:10.1007/s00223-017-0319-7.
- [184] M.L. Bouxsein, S.K. Boyd, B.A. Christiansen, R.E. Guldberg, K.J. Jepsen, R. Müller, Guidelines for assessment of bone microstructure in rodents using micro-computed tomography, *J Bone Miner Res*. 25 (2010) 1468–1486. doi:10.1002/jbmr.141.
- [185] N.X. Chen, S.M. Moe, Vascular Calcification: Pathophysiology and Risk Factors, *Curr Hypertens Rep*. 14 (2012) 228–237. doi:10.1007/s11906-012-0265-8.
- [186] S. Gohin, A. Carriero, C. Chenu, A.A. Pitsillides, T.R. Arnett, M. Marenzana, The anabolic action of intermittent parathyroid hormone on cortical bone depends partly on its ability to induce nitric oxide-mediated vasorelaxation in BALB/c mice, *Cell Biochem Funct*. 34 (2016) 52–62. doi:10.1002/cbf.3164.
- [187] R.N. Moorthi, W. Fadel, G.J. Eckert, K. Ponsler-Sipes, S.M. Moe, C. Lin, Bone marrow fat is increased in chronic kidney disease by magnetic resonance spectroscopy, *Osteoporos Int*. 26 (2015) 1801–1807. doi:10.1007/s00198-015-3064-7.
- [188] E.A. Swallow, M.W. Aref, N. Chen, I. Byiringiro, M.A. Hammond, B.P. McCarthy, et al., Skeletal accumulation of fluorescently tagged zoledronate is higher in animals with early stage chronic kidney disease, (2018) 1–8. doi:10.1007/s00198-018-4589-3.
- [189] R.N. Moorthi, S.M. Moe, Recent advances in the noninvasive diagnosis of renal osteodystrophy, *Kidney Int*. 84 (2013) 886–894. doi:10.1038/ki.2013.254.

- [190] F.H. Sim, P.J. Kelly, Relationship of Bone Remodeling, Oxygen Consumption, and Blood Flow in Bone, *J Bone Joint Surg Am.* 52 (1970) 1377–1389.
- [191] L. Ou-Yang, G.-M. Lu, Dysfunctional microcirculation of the lumbar vertebral marrow prior to the bone loss and intervertebral discal degeneration, *Spine.* 40 (2015) E593–600.
- [192] L.I. Plotkin, R.S. Weinstein, A.M. Parfitt, P.K. Roberson, S.C. Manolagas, T. Bellido, Prevention of osteocyte and osteoblast apoptosis by bisphosphonates and calcitonin, *J. Clin. Invest.* 104 (1999) 1363–1374. doi:10.1172/JCI6800.
- [193] L.I. Plotkin, S.C. Manolagas, T. Bellido, Dissociation of the pro-apoptotic effects of bisphosphonates on osteoclasts from their anti-apoptotic effects on osteoblasts/osteocytes with novel analogs, *Bone.* 39 (2006) 443–452. doi:10.1016/j.bone.2006.02.060.
- [194] C. Duan, MRI in Cancer, 2017.
- [195] N. Kobayashi, Y. Inaba, U. Tateishi, H. Ike, S. Kubota, T. Inoue, et al., Comparison of 18F-fluoride positron emission tomography and magnetic resonance imaging in evaluating early-stage osteoarthritis of the hip, *Nucl Med Commun.* 36 (2015) 84–89. doi:10.1097/MNM.0000000000000214.
- [196] Monroy, M. A., Fang, J., Li, S., & in, L. F. F. (2015). Chronic kidney disease alters vascular smooth muscle cell phenotype. *Front Biosci.*
- [197] D. Togawa, K.-U. Lewandrowski, The Pathophysiology of Spinal Metastases, in: *Cancer in the Spine*, Humana Press, Totowa, NJ, 2006: pp. 17–23. doi:10.1007/978-1-59259-971-4\_3.
- [198] K. Kita, K. Kawai, K. Hirohata, Changes in bone marrow blood flow with aging, *J. Orthop. Res.* 5 (1987) 569–575. doi:10.1002/jor.1100050412.
- [199] L. Balducci, W.B. Ershler, J.M. Bennett, *Anemia in the Elderly*, Springer Science & Business Media, Boston, MA, 2007. doi:10.1007/978-0-387-49506-4.
- [200] Teicher, BA, et al. Antiangiogenic agents and targets: A perspective. (2011). *Antiangiogenic agents and targets: A perspective.*, *Biochem Pharmacol*, 2011 vol. 81(1) pp. 6-12. <http://doi.org/10.1016/j.bcp.2010.09.023>

## CURRICULUM VITAE

**Mohammad W. Aref**

### **Education**

- 2013 - Present      Doctor of Medicine  
Indiana University School of Medicine
- 2015 - 2019        Doctor of Philosophy  
Major: Anatomy and Cell Biology  
Indiana University
- 2010 – 2013        Bachelor of Science  
Major: Biomedical Engineering  
Indiana University-Purdue University at Indianapolis

### **Research Interests**

#### *Intersections of the skeletal and vascular systems*

What systemic, vascular, and skeletal factors play a role in bone dysfunctions and skeletal fractures? What physiologic mechanisms of skeletal homeostasis and mineral metabolism play active roles in systemic disease? What are the factors within disease processes that cause the dysregulation of these physiologic mechanisms? How can this dysregulation be inhibited or reversed in patients with such diseases?

### **Research Experience**

- 2015 - present      Medical Scientist Training Program  
Indiana University School of Medicine  
Mentor: Matthew R. Allen, Ph.D.; Clinical mentor: Sharon Moe, M.D.  
*\*Studying the interactions of the skeletal and vascular systems in Chronic Kidney Disease*
- 2017                    Community Health Research/Quality Improvement Research  
Indiana University Student Outreach Clinic  
Role: Clinic Research Director  
Mentor: Javier Sevilla-Martir, M.D.  
*\*Directed and implemented research projects with the goal of better serving our underserved and underinsured neighbors on the near-east side of Indianapolis*
- 2018 - present      Patient Centered Outcomes Research for Community Health  
University of Chicago

- Role: Project Leader  
Mentor: Aasim Padela, M.D.  
*\*Planning and implementing a Community Engagement Research Project focused around patient-centered outcomes.*
- 2017 Interprofessional Education Research in Community Clinic Setting  
Indiana University School of Medicine  
Role: Research Team Member  
Mentors: Javier Sevilla-Martir, M.D., Andrea Pfeifle, Ed.D. P.T. FNAP  
*\*Participated in research measuring the impact of the interprofessional nature of a community clinic on patient care, patient satisfaction, and interprofessional education.*
- 2016 (summer) ASN Kidney TREKS Program (Kidney Research Intensive)  
American Society of Nephrology  
Role: Kidney Star (Young Investigator Award)  
Mentor: Dr. Mark Zeidel, MD  
*\*Studied kidney physiology through a variety of marine models.*
- 2014 (summer) Student Research Program in Academic Medicine  
Indiana University School of Medicine  
Role: Summer Research Intern  
Mentor: Matthew R. Allen, PhD  
*\*Developed protocol for mechanical testing (reference point indentation) of cartilage.*
- 2012 - 2013 Bone Biology Research  
Indiana University School of Medicine  
Role: Hourly Research Assistant  
Mentor: Matthew R. Allen, PhD  
*\*Developed MATLAB code to gather mechanical information from reference point indentation testing.*
- 2012 Product Development (Device Design and Development)  
Riley Children's Hospital  
Role: Student Researcher  
Advisor: Megan Marine, MD  
*\*Designed device to automate intussusception reduction in children.*
- 2011 Life Health Science Internship  
Indiana University School of Medicine

Mentor: Matthew R. Allen, PhD

*\*Performed histological analysis in a research project determining the anabolic potential of a traditional medicinal compound.*

## Grants

Agency: National Institutes of Health (F30)

Grant: NIH F30 – F30 DK115162

Title: Bone vascular alterations in chronic kidney disease

PI: Aref, Mohammad

Dates: Sep 2017 – May 2021

Agency: Clinical and Translational Sciences Institute of Indiana

Grant: CTSI Predoctoral – UL1TR002529

Title: Bone vascular alterations in chronic kidney disease

PI: Aref, Mohammad

Dates: Jul 2017 – Jul 2019

Agency: National Institutes of Health (T32)

Grant: NIH T32 – AR 065971-01A1

PI: Burr, David B

Role: Trainee

Dates: Jun 2015 – Jun 2017

## Peer-reviewed Publications

1. **MW Aref**, MA Gallant, JM Organ, JM Wallace, CL Newman, DB Burr, DM Brown, MR Allen. In vivo reference point indentation reveals positive effects of raloxifene on mechanical properties following six months of treatment in skeletally mature beagle dogs. *Bone*. 56: 449-453, 2013. PMID: PMC3873633. <http://hdl.handle.net/1805/3375>
2. AP Baumann, **MW Aref**, TL Turnbull, AG Robling, GL Niebur, MR Allen, and RK Roeder. Development of an in vivo rabbit ulnar loading model. *Bone*. 75: 55-61, 2015. PMID: 25683214.
3. JB Krege\*, **MW Aref\***, EM McNerny, JM Wallace, JM Organ, MR Allen. Reference point indentation is insufficient for detecting alterations in traditional mechanical properties of bone under common experimental conditions. *Bone*. 87:97-101, 2016.
4. **MW Aref**, EM Mchnerny, DM Brown, KJ Jepsen, and MR Allen. Zoledronate treatment has different effects in mouse strains with contrasting baseline bone mechanical phenotypes. *Osteoporosis International*. 27:3637-3643, 2016.

5. MR Allen, **MW Aref**. What animal models have taught us about the safety and efficacy of bisphosphonates in chronic kidney disease. *Current Osteoporosis Reports*. 15:171-177, 2017.
6. MR Allen, **MW Aref**, CL Newman, JR Kadakia, JM Wallace. Raloxifene neutralizes bone brittleness induced by anti-remodeling treatment and increases fatigue life through non-cell mediated mechanisms. *Actualizaciones en Osteología*. 2016. Under revision.
7. CN Meixner, **MW Aref**, A Gupta, EM McNerny, D Brown, JM Wallace, MR Allen. Raloxifene improves bone mechanical properties in mice previously treated with zoledronate. *Calcified Tissue International*. 1-17, 2017.
8. **MW Aref**, E Akans, MR Allen. Assessment of regional bone tissue perfusion in rats using fluorescent microspheres. *Bone Reports*. 6:140–144, 2017.
9. RA Larsen, JL Peveler, JB Klutzke, DL Hickman, **MW Aref**, JM Wallace, et al. Effects of daily restraint with and without injections on skeletal properties in C57BL/6NHsd mice. *Lab Animal*, 46(7), 299–301, 2017.
10. MR Allen, E McNerny, **MW Aref**, JM Organ, CL Newman, B McGowan, et al. Effects of combination treatment with alendronate and raloxifene on skeletal properties in a beagle dog model. *PloS one* 12 (8), e0181750, 2017.
11. HM Davis, **MW Aref**, A Aguilar-Perez, R Pacheco-Costa, K Allen, S Valdez, et al. Cx43 overexpression in osteocytes prevents osteocyte apoptosis and preserves cortical bone quality in aging mice. *JBMR Plus*, 1–33, 2018. <http://doi.org/10.1002/jbm4.10035>
12. **MW Aref**, EA Swallow, N Chen, SM Moe, MR Allen. Skeletal vascular perfusion is altered in chronic kidney disease. *Bone Reports*, 8, 215–220. 2018. <http://doi.org/10.1016/j.bonr.2018.05.001>
13. EA Swallow, **MW Aref**, N Chen, I Byiringiro, MA Hammond, BP McCarthy, et al. (2018). Skeletal accumulation of fluorescently tagged zoledronate is higher in animals with early stage chronic kidney disease. *Osteoporosis International*, 29(9), 2139–2146. <http://doi.org/10.1007/s00198-018-4589-3>
14. R Pacheco-Costa, HM Davis, EG Atkinson, JE Dilley, I Byiringiro, **MW Aref**, et al. (2018). Reversal of loss of bone mass in old mice treated with mefloquine. *Bone*, 114, 22–31. 2018. <http://doi.org/10.1016/j.bone.2018.06.002>
15. HM Davis, AL Essex, S Valdez, PJ Deosthale, **MW Aref**, MR Allen, A Bonetto, LI Plotkin. Short-term pharmacologic inhibition of RAGE suppresses bone turnover and muscle atrophy in aging. *Submitted to Aging Cell*. (2018).

16. EM McNerny, DT Buening, **MW Aref**, N Chen, SM Moe, and MR Allen. Time course of rapid bone loss and cortical porosity formation observed by longitudinal microCT in a rat model of CKD. *Submitted to Bone*. (2018).

17. HM Davis, PJ Deosthale, R Pacheco-Costa, AL Essex, EG Atkinson, **MW Aref**, JE Dilley, T Bellido, M Ivan MR Allen, LI Plotkin. Osteocytic miR21 deficiency improves bone strength independent of sex despite having sex divergent effects on osteocyte viability and bone turnover. *Submitted to Nature Communications*. (2018).

18. EL Clinkenbeard, M Noonan, JC Thomas, P Ni, JM Hum, **MW Aref**, EA Swallow, SM Moe, MR. Allen, and KE White. Increased FGF23 protects against detrimental cardio-renal consequences during elevated blood phosphate in CKD. *Submitted to JCI Insight*. (2018).

19. **MW Aref**, EA Swallow, CA Metzger, N Chen, SM Moe, MR Allen. Suppression of parathyroid hormone normalizes chronic kidney disease-induced elevations in cortical bone vascular perfusion. *Submitted to Osteoporosis International*. (2018).

### **Invited Presentations**

Venue: European Calcified Tissue Society PhD Training Course – Amsterdam, Netherlands

Title: Skeletal Vascular Alterations in Chronic Kidney Disease

Year: 2018

Venue: Purdue University Social Justice Seminar – West Lafayette, IN

Title: A Forgotten Tissue in a Silent Disease: Skeletal Deterioration in Chronic Kidney Disease

Year: 2018

### **Awards**

2018 ASBMR Young Investigator Award – ECTS PhD Training Course

2018 Sherry Queener Graduate Student Excellence Award – Top Graduate Student Award

2018 Elite 50 Award – Top 50 Graduate Student Award

2017 Indiana University School of Medicine Seed Grant for Student Development

2017 Mayo Clinic Transform Conference Scholarship



2017 Christopher Hrvoj Travel Award  
2012 IUPUI Top 100 Student – Top 100 Undergraduate Student Award  
2010-2017 Bepko Scholars and Fellows Fellowship Program  
2010-2013 School of Engineering and Technology Scholarship

### **Teaching Experience**

Course: G819 Bone Biology  
Role: Lecturer  
Term: Spring 2018 (30 students)

*Delivered one lecture (bone modeling and remodeling; 1.5 hour) in this team-taught course*

Course: P547 Philosophy of Philanthropy  
Role: Presenter  
Term: Fall 2018 (25 students)

*Lead one discussion (How service brings us to life; 1 hour) in this discussion-based course*

### **Mentoring**

Herron School of Design Thinking Masters Committee Member (2018)